THE STRUCTURAL CHARACTERIZATION OF MAMMALIAN REOVIRUS RNA-DEPENDENT RNA POLYMERASE, CAPSID MORPHOLOGY, AND CAPSID DYNAMICS

By

Israel Isaac Mendez

A Thesis
Submitted to the Faculty of Graduate Studies
in Partial Fulfillment of the Requirements
for the Degree of

Master of Science

Department of Medical Microbiology and Infectious Diseases
University of Manitoba
Winnipeg, Manitoba
Canada

THE UNIVERSITY OF MANITOBA

FACULTY OF GRADUATE STUDIES

*****

COPYRIGHT PERMISSION PAGE

The Structural Characterization of Mammalian Reovirus RNA-Dependent RNA Polymerase, Capsid Morphology, and Capsid Dynamics

BY

Israel Isaac Mendez

A Thesis/Practicum submitted to the Faculty of Graduate Studies of The University of Manitoba in partial fulfillment of the requirements of the degree of

Master of Science

TABLE OF CONTENTS

ACKNOWLEDGEMENTS

I would like to deeply thank my supervisor, Dr. Kevin Coombs, who has been more than a supportive mentor but also a friend. It is he who has given me the passion for research and discovery. By promoting independent thought through many insightful discussions, he has taught me that we are only limited by our imagination. He has shown me my hidden potential and for that I am ever grateful.

I would like to thank all the past and present members of the Coombs lab for support, friendship and advice. A sincere thank you to Dr. Paul Hazelton who provided enormous help and guidance. A sincere thank you to Megan Patrick, Tammy Stuart, Magdalena Swanson, Laura Hermann, and Natalie Keirstead for your love and friendship. I would also like to thank Dr. Yi-Min She who was absolutely wonderful to work with, possibly one of the most thoughtful persons I know.

In no particular order, I would like to thank my committee members Dr. Xi Yang, Dr. Harvey Artsob and Dr. Peter Loewen for their insightfulness and encouragement. I would also like to thank Dr. Werner Ens for providing me with a "home" at the Department of Physics and opening the doors to the world of mass spectrometry.

I would like to thank all of my friends, especially Clarence, Boo and Mike, who have offered support and relentlessly reminded me that life is not all about work.

I would like to thank God for guiding my path and giving me hope.

I would also like to thank my sister, Ursula, who has always been there by my side and will always be my best friend.

Last but not least, I would like to thank my parents most of all; for teaching me to challenge myself, for instilling in me the value of education, the appreciation of science, and the perseverance, determination and strength to accomplish any hurdle. They are the true wind beneath my wings.

DEDICATION

I would like to dedicate this to my dearest sister, Ursula, who always makes me smile.

You are the only one who can make my stomach hurt so much by laughing.

I LOVE YOU.

LIST OF FIGURES

LIST OF TABLES

ABBREVIATIONS

(-) RNA	minus sense ribonucleic acid
(+) RNA	plus sense ribonucleic acid
ATP	adenosine triphosphate
BSA	bovine serum albumin
cDNA	copy deoxyribonucleic acid
CTP	cytosine triphosphate
dATP	deoxyadenosine triphosphate
dCTP	deoxycytosine triphosphate
dGTP	deoxyguanosine triphosphate
DMSO	dimethyl sulfoxide
DNA	deoxyribonucleic acid
DOC	deoxycholate
DPI	days post infection
DTT	dithiothreitol
dTTP	deoxythymidine triphosphate
EDTA	ethylenediamine tetraacetate
EOP	efficiency of plating
ESI	electron spray ionization
FCS	fetal calf serum
GTP	guanosine triphosphate
HO	homogenization buffer
ISVP	intermediate/infectious subviral particle

MALDI	matrix assisted lazer desorption ionization
MOI	multiplicity of infection
mRNA	messenger ribonucleic acid
PBS	phosphate buffered saline
PBS/EDTA	phosphate buffered saline/ethylenediamine tetraacetate
PCR	polymerase chain reaction
PFU	plaque forming unit
Px	passage (x = passage number)
Qq	quadrupole-quadrupole
RdRp	RNA dependent RNA polymerase
RNA	ribonucleic acid
Rnasin	RNase inhibitor
RT	reverse transcription
SDS	sodium dodecyl sulfate
SDS-PAGE	sodium dodecyl sulfate polyacryamide gel electrophoresis
T1L	serotype 1 Lang
T3D	serotype 3 Dearing
TBE Buffer	tris/ boric acid/ EDTA buffer
TFA	trifluoroacetic acid
TOF	time of flight
TRB	transcription reaction buffer
ts	temperature sensitive
UTP	uridine triphosphate
VSP	viable serum protein

ABSTRACT

Viruses maintain high structural stability during the extracellular portions of their replicative cycles, yet are significantly dynamic during other stages in their life cycle. Despite the extensive studies that have characterized the various structural proteins found within the capsid layers of reovirus, little is still known with regards to the proteins within it and to the overall dynamics of the virus particle. This study serves to further characterize the interior particle protein λ3, the RNA dependent RNA polymerase, and to offer evidence that reovirus has the capacity to undergo extensive conformational changes. In addition, the environmentally safe compound Vertrel XF was identified as a suitable substitute for the organic solvent Freon 113, extensively used in virus purification.

Factors affecting protein configuration, specifically of the RdRp, can have detrimental effects on transcription. To examine such factors, temperature-sensitive mutants *tsD*357 and *tsG*453, along with reassortant analysis were used. Although replication by *tsD*357 is impaired at elevated temperatures (as implied by its "temperature sensitivity"), purified *tsD*357 virions are less susceptible to heat-induced loss of infectivity than their wild-type parent type 3 Dearing (T3D). Furthermore, purified cores derived from *tsD*357 are less sensitive to heat-induced loss of transcriptase activity than T3D cores. This phenotype was mapped to the L1 gene. The L1 gene was sequenced and shown to contain two non-silent mutations which when analysed by various computer algorithms, suggests that a substitution at amino acid 399 causes a significant change to the protein's secondary structure. These results suggest that an altered RdRp can either stabilize or facilitate transcription. When *tsG*453 core particles were examined more closely, a phenotypic difference in transcription when compared to its

wild-type parent was mapped to the L1 gene. Despite mapping the temperature sensitive lesion to the S4 gene, these results indicate the presence of a previously undetected lesion in the L1 gene or some novel role of the S4 gene in transcription.

To investigate the dynamic nature of the virus, purified virions and cores were analysed by MALDI QqTOF mass spectrometry. Analysis of virion and core particles revealed conformational differences between different strains of reovirus. Furthermore, conformational changes that did not disrupt capsid integrity were observed in virions in response to different pH's. Cores were shown to undergo a conformational shift when they switch from a non-transcribing state to a transcribing one. These results offer conclusive evidence that the proteins that make up the viral capsids interact in such a manner that promotes both particle stability and flexibility.

1. INTRODUCTION

1.1. Mammalian reovirus introduction.

Mammalian reovirus is the prototype virus from the genus *Orthoreovirus*, one of nine genera from the viral family *Reoviridae* (van Regenmortel *et al.*, 2000). Five of the nine genera cover viruses that are capable of infecting plants, insects, and fish while the other four, *Coltivirus*, *Orbivirus*, *Rotavirus* (a notable pathogenic genera), and *Orthoreovirus* are capable of infecting mammals. Mammalian reoviruses are capable of infecting a wide range of mammalian species including humans (Rosen 1962). The acronym *reo* within the name reovirus stands for *r*espiratory and *e*nteric *o*rphan which connotes that the virus is capable of infecting the respiratory or enteric systems without causing any serious pathogenesis in humans (Sabin 1959).

Reoviruses in nature are typically found in a variety of water sources which are thought to be the primary source of enteric infections. These viruses pose a greater risk to infants and immuno-compromised hosts than they do to normal healthy individuals. Study of these viruses over the past several decades have rendered them as a functional model to study entry of non-enveloped animal viruses into host cells and their corresponding pathogenesis. Some more notable findings include the discovery of Kozak's sequence, receptor mediated endocytosis and 5' mRNA capping (Silverstein S.C. & Dales 1968; Furuichi *et al.*, 1975a; Furuichi *et al.*, 1975b; Kozak 1981; Kozak 1982). Furthermore, the use of reoviruses have recently been explored as novel oncolytic agents (Coffey *et al.*, 1998; Norman & Lee 2000).

1.2. Virion structure.

Mammalian reoviruses are non-enveloped viruses made up of eight structural proteins arranged in two concentric icosahedral capsid layers (Figure 1). This double layered protein shell houses a genome which consists of ten double stranded RNA (dsRNA) segments. There are three large segments named L1, L2, and L3 (L for large), three medium segments named M1, M2, and M3 (M for medium), and four smaller segments named S1 through S4 (S for small), each of which can be easily resolved by electrophoresis in a polyacrylamide gel (Figure 1)(Shatkin *et al.*, 1968). Each of these genes, with the exception of S1 which has two different initiation codons, are monocistronic; that is, one gene encodes a single protein. Together, the ten genes encode eight structural proteins and three non-structural proteins which are also resolvable by electrophoresis (Figure 1) (Both *et al.*, 1975; McCrae & Joklik 1978).

Reoviruses exist in nature in three forms: virion, ISVP (infectious or intermediate subviral particle) and core (Figure 1). The virion contains a full complement of the eight structural proteins. Cryoelectron microscopic analysis indicates a diameter of 85 nm(Metcalf *et al.*, 1991; Dryden *et al.*, 1993). Virions have a T = 13 icosahedral symmetry whose outer capsid is made up of 600 copies each of σ3 (encoded by S4) and μ1 (encoded by M2) (Dryden *et al.*, 1993). At each of the 12 vertices, five monomers of λ2 (encoded by L2) form a pentameric complex, extending about 9.5 nm from the surface, for a total of 60 copies (Dryden *et al.*, 1993). At the surface of each vertex, and interacting with λ2, lies a folded arrangement of σ1 monomers (encoded by S1), the cell attachment protein. Originally believed to exist as tetramers (Bassel-Duby *et al.*, 1987; Fraser *et al.*, 1990), recent evidence suggests that σ1 may be present as trimers (Strong *et al.*, 1991; Turner *et al.*, 1992; Lee &

A.

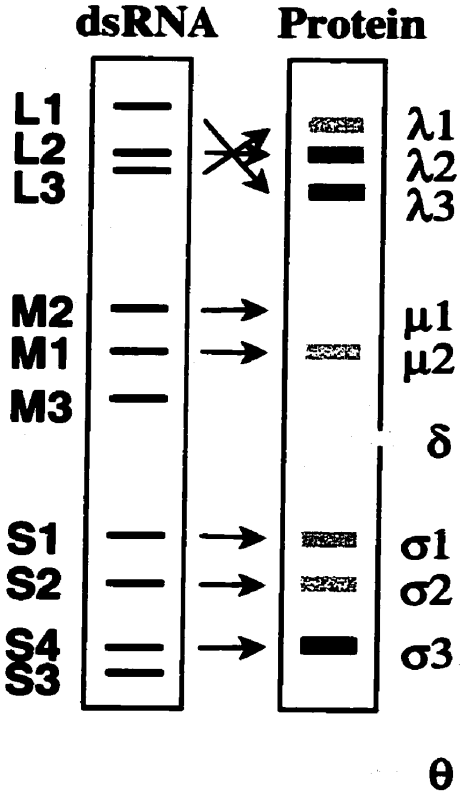
dsRNA
Protein
L1
L2
L3
M2
M1
M3
S1
S2
S4
S3
λ1
λ2
λ3
μ1
μ2
δ
σ1
σ2
σ3
θ

B.

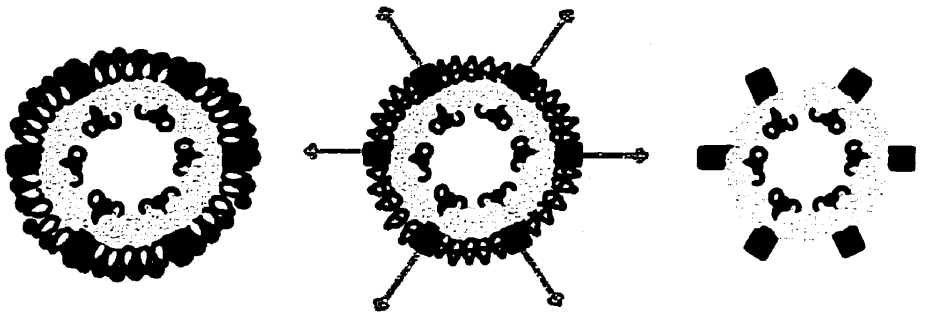
Virion
ISVP
Core

C.

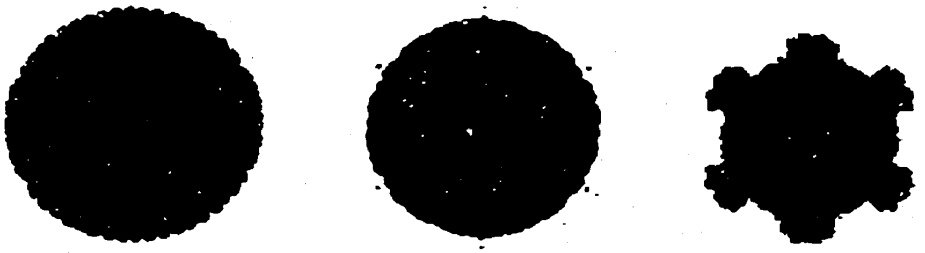

Figure 1. Mammalian reovirus genotype, protein profile, and particle structural elements. A. The migration of serotype 1 Lang (T1L) genomic segments as seen by SDS polyacrylamide gel electrophoresis (SDS-PAGE) and the migration of the corresponding proteins they encode. The genes cluster into three groups: the L (large) genes, the M (medium) genes, and the S (small) genes. δ and φ are μ1 cleavage products generated during proteolysis of virions and are present in ISVPs only (Nibert & Fields, 1992). For the migration of T3D genomic segments, please see Figure 4. **B.** Schematic representation of the three particle forms of reovirus: virion, ISVP and core. Proteins in both capsids are colour coded to match the proteins resolved in A. **C.** Cryoelectron microscopic images of the virion, ISVP and core which are 85, 80, and 60 nm respectively (Dryden *et al.*, 1993).

Leone 1994). Virions are proteolytically processed within the host to generate virion derivative ISVP's and cores, 80 nm and 60 nm respectively (Dryden *et al.*, 1993). ISVPs may be formed extracellularly via proteolysis of the virion by proteases such as pepsin in the stomach, or chymotrypsin or trypsin in the intestinal tract (Vander *et al.*, 1994). During conversion to ISVP, σ3 is digested away, μ1 is specifically cleaved into δ and φ, and the σ1 fibres extend outwards, possibly to facilitate cell attachment. ISVPs can be further processed to cores with the loss of all μ1 cleavage products and σ1 proteins to yield the inner capsid of reovirus which consists of only five structural proteins: λ1 (encoded by L3), λ2, λ3 (encoded by L1), μ2 (encoded by M1), and σ2 (encoded by S2). During proteolysis, λ2 has been shown to undergo a significant conformational change (Dryden *et al.*, 1993).

Proteins λ1 and σ2, both present in roughly 120 copies, make up the lattice of the inner capsid where λ1 is thought to form a smooth surface punctuated with low lying ridges upon which σ2 binds (Reinisch *et al.*, 2000). Protein λ2 exists as described above. Internal core proteins λ3, the RNA-dependent RNA polymerase (RdRp) and μ2, the putative polymerase cofactor, are both found internal to the core and are present in low copy number. Protein λ3 is located at the base of each of the 12 vertices as a single copy and each is believed to be associated with one or two copies of μ2. Both ISVPs and cores can be generated *in vitro* through proteolytic digestion (Mayor & Jordan 1968). ISVPs are infectious but not transcriptionally competent whereas cores are transcriptionally competent but not infectious, having lost its cell attachment protein.

1.3. Virion life cycle

1.3.1. Early events. The predominant route of infection in a host is enteric. Once

inside, the virion initiates infection within the respiratory or enteric systems. During a gastro-intestinal infection, the virion must go through the stomach and endure an acidic pH that can be as low as 0.82 (Vander *et al.*, 1994). Virions are notable for their remarkable stability as they are able to maintain their morphology at pH's as low as 2.0 and still retain their infectious nature (Stanley 1967; Fields & Eagle 1973). Typical cells targeted, or recognized, by the virions are the epithelial cells that line the gastro-intestinal tract and respiratory tract.

For an overview of the reovirus life cycle, please see Figure 2. The first step critical in reovirus infection is the attachment to cellular surface molecules. Both virions and ISVP's are capable of binding to a cellular receptor. Which proteins serve as receptors remains in question; however, evidence has pointed out sialic acid, other sialoglycoproteins, EGF (epithelial growth factor) receptor, and the junction adhesion molecule as possible reovirus receptors (Gentsch & Hatfield 1984; Paul *et al.*, 1989; Choi *et al.*, 1990; Tang *et al.*, 1993; Barton *et al.*, 2001). The virus attaches to the receptor via its cell attachment protein σ1 (Lee *et al.*, 1981). Binding of the virion to the receptor leads to a conformational change in the viral capsid as cell-bound virions have been shown to be more resistant to pepsin digestion than unbound virions (Fernandes *et al.*, 1994). Furthermore, this conformational change is totally reversible as bound virions reverted back to their pepsin sensitive state once released from the cell surface (Fernandes *et al.*, 1994). An altered conformational state may be necessary for viral entry and subsequent uncoating.

Protein σ1 is the main determinant of reovirus serotype as it is the protein encoded from the least conserved gene amongst reovirus, conserved as little as 26% between some serotypes (Duncan *et al.*, 1990). There are three major prototypic reovirus serotypes: Type

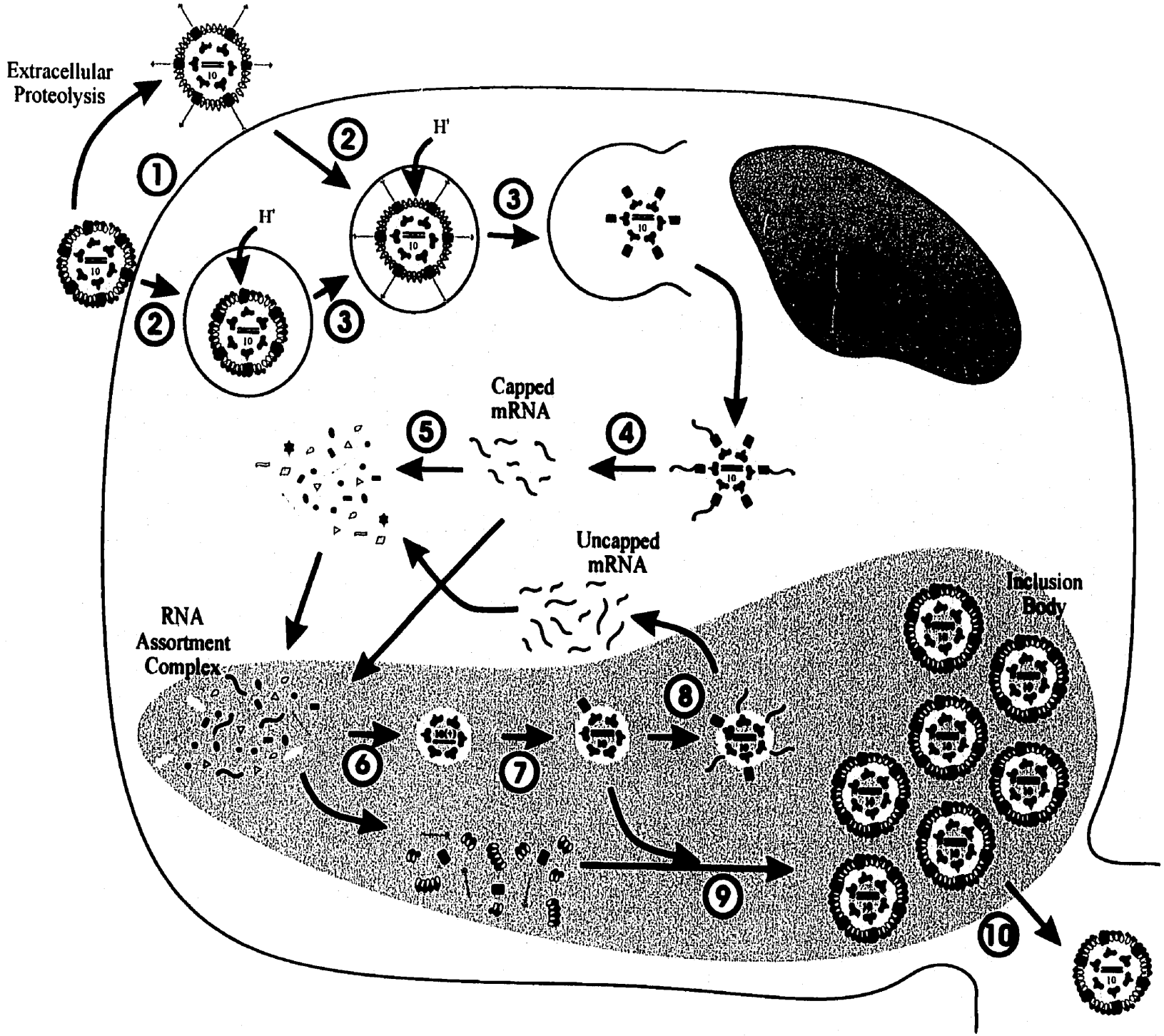
Extracellular
Proteolysis
H'
H'
Capped
mRNA
Uncapped
mRNA
RNA
Assortment
Complex
Inclusion
Body
1
2
2
3
3
4
5
6
7
8
9
10

Figure 2. The reovirus life cycle. ① Virions or ISVPs must first attach to a cell surface receptor, present on a variety of cell types. ISVPs can be generated extracellularly through proteolytic digestion of the outer capsid proteins. ② After adsorption, virions or ISVPs are invaginated through receptor-mediated endocytosis. ISVPs can bypass the endocytic pathway and instead, directly penetrate the membrane. ③ Endosomes carrying viral particles will fuse with lysosomes upon which lysosomal enzymes, under acidic conditions, will mediate uncoating of the virion or ISVP outer capsid to generate and release the core particle. ④ Cores are the transcriptionally active component of reovirus and will initiate primary transcription to generate capped mRNA. ⑤ Nascent transcripts will be translated by host cellular ribosomes to produce viral proteins. ⑥ Viral proteins and primary plus strand transcripts will come together in an RNA assortment complex, possibly mediated by non-structural and certain structural reovirus proteins. Assembly occurs to generate core-like replicase intermediate particles that contain a full complement of plus strand transcripts. ⑦ These sub-viral particles will then undergo replication to generate complimentary minus strand templates that are not liberated to the cytoplasm. ⑧ These minus strand RNAs serve as the template for subsequent secondary transcription to yield uncapped plus strand mRNA. ⑨ Secondary uncapped transcripts are then translated to generate more viral proteins. ⑩ Proteins and plus strand capped transcripts will assemble to generate progeny virions. These virions will often aggregate to form *inclusion bodies*. Virions are then released through cell lysis through a mechanism incompletely understood.

1 Lang (T1L), Type 2 Jones (T2J) and Type 3 Dearing (T3D). Differences among these strains will be discussed in further detail in later sections.

Once attached, the virion or the ISVP is adsorbed into clathrin coated pits via receptor mediated endocytosis (Borsa *et al.*, 1979; Georgi *et al.*, 1990; Rubin *et al.*, 1992). Evidence also suggests that ISVPs can directly cross through the membrane, bypassing endocytic uptake (Borsa *et al.*, 1979). Once adsorbed into endosomes, the endosomes will then fuse with lysosomes. An influx of ions via proton pumps present on the lysosomal membrane will cause the pH to drop to as low as 4.0. This acidic environment, in conjunction with the presence of acid-dependent lysosomal proteases such as cathepsins, will proteolytically process the virion or ISVP to core particles that are subsequently released to the cytoplasm.

1.3.2. Transcription and replication. Cores in the cytoplasm are transcriptionally active as they bear self-sustained transcriptional machinery, and will initiate synthesis of 5'-capped, non-polyadenylated messenger RNA (mRNA) from each of their ten genomic stands (Faust *et al.*, 1975; Furuichi *et al.*, 1975b). Reovirus bears its own RNA polymerase, a property unique to all RNA viruses with the exception of retroviruses, as no currently known cellular enzymes are capable of transcribing or replicating RNA. Core protein λ3, the RNA-dependent RNA polymerase (RdRp) (Drayna & Fields 1982a; Koonin *et al.*, 1989; Morozov 1989; Starnes & Joklik 1993) and μ2, the putative polymerase cofactor (Wiener *et al.*, 1989; Yin *et al.*, 1996) are the internal core enzymes responsible for transcription and subsequent replication. Protein λ3 has been the only structural protein demonstrated to possess polymerase activity *in vitro* (Starnes & Joklik 1993). Genetic studies that use reassortants (see section 1.4 for a review on reassortants) showed that the L1 gene, which encodes λ3, controlled the pH optimum of transcription amongst the three different serotypes (Drayna &

Fields 1982a). Furthermore, sequence analysis of the L1 gene revealed GDD motifs conserved in all viral polymerases (Morozov 1989; Bruenn 1991). Putative polymerase cofactor μ2 has been shown to be responsible for the optimal temperature of transcription characteristic in cores (Yin *et al.*, 1996) and may further function as an NTPase (Noble & Nibert 1997). Core spike protein λ2 is responsible for the 5'mRNA capping as it possesses guanylyltransferase activity (Shatkin *et al.*, 1983; Cleveland *et al.*, 1986) and possibly methyltransferase activity (Seliger *et al.*, 1987; Reinisch *et al.*, 2000) Core capsid protein λ1 has recently been shown to possess NTPase/helicase activity (Bisaillon *et al.*, 1997; Bisaillon & Lemay 1997a), RNA 5'-triphosphatase activity (Bisaillon & Lemay 1997b), and can bind nucleic acids nonspecifically (Lemay & Danis 1994). The genome of reovirus is double stranded; therefore, unwinding the RNA duplexes, necessary for transcription, would require energy, energy that perhaps λ1 provides.

Cryoelectron microscopic analysis of cores have suggested that cores undergo a conformational change when switching from a non-transcribing state to a transcribing one (Yeager *et al.*, 1996). Upon activation, the λ2 monomers are thought to undergo a shift in conformation, exposing an 8 nm channel, that allows for 5'-mRNA capping and mRNA extrusion (Dryden *et al.*, 1993; Yeager *et al.*, 1996; Reinisch *et al.*, 2000). The nascent plus strand RNA transcripts, or mRNA, are then released via these λ2 channels to the cytosol (Gillies *et al.*, 1971, Bartlett *et al.*, 1974).

The nascent mRNA's, the product of *primary transcription*, are next translated by host cellular ribosomes to generate viral proteins. These proteins will associate with primary transcripts to form what are known as RNA assortment complexes. A full complement of genes is packaged into replicase intermediate particles, devoid of an outer capsid and devoid

of inner capsid core protein λ2, through a poorly understood process. Unknown tight signaling, possibly through short conserved regions at the 5' and 3' ends of each gene (Antczak *et al.*, 1982), must exist that mediate assortment such that only viral mRNA, not cellular mRNA, and that only one of each of the ten segments, is packaged (Zou & Brown 1992; Chapell *et al.*, 1994). Structural protein σ3 and both non-structural proteins translated from early transcripts, μNS and σNS, all have the capacity to bind ssRNA and may alone, or in cooperation, play a role in assortment (Huismans & Joklik 1976; Antczak & Joklik 1992). Just as genetic assortment remains poorly understood, so is core-like replicase intermediate particle capsid assembly. Certain core proteins, such as λ1 and σ2, have been shown to self-associate when co-expressed while others, such as λ2, in the absence of the remaining proteins, fail to do so (Mao & Joklik 1991; Xu *et al.*, 1993). The requirement to preform certain protein complexes prior to complete core capsid assembly remains unknown.

Like many structural proteins in virus, σ3 plays several regulatory roles aside from its structural one. Through its ability to bind dsRNA, a feat considered to occur only upon dimerization (Olland *et al.*, 2001), σ3 is thought to counteract the reovirus induced host antiviral defence mechanisms. dsRNA-dependent protein kinase PKR, in the presence of dsRNA, will phosphorylate the α-subunit of initiation factor eIF-2 which shuts off translational initiation, thereby interfering with viral protein synthesis (Huismans & Joklik 1976; Sharpe & Fields 1982; Imani & Jacobs 1988; Lloyd & Shatkin 1992; Beattie *et al.*, 1995; Clemens 1996; Schmechel *et al.*, 1997; Yue & Shatkin 1997). By sequestering dsRNA, σ3 removes PKR's potent inducer. Protein σ3 also has the capacity to bind ssRNA and may play a role in the assortment complex during particle assembly (Antczak & Joklik 1992).

Once the mRNA transcripts are packaged, they serve as template for minus strand synthesis by the RdRp. Minus strand synthesis initiates from the 3' end of each plus strand, possibly mediated through specific polymerase recognition sequences common to all genes. Once synthesized, the minus strands remains within the replicase particle. These particles are able to carry out further transcription, termed *secondary transcription*, whose mRNA transcripts are reportedly uncapped due to a decreased particle presence of λ2 (Zweerink *et al.*, 1972; Morgan & Zweerink 1975; Zarbl *et al.*, 1980). These uncapped transcripts are the greater source of all transcripts during an infection (Ito & Joklik 1972a; Zarbl & Millward 1983), and serve to be translated into proteins. Whether or not the transcripts are packaged and serve as template for minus-strand synthesis remains unknown.

1.3.3. Late events. The steps leading to virion capsid assembly remain poorly understood but are believed to involve the addition of preformed outer capsid protein complexes onto self-assembled core particles. Outer capsid protein complexes between μ1 and σ3 must preform before their subsequent condensation onto the core particles, to form the outer capsid layer (Shing & Coombs 1996). The σ1 oligomers are believed to self-assemble and then attach to the particle vertices via sequence mediated interactions with the pentameric spike proteins, λ2 (Mah *et al.*, 1990; Leone *et al.*, 1991). What triggers virion release from infected cells is unknown but once virions are assembled, they eventually are liberated from the cell through an inefficient means of cell lysis.

1.4. Reovirus genetics

1.4.1. Reassortment. The genetic system of reovirus has properties that have made it an attractive and successful model to delineate the molecular and pathogenic basis of

viruses. Each of the ten dsRNA segments are of a different size; therefore, their migration profiles or *electropherotypes*, are easily distinguishable in polyacrylamide gels (Shatkin *et al.*, 1968). When a cell is co-infected with two or more different strains of reovirus, genes from the parents can mix, a process termed *assortment*. Progeny virions whose genomes consist of a mixed set of genes from the parents are called *reassortants*. Homologous genes from different reovirus strains are distinguishable under electrophoresis; thus, it is possible to identify which genes came from which parent when the electropherotypes of reassortants are viewed in polyacrylamide gels. For a schematic example, please see Figure 3.

If reassortment was completely random, there would be 2^n (where n equals the number of gene segments) possible reassortants, including two parental types. In reovirus, one may expect up to 1,024 (2^{10}) different gene combinations of which two are parental and the rest are reassortants (Figure 3). However, when cells are co-infected with two different strains of reovirus, resultant progeny consists of only 3-25% reassortants (Fields 1971). This nonrandom segregation phenomena remains to be explained; however, two possible mechanisms have been suggested. The first relies on separate areas of replication of two invading virions within a cell in which RNA may be poorly exchanged between the two regions (Joklik & Roner 1995). The second possibility is that heterologous viral RNA/protein will not interact as efficiently if they come from different parents, which would lead to a decrease in the observed number of reassortants (Roner *et al.*, 1990). A third possibility is that perhaps all 1,024 possible reassortants *are* generated; however, because of the various proteins present in the capsids, many may not be stable or allow for infections, and hence their passaging and propagation to high enough titres for identification is not possible as their capacity to survive is severely limited.

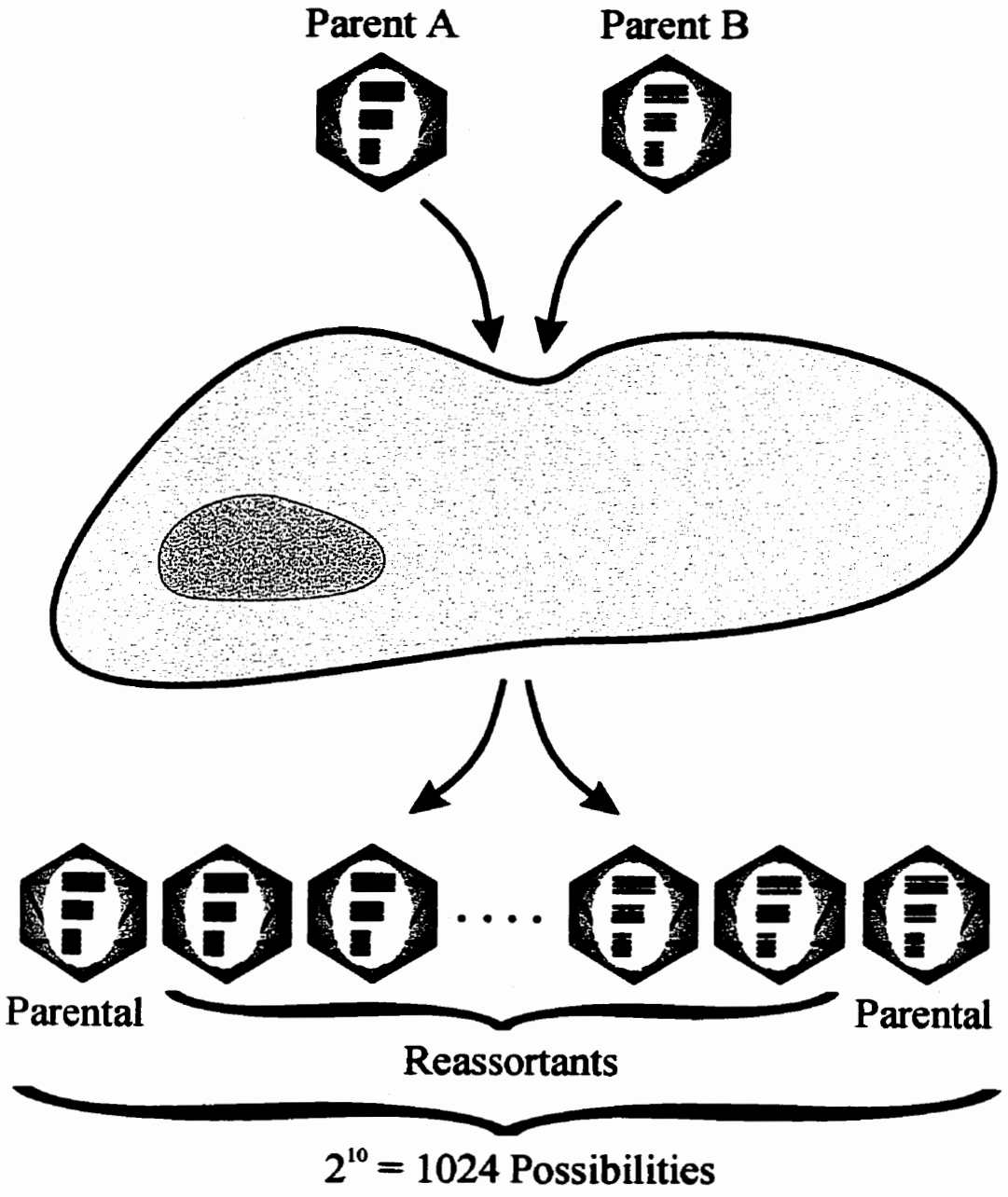
Parent A
Parent B
Parental
Parental
Reassortants
$2^{10} = 1024$ Possibilities

Figure 3. Co-infection and the generation of reassortant progeny virions. During a mixed or a co-infection, the incoming virions, or parents, will both undergo transcription and replication. The assortment complex will then consist of RNA and viral proteins from both parents. Assortment can then occur to generate reassortants, progeny virions that contain a mixed set of genes from both parents. If reassortment were a completely random process, 1024 (2^n where n = the number of gene segments) possible reassortants can be assembled. Two of the 1024 would result in parental like virions, whereas the other 99.8% of progeny virions would be reassortants. The hybrid genomes of reassortants can be resolved by SDS polyacrylamide gel electrophoresis and which genes came from which parent can be determined if the parental strains have different electropherotypes, i.e. are different serotypes.

1.4.2. Reassortant mapping. The segmented nature of the virus and the virus's capability to undergo assortment to generate reassortants provides researchers with an exploitable tool to characterize proteins and their roles in the reovirus life cycle. For example, if T1L virions grew optimally under condition A whereas T3D preferentially grew under condition B, T1L x T3D reassortants can be generated and isolated for analysis of growth conditions. One set of reassortants will grow better under condition A whereas the other set will favor condition B. The electropherotypes of the reassortants can be determined by comparing their gene migrations to that of their parents. The reassortants would then be organized according to their preferred growth conditions, A or B. Analysis of their electropherotypes may single out a gene that comes from one parent in one set of reassortants, and from the second parent in the other set of reassortants (Figure 4). If all other genes are randomly distributed among the reassortants, then the singled out gene is responsible for the phenotypic difference towards growth conditions observed among the two parents. Such use of reassortants to phenotypically identify or "map" a gene is termed *reassortant mapping*.

1.5. Temperature sensitive mutants

Many protein function determinations and other related discoveries have been attributable to the existence of reovirus *temperature sensitive (ts)* mutants. For example, use of reovirus *ts* mutants have led to advances in viral structure (Drayna & Fields 1982b), viral assembly (Shing & Coombs 1996; Hazelton & Coombs 1999; Becker *et al.*, 2001) viral pathogenesis (Keroack & Fields 1986; Bodkin & Fields 1989) and protein and enzymatic functioning (Drayna & Fields 1982; Drayna & Fields 1982a; Coombs 1996). Originally *ts*

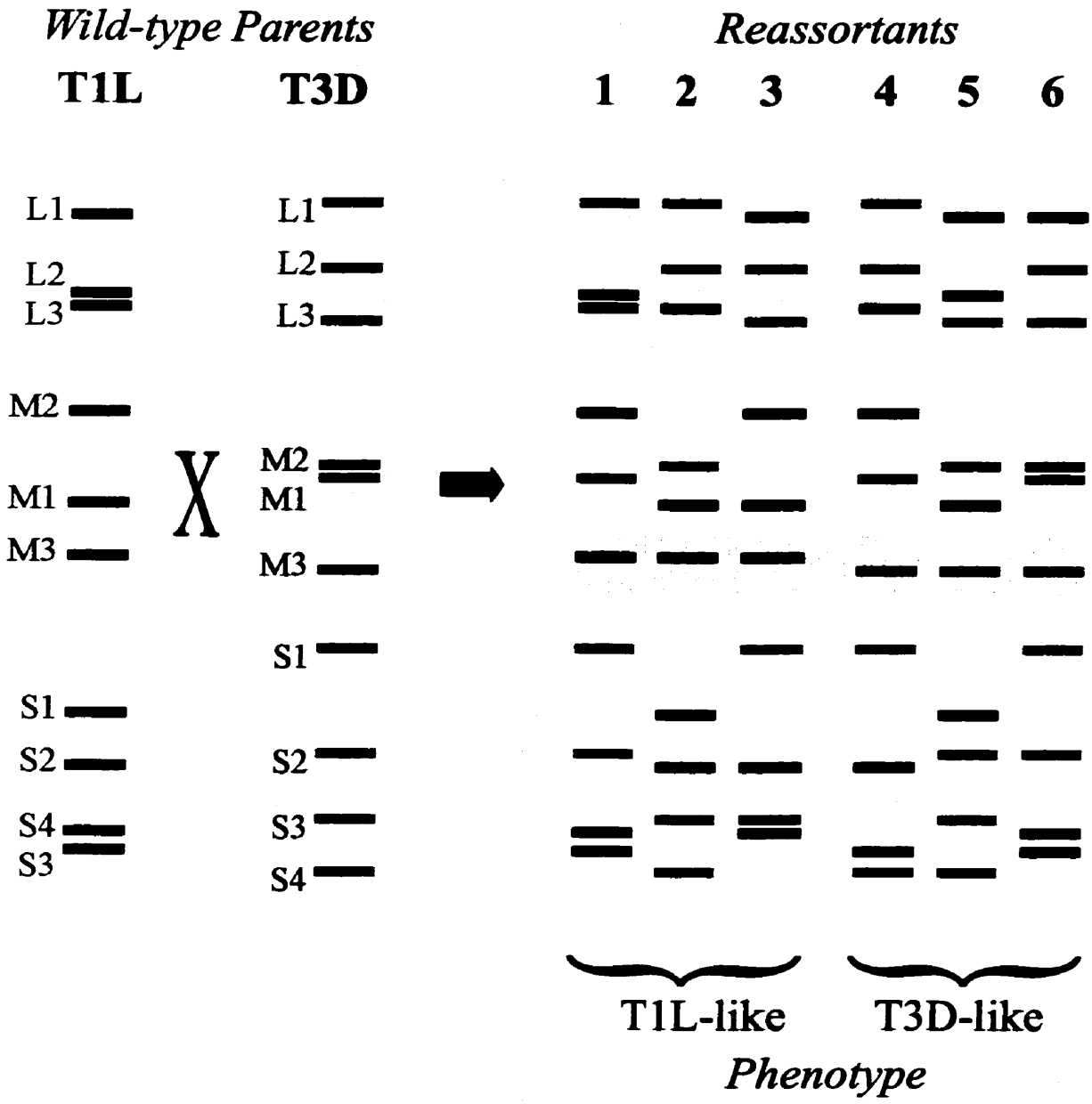
Wild-type Parents
T1L
T3D
Reassortants
1
2
3
4
5
6
L1
L2
L3
M2
M1
M3
S1
S2
S4
S3
T1L-like
T3D-like
Phenotype

Figure 4. Reassortant mapping. If a phenotypic difference exists between two different parental strains, reassortants generated from the two parents can be used to identify which gene and hence which protein is responsible. In this example, reassortants were generated from a T1L x T3D co-infection and their electropherotypes resolved by SDS-PAGE. The reassortants were studied to determine whether they behaved more like one parent or the other. One group of reassortants (1, 2 and 3) behave like parent T1L under a specific set of conditions. The other group of reassortants (4, 5 and 6) behave like parent T3D under the same set of conditions. By examining the electropherotypes of the reassortants, the T1L-like group all derived their M3 gene from T1L whereas the M3 gene in the T3D-like group comes from T3D. The fact that all other genomic segments are randomly distributed indicates that the phenotypic difference between the two groups is attributed to the M3 gene. Hence the M3 gene, which encodes the nonstructural protein μNS, defines the observed growth behavior between the T1L and T3D parents.

mutants were generated by chemical treatment of virions with mutagens such as nitrous acid, nitrosoguanidine, 5'-fluorouracil or proflavin (Ikegami & Gomatos 1968; Fields & Joklik 1969). To identify a *ts* mutant, mutagen treated stocks of virus were diluted and plated at 30°C (Ikegami & Gomatos 1968) or 31°C (Fields & Joklik 1969) as the *permissive* temperature. Individual plaques were identified early in the infection and marked. Infections were then incubated at a higher *non-permissive* temperature of 37°C (Ikegami & Gomatos 1968) or 39°C (Fields & Joklik 1969). Plaques that did not continue to grow were identified as *ts* mutants.

Therefore *ts* is a conditionally-lethal property defined as the impairment of replication at elevated temperatures. Furthermore, a reovirus' temperature sensitivity is a function of both the infected cells and the virus. The standard means of measuring a clone's temperature sensitivity is to compare the viral titre at a high, non-permissive temperature, typically at 39°C, to the viral titre at a low, permissive temperature, typically at 32°C. The viral titre at the non-permissive temperature is divided by the titre at the permissive temperature to generate an *efficiency of plating* (EOP) value. Non-*ts* clones, having grown equally well at both temperatures, will have an EOP value near 1 ± 10 whereas *ts* clones will have a value significantly lower than the wild-type value; usually by a difference of at least one magnitude of 10 (Coombs 1998).

As *ts* clones were created, they were organized into ten groups, one for each gene segment. In certain cases, reassortant mapping was used to identify which gene was responsible for the *ts* phenotype and hence contained the *ts* lesion. Sometimes though, reassortant analysis failed to identify which gene possessed the lesion. Originally however, an analytical method, recombinational analysis, was developed to identify which group a *ts*

clone belonged to. When an ungrouped ts clone co-infects cells with a *ts* clone from a known group, reassortment can occur. If both parents have a *ts* lesion in different genes, their progeny virions will either be a single mutant, a double mutant (having picked up the two genes with *ts* lesions) or wild-type like, only the latter of which can grow efficiently at both permissive and non-permissive temperatures. If both parents were to contain a *ts* lesion in the same gene, then all subsequent progeny would be *ts*. In such a case, by knowing where the lesion lies in one parent then implies that the second parent must have the lesion in that same gene. However, such a clear discrepancy is not often the case. Often, phenomena now known as *complementation*, the mixing of proteins not genes, or *genetic interference*, the ability of a virus to decrease the yield of another virus during a co-infection, may interfere with recombination (Ito & Joklik 1972a; Chakraborty *et al.*, 1979). Therefore, to measure a clone's ability to recombine with another, the following formula was generated as a measure of recombination:

$$\frac{(AB)_{NP} - (A+B)_{NP}}{(AB)_{P}} \times 100$$

where A and B are the viral titres of two parental *ts* mutants and where NP = non-permissive temperature of 39°C and P = permissive temperature of 32°C (Fields & Joklik 1969). *ts* mutants were assigned originally to one of five groups depending on which gene contained the *ts* lesion, a categorical system based on their recombination values (Cross & Fields 1972). Subsequent *ts* clones that did not fall into any of the five groups were placed in newly assigned groups (Fields & Joklik 1969; Ramig & Fields 1979; Coombs 1996).

1.6. Objectives of this study

There are two arms of investigation in my thesis work, demarcated primarily by the methodologies involved, but only one focus: to further our knowledge on protein structure and function within mammalian reovirus. Despite the extensive study of reovirus over the past three decades, very little is known about protein orientation and interactions within the viral capsid, the role of such interactions and the locations of those interactions. Furthermore, little is known with regards to the enzymatic proteins within the capsid, specifically with respect to λ3, the RdRp, and how they functionally carry out transcription.

All of my studies at one point or another required virions in a purified state in the absence of cellular debris. The method past employed in the lab involved organic solvent extraction of virions from cellular components. The solvent used was Freon 113 (1,1,2-trichloro-1,2,2-trifluoroethane)(Freon)(DuPont, Wilmington, DE) which for decades has been a key component of some viral purification methods (Gomatos & Tamm 1963; Gschwender & Traub 1978; Berman *et al.*, 1981; Richt *et al.*, 1993; Liebermann & Mentel 1994). This organo-aliphatic compound has been ideal in extracting lipids and lipid bilayers without extracting proteinaceous (and hence polar) material such as non-enveloped viruses, a feat attributable to its unique physical and chemical properties. However, as Freon has been implicated in ozone layer depletion, its use has been progressively eliminated which will lead to inevitable prohibition (Taylor 1996). The future unavailability of Freon would remove a vital step in virus purification, an important first step in many biochemical and structural studies. Therefore before any further experimentation could be done with viruses, I had to find a way to circumvent such a problem. A logical solution to this obstacle is to substitute it with another solvent that shares similar properties to it yet has low toxicity and

environmental hazards. I have analysed the capacity of other suitable solvents, based on their solubility parameters, to effectively purify large quantities of virus without any ill effects on virion morphology and infectivity. The identification of Vertrel XF as a suitable solvent has allowed for virion purification, an essential prerequisite for my further studies.

Two temperature sensitive mutants were examined more in depth after initial observations went unexplained. Mutant *tsD*357 is a *ts* mutant from Group D (Cross & Fields 1972), which has its *ts* lesion mapped to the L1 gene, which encodes the RdRp, λ3 (Ramig *et al.*, 1978; Drayna & Fields 1982a; Koonin *et al.*, 1989; Morozov 1989; Starnes & Joklik 1993). At non-permissive temperatures, *tsD*357 infected cells have been shown to produce progeny virions devoid of genomic material (Fields *et al.*, 1971). Additionally, decreased amounts of ssRNA and protein (Cross & Fields 1972; Fields *et al.*, 1972) and less than 0.1% dsRNA (Cross & Fields 1972; Ito & Joklik 1972b) were also found, all of which are suggestive of a defective polymerase. Within our lab, plots of viral titres over increasing non-permissive temperatures, have revealed that *tsD*357 virions appeared to be more stable than their wild-type parent T3D. That is to say, the *rate* not the actual titre, of T3D viral titres dropped off sooner than *tsD*357 viral titres in response to increasing temperatures. This suggests that *tsD*357 virions are more thermal stable than T3D, despite having a *ts* characteristic. To further these observations, *purified* virions as well as their derivative core particles were reexamined for thermal stability. Reassortants were used to map observed phenotypic differences from wild-type parent and results revealed a thermally stable RdRp. Sequence analysis of the L1 gene revealed three mutations, one of which, located in the catalytic portion of the enzyme, confers a dramatic change in the protein secondary structure and may be responsible for both the *ts* characteristic and thermal stability of the polymerase.

A second mutant, *tsG*453, was examined more closely after a previous study revealed a transcriptional difference when compared to its wild-type parent, T3D (Coombs 1996). Three point mutations were already identified in *tsG*453, one or all of which are responsible for temperature sensitivity, in its S4 gene which encodes the outer capsid protein σ3 (McCrae & Joklik 1978; Mustoe *et al.*, 1978a; Mustoe *et al.*, 1978b; Danis *et al.*, 1992; Shing & Coombs 1996). At the non-permissive temperature, *tsG*453 produces reduced amounts of protein and RNA (Cross & Fields 1972; Fields *et al.*, 1972; Danis *et al.*, 1992; Shing & Coombs 1996). Past experiments have also shown that at the non-permissive temperature, *tsG*453 infected cells fail to yield complete virions but instead produce large amounts of core-like particles (Morgan & Zweerink 1974, Danis *et al.*, 1992). It was concluded that outer capsid assembly required μ1/σ3 interactions which were prevented by a misfolded σ3 protein (Shing & Coombs 1996). To investigate an earlier observed transcriptional difference whereby *tsG*453 cores appeared more temperature-sensitive than wild-type parent T3D cores, *tsG*453 purified virions and cores were studied in parallel with *tsD*357. Virion particles preheated at higher temperatures appeared to have a loosely associated σ3 shell, indicative of a weak μ1/σ3 interaction which may play a role in decreased infectivity. Upon examination of heat treated cores, there was a significant decrease in transcriptase capabilities compared to wild-type parent T3D. Reassortant analysis indicates that the L1 gene is responsible. This would suggest that *tsG*453 is a double mutant, not a single mutant as previously thought, or alternatively, if no gene permutations are present in any phenotypically responsible gene, may suggest a novel role of gene controlled transcription in reovirus.

To examine viral protein interactions within the capsid first requires prerequisite knowledge about protein orientation. Understanding a protein's orientation will tell us about

possible regions available for protein binding as well as the regions that are surface exposed. To answer such questions, I analysed purified virion and core particles by mass spectrometry, a technique novel to reovirus. In conjunction with time limited proteolysis, mass spectrometric analysis have revealed primary surface exposed regions within virion capsid proteins and within core capsid proteins. Two surface exposed regions were identified in outer capsid protein μ1 which is situated beneath σ3, suggestive of possible regions capable of σ3 binding. Furthermore, analysis of an unidentified peptide yields evidence that σ3 is acetylated at its N-terminus, a structural novelty never before observed in this or other reovirus proteins. Core capsid digestions revealed surface exposed regions on core capsid protein λ1 which were originally thought to be internal to the capsid.

To further our understanding of the dynamics of the virion and core as a whole, flexibility of the virion or core while maintaining particle stability was probed by looking for non-disruptive conformational changes. Past evidence has indicated individual protein conformational changes occur during the course of the reovirus life cycle, namely during cell attachment (Fernandes *et al.*, 1994) and uncoating (Dryden *et al.*, 1993). Past studies have also provided some evidence to capsid conformational changes, both in virions (Fernandes *et al.*, 1994) and cores (Yeager *et al.*, 1996). Using mass spectrometry, I have identified conformational changes within virions that were environment dependent, and within cores when they switch to an active state of transcription.

Combined evidence provided in these studies shed new light on the dynamics of reovirus during the course of an infection, evidence which can be extrapolated to other RNA viruses and to all viruses in general.

2. MATERIALS AND METHODS

2.1 Stock cells and viruses. Mammalian reovirus type 1 Lang (T1L) and type 3 Dearing (T3D) are laboratory stocks. Temperature sensitive (ts) mutant clones *tsD*357 and *tsG*453 [originally derived from reovirus T3D as described (Fields & Joklik 1969; Cross & Fields 1972)], and T1L x *tsD*357 and T1L x *tsG*453 [originally isolated as described (Shing and Coombs, 1996)] are laboratory stocks. All viruses are grown in the fibroblast mouse cell line, L929. The cells are a continuous cell line derived from transformed cells epithelial in origin and can be subcultured indefinitely. The cells are maintained at an optimum density of 4.5 - 5.0 x 10^5 cells/ml at 37°C in suspension culture in Joklik's modified minimal essential medium (MEM)(Gibco, Grand Island, NY) supplemented with 2.5% fetal calf serum (FCS)(Intergen, Purchase, NY), 2.5% viable serum protein (VSP)(Biocell, Carson CA), and 2 mM ℓ-glutamine. To maintain an optimal density the cells are counted daily on a haemocytometer using a light microscope. A volume of cells is then replaced with fresh supplemented MEM to lower the concentration of the cells to the optimum level. Viral infections are carried out in either cell monolayers (grown in the presence of 5% CO_2 at 37°C) or suspension (grown at 33.5°C) that are further supplemented with 100U/ml of penicillin, 100 μg/ml streptomycin sulfate, and 1 μg/ml amphotericin-B as previously described (Coombs *et al.*, 1994).

2.2. Virus passaging and plaque assay.

2.2.1. Virus passaging. Wild type, *ts* mutants and reassortant virus stocks were amplified through three passages (P_1, P_2, P_3) in mouse L929 cells grown in supplemented MEM (as described above). Cells were either diluted to 4.2 - 4.5 x 10^5 cells/ml and incubated

overnight at 37°C in a 5% CO_2 atmosphere for next-day infections or were diluted to 1.1 x 10^6 cells/ml for immediate infection. Cells were grown in T25 Corning flasks (Fisher, Nepean, ON) until they reached 90% confluency. Most of the media was then removed (some saved as "pre-adaptive" media) and the cells were subsequently infected with 0.5 ml of the P_0 stock. Virus was allowed to adsorb to the cell monolayer under minimal volume of media for 1 hour at room temperature with periodic mixing every 10 to 12 minutes. A volume of 4.5 ml of fresh MEM (supplemented as described above for virus infections and also include a 30% volume of pre-adaptive media) was then added to each flask and the infected monolayers were incubated at 37°C for wild type clones and at 32°C for *ts* and reassortant clones. Cells were examined daily with the light microscope to check for cytopathic effect (CPE). Once the monolayers displayed ~ 90% CPE, the T25 flasks were frozen in a -80°C freezer. After three rounds of freeze/thawing, the cell aliquots (P_1) which contained the virus were collected. A volume of 0.5 ml of P_1 virus stock was then used to infect cell monolayers in T75 flasks to generate a subsequent round of amplified virus (P_2) in a similar manner. When a third passage of virus (P_3) was required, cell monolayers in T75 flasks were infected with virus at a multiplicity of infection (MOI) of one plaque forming unit (PFU) per cell. On day two of the infection, 2/3 of the media was removed and replaced with fresh supplemented MEM. The cells were subsequently harvested as described above. The dsRNA genomes of all virus stock types were extracted from the cytoplasm and the presence of viruses were confirmed in SDS-PAGE as described below.

2.2.2. Virus Plaque Assay. Mouse L929 cells were plated at a concentration of 1.1 x 10^6 cells/ml onto Corning Costar 6-well cluster dishes (Fisher, Nepean, Ontario) to form monolayers and were grown in a 5% CO_2 atmosphere at 37°C for wild type clones and at

32°C for *ts* and reassortant clones. Serial 1:10 dilutions of virus were made in gel saline (137 mM NaCl, 0.2 mM $CaCl_2$, 0.8 mM $MgCl_2$, 19 mM HBO_3, 0.1 mM $Na_2B_4O_7$, 0.3% [wt/vol] gelatin). A volume of 100 μl of each dilution was used to infect cell monolayers (day 1) under minimal volume media. The virus was allowed to adsorb for one hour with periodic mixing every 10 to 12 minutes. After adsorption, each well was overlayed with 3 ml of a 50:50 ratio of 2% agar and 2 x Medium 199 supplemented with 2.5% FCS, 2.5%VSP and a final concentration of 2 mM ℓ-glutamine, 100U/ml of penicillin, 100 μg/ml streptomycin sulfate, and 1 μg/ml amphotericin-B. The cells were incubated at 37°C for wild type clones and at 32°C for *ts* and reassortant clones. The cells were fed with 2 ml fresh agar/199 (supplemented as above) at 3 days post infection (dpi) for cells grown at 39°C, at 4 dpi for cells grown at 37°C, or at 6 dpi for cells grown at 32°C. Cells were then stained with a 0.04% neutral red solution (neutral red in a 1:1 ratio of 2X phosphate buffered saline (PBS) to 2% agar) at 6 dpi for cells grown at 39°C, at 7 dpi for cells grown at 37°C, or at approximately 14 dpi for cells grown at 32°C. Viral plaques were counted 18 to 24 hours after they were stained and the viral titres were calculated.

2.3. Purification of reovirus particles.

2.3.1. Virus amplification. To purify enough virus particles, batch infections ≥1 L were set up. For each litre of batch infection for purification, a total of 6.5×10^8 suspension grown cells were centrifuged at 700 rpm for 10 minutes in an IEC floor centrifuge. The resultant pellet was re-suspended in fresh MEM supplemented with 2.5% FCS, 2.5% VSP, 100U/ml of penicillin, 100 μg/ml streptomycin sulfate, and 1 μg/ml amphotericin-B to a final volume so that upon viral addition, the final concentration was no higher than 2.0×10^7

cells/ml. Virus from a P_2 or P_3 stock was added at an MOI of 5 PFU/cell and allowed to adsorb with periodic mixing every 10 to 12 minutes. After one hour, the infected cells were diluted to a concentration of 6.5×10^5 cells with 75% fresh MEM supplemented as described above and 25% pre-adaptive medium from cell suspension. The infected cells in suspension were then incubated at 33.5°C for 65 hours. Longer incubation times were needed for certain clones and cell harvesting did not occur until 60% cell death was observed by Trypan Blue staining using a haemocytometer. After incubation, the cells were centrifuged at 3,500 rpm for 20 minutes in a fixed-angle rotor (JA-10) in a Beckman RC centrifuge (Beckman, Mississauga, ON). The cells were resuspended in 12 ml HO Buffer (Homogenization buffer, 10 mM Tris, pH 7.4, 250 mM NaCl, 10mM β-mercaptoethanol) and transferred to a 30 ml COREX tube. Suspensions were either frozen and stored at -80°C or used immediately for purification.

2.3.2. Virus Purification. Cells suspended in HO were thawed if frozen and kept on ice. Samples were sonicated for 10 seconds to disrupt both cells and clump formation during freeze-thaw. Cell membranes were further disrupted with the addition of 1/50 sample volume of 10% DOC (desoxycholate) followed by vortexing and incubation on ice for 30 minutes. Then, 2/5th volume of Freon 113 (1,1,2-tricholoro-1,2,2-trifluoroethane) (Caledon Laboratories LTD, Georgetown, ON) or Vertrel XF (1,1,1,2,3,4,4,5,5,5-decafluoropentane) (DuPont Chemicals, Wilmington, DW) was added to the suspension and made into an emulsion by sonication for 30 seconds or more at 35% duty cycle with the sonicator probe (Vibra Cell) (Sonics & Materials Inc., Danbury, CN). Another 2/5th volume of the same organic solvent was added and the solution was re-emulsified and then centrifuged at 9,000 rpm for 10 minutes in a fixed-angle rotor (JA-20) in a Beckman RC centrifuge (Beckman, Mississauga,

ON). The resultant solution separated into two phases: an aqueous phase on the top and an organic phase on the bottom. The top phase was collected using a plastic pipette and transferred into a fresh 30 ml COREX tube. Identical organic solvent was added at 9/10th the volume of the collected phase. The solution was re-emulsified and re-centrifuged as described above. If the aqueous phase was not clear enough, the sample was solvent-extracted a third time. The resulting aqueous phase was then layered onto a pre-formed 1.2 - 1.4 gm/cc cesium chloride gradient made in a SW-28 polypropylene tube (Beckman Instruments Inc., Palo Alto, CA) and ultracentrifuged in a Beckman SW-28 rotor at 25,000 rpm for a minimum of 5 hours. Purified viruses formed a band that was collected through bottom puncture, their densities checked using a refractometer (Bausch and Lomb, USA), and then loaded into dialysis tubing for extensive dialysis against D-Buffer (Dialysis Buffer, 150 mM NaCl, 15 mM $MgCl_2$, 10 mM Tris, pH 7.4) to remove cesium chloride. Virus and Top Component were collected into appropriate vessels and stored at 4°C or frozen with the addition of 25% glycerol at -80°C. The concentration of purified virions was measured (before the addition of glycerol) by UV spectroscopy where the relationship 1 $OD_{260} = 2.1 \times 10^{12}$ particles/ml (Smith *et al.*, 1969).

2.4. Determination of temperature sensitivity. An efficiency of plating (EOP) assay was used to determine whether a virus clone was *ts*. Sub-confluent 6 well tissue culture plates were infected with serial 1:10 dilutions of a virus stock in duplicate and incubated at 32.0°C (permissive temperature) and 39.0°C (non-permissive temperature) as described in section 2.2.2. The viral titre obtained at each temperature was determined by plaque counts. To determine *ts* status, the following formula was used to calculate the EOP ratio:

$$EOP = \frac{\text{Viral titre at non-permissive temperature}}{\text{Viral titre at permissive temperature}}$$

Non-ts clones will have an EOP value near 1 ● 10 whereas *ts* clones will have a value significantly lower than the wild-type value; usually a difference of at least one magnitude of 10 (Coombs 1998).

2.5. Reassortant mapping

2.5.1. Cytoplasmic extraction of viral dsRNA. L929 cell monolayers were set up in Corning P60 culture dishes. After they reach sub-confluency, the cells were infected with 0.3 ml of virus P2 lysate stock and overlayed with 75% completed MEM and 25% pre-adaptive media (as described in section 2.2.1). Infections were incubated at 32°C for 6 days or until ~90% CPE was observed. Cells were then harvested by "scraping" the cell monolayer free and transferred to centrifuge tubes. Cells were pelleted under centrifugation at 1100 rpm in the IEC floor centrifuge. The cell pellets were resuspended in 0.45 ml of NP-40 buffer (140 mM NaCl, 1.5 mM $MgCl_2$, 10mM Tris, pH 7.4) and the cell membranes dissolved by adding 50 µl of 5% NP-40 detergent, vortexed to mix and incubated for a minimum of 30 minutes on ice. Cellular nuclei and organelles were pelleted under centrifugation at 2800 rpm in the Biofuge (VWR Scientific, Toronto, ON) for 10 minutes. Resultant supernatants were collected and transferred to a sterile microfuge tube (Fisher, Nepean, ON). Samples were either frozen at -20°C or used immediately. A pre-mixed solution was prepared (30 µl of 1 M Tris, pH 7.8, 3 µl of 200 mM EDTA, pH 8, 60 µl of 10% SDS) and added to each sample. Samples were then heated for 15 minutes at 42°C and the viral dsRNA genomes were purified by phenol/chloroform extraction (sequential addition of 14 µl of 5 M NaCl and 600 µl of

phenol/chloroform at a 1:1 ratio). Samples were mixed thoroughly by vortexing and then reheated to 42°C for 30 seconds followed by centrifugation at 12,500 rpm in a microfuge for 5 minutes. The resulting top aqueous phase was collected and transferred to a sterile microfuge tube and placed on ice. To precipitate the dsRNA, sodium acetate to a final concentration of 0.1 mM and 2.5 volumes of ice-cold ethanol were added to the samples which were then stored overnight at -20°C. The precipitated dsRNA was then pelleted at 12,500 rpm for 30 minutes at 4°C in the Biofuge. To dry the RNA, samples were lyophilized (SC100 speed-vac, Savant, Holbrook, NY) for 30 minutes, then resuspended in 35 µl of 1X electrophoresis sample buffer (240 mM Tris-HCl, pH 6.8, 1.5% dithiothreitol, 1% SDS). Samples were stored at -20°C if not used immediately.

2.5.2. Identification of reassortants by sodium dodecyl sulfate polyacrylamide gel electrophoresis (SDS-PAGE). RNA samples prepared (as described in section 2.5.1) were resolved by SDS-PAGE as described in section 2.6. Reassortants were identified by comparing the migration of the RNA gene segments to parental wild-type controls as described (Sharpe *et al.*, 1978, Nibert *et al.*, 1996).

2.6. SDS-PAGE. All samples to be resolved by SDS-PAGE were dissolved in 1X electrophoresis sample buffer (240 mM Tris-HCl, pH 6.8, 1.5% dithiothreitol, 1% SDS). 9% or 10% SDS slab gels (16 x 16 x 0.1 cm or 16 x 16 x 0.15 cm) for RNA analysis were poured and polymerized overnight. For protein analysis, a 15% or a 5-15% gradient SDS gel was poured and polymerized for 4 hours (for the 15% gel) or overnight (for the gradient gel). RNA and protein samples were heated to 65°C and 95°, respectively, for 5 minutes. Equal volumes of sample were loaded into wells and resolved at 18 mA for 40 hours for RNA

samples or at 5 W for 4 to 5 hours for protein samples. For RNA visualization, gels were stained with 0.1% ethidium bromide, visualized under UV light and photographed with Polaroid 667 film or visualized using a Gel Doc 2000 (BioRad) apparatus. For protein visualization, gels were fixed in acetic acid/methanol and then stained with Coomassie Brilliant Blue. For preservation, gels were dried between cellophane layers or onto filter paper at 80°C for 2 hours on a Gel Dryer (Slab Gel Dryer, SGD4050, Savant).

2.7. Generation and purification of core particles. To generate cores, high concentrations of purified virions were required; $\geq 5 \times 10^{12}$ particles/ml for T3D or 10 fold higher for other strains, a phenotype shown to be attributed to the M2 gene (encoding the outer capsid protein μ1/μ1C) (Drayna & Fields 1982a). Virions were adjusted to a final concentration of 6×10^{13} particles/ml with D buffer. 1/10th the volume of 2.2 mg/ml TLCK-treated α-chymotrypsin (made up in D buffer) was added to the virions which were then incubated, with periodic mixing, at 37°C for 2 to 3 hours (Joklik 1972). Successful concentration of virus and generation of cores was indicated by a change in colour and by the appearance of a flocculent late in the incubation. At the end of the core incubation, α-chymotrypsin was inhibited with the addition of 1X PMSF (p-phenylmethylsulfonyl fluoride) followed by vortexing and incubation on ice. The mixture was layered onto a pre-formed 1.3-1.55 gm/cc cesium chloride density gradient in a ½" x 2½" SW-41 ultracentrifuge tube (Beckman Instruments Inc., Palo Alto, CA) and ultracentrifuged in a Beckman SW-41 rotor at 35,000 rpm for a minimum of 3 hours. Purified cores formed a band that was collected and loaded into dialysis tubing for extensive dialysis against Core Buffer (1 M NaCl, 100 mM $MgCl_2$, 25 mM HEPES, pH 8.0). Cores were collected in a 1.5 ml centrifuge tube (Fisher, Nepean, ON) and stored

at 4°C or frozen with the addition of 25% glycerol at -80°C. The concentration of purified cores was measured (before the addition of glycerol) by UV spectroscopy where 1 OD_{260} = 4.2×10^{12} particles/ml (Coombs *et al.*, 1990). To confirm core purity, an aliquot of cores was run on a mini-SDS-PAGE gel to observe the characteristic protein profile or viewed by electron microscopy as detailed in section 2.9.

2.8. Transcription assay. The transcription assay is modified from previous methods (Skehel & Joklik 1969; Drayna & Fields 1982a). A typical transcriptase reaction is carried out in a final volume of 50 µl in a silanized, RNAse-free 1.5 ml centrifuge tube (Fisher, Nepean, ON)(for mass spectroscopic and electron microscopy analysis, the final volume was scaled down to 20 µl). As the transcription reaction is saturable by the concentration of cores, $\leq 3.5 \times 10^{11}$ total gradient purified core particles in ≤4.5 µl were used. Transcriptase activity was reported to be highest between 8-10 mM $MgCl_2$; therefore, the amount of core buffer must be carefully monitored (Yin *et al.*, 1996). Cores were diluted in core buffer, 75U RNAsin (Boehringer, then later, 5 Prime 3 Prime Inc. Boulder, CO), 2X TRB (Transcription Reaction Buffer: 2 mM each of ATP, CTP, GTP, and UTP (Sigma Chemicals); 3 mM phosphoenol pyruvate (Sigma); 0.1 mg/ml pyruvate kinase (Sigma), 200 mM HEPES, pH 8.0), and diethyl pyrocarbonate (DEPC) treated water to bring the final volume to 50 µl. To reduce variability due to pipetting errors, a single larger reaction mixture was prepared and then divided into equal aliquots. The reactions were labelled by the addition of 0.1 µCi α-^{32}P-UTP (NEN-Mandel, Mississauga ON). The reaction was then incubated at 37-65°C (optimum is 48°C for T1L and 52°C for T3D) for one hour and stopped by chilling on ice. The core-generated messenger RNA (mRNA) was precipitated with 8 volumes of ice-cold

5% trichloroacetic acid (TCA), collected onto filters (Fisher, Nepean, ON), and washed with excess 5% TCA and ice-cold ethanol. The level of radioactivity present on the filters was determined on a Beckman LS 5000CE scintillation spectrophotometer and is indicative of the level of transcriptase activity.

2.9. Electron microscopy of reovirus particles. Virion or core particles were prepared for viewing by electron microscopy by a standard drop method described elsewhere (Hammond *et al.*, 1981; Hazelton & Coombs 1995). Briefly, a drop of untreated virions or cores were placed on clean parafilm (in the case of transcribing cores, samples were treated and fixed by adding 9 volumes of 0.1% gluteraldehyde in PBS (phosphate buffered solution)). In some instances, virions were diluted 100 fold with 0.1% glutaraldehyde in dialysis buffer to stabilize viral structures. 400-mesh electron microscope copper grids (3.05mm), pre-carbon-coated with Formvar, were placed carbon-side down onto the surface of the sample drop for ~30 seconds. Excess sample was wicked away by touching filter paper to an edge of the grid. The sample was then negatively stained with 1.2 mM phosphotungstic acid, pH 7.0 for ~30 seconds. Excess stain was wicked away as previously described. Samples were then viewed with the use of a Philips model 201 transmission electron microscope at magnifications between 50,000X and 100,000X. Electron micrographs were photographed onto Kodak 5303 direct positive film and printed onto Kodak Polycontrast III paper.

2.10. Determination of the T3D and *tsD*357 L1 gene sequences.

2.10.1. Virus template preparation. Virus template was obtained from purified T3D or *tsD*357 virions. In a 0.6 ml silanized centrifuge tube (Fisher, Nepean, ON), virions were

diluted in D-Buffer, 50 mM Tris, pH 8.0, 1.7 mM EDTA, pH 8.0, and 10% SDS. The mixture was vortexed and incubated at 42°C for 15 minutes. The genomic dsRNA was isolated by two rounds of phenol/chloroform extraction as described in section 2.5.1 followed by one round of chloroform only extraction. dsRNA was precipitated overnight at -20°C with sodium acetate to a final concentration of 0.1 mM and 2.5 volumes of ice-cold ethanol. The dsRNA pellet was then resuspended in 20 µl 90% DMSO (dimethyl sulfoxide) and 10% 10 mM Tris, pH 6.8. Template was either used immediately or stored at -20°C.

2.10.2. Primer design specific for the L1 gene. The nucleotide sequence of the T3D L1 gene is known (Wiener & Joklik 1989) and is available on GenBank (Accession # M31058); however, the GenBank sequence contains errors within the first 24 nucleotides. Therefore, primers were designed for recognition of the L1 gene sequence reported by Wiener and Joklik. As T1L and T3D show high homology in the L1 gene, 12 internal primers were designed and targeted to conserved areas spaced apart to allow for sequencing of the entire gene in both directions. The four end primers that were used for sequencing were created by a former student in the lab, Rashmi Goswami. The primers were designed using PrimerSelect (DNASTAR Inc., Madison, WI) and ordered in a desalted form from GIBCO-BRL (Life Technologies) (see Figure 5 for primer specifics). Primers were resuspended in DEPC-treated water and their concentration determined by UV spectroscopy.

2.10.3. Reverse transcriptase polymerase chain reaction (RT-PCR). dsRNA template was converted to ssDNA by RT. The L1 gene is 3.85 kb long; therefore due to its large size, the gene was amplified into two overlapping parts: a 2.75 kb and a 1.30 kb product. A volume of 6 µl of purified template (dsRNA) prepared as described in section 2.10.1, was melted in a heating block (PRC-100; MJ Research Inc., Watertown, MA) at 50°C

Primer A

1 5' gctacacgtt ccacgacaat gtcatccatg atactgactc agtttggacc gttcattgag agcatttcag gtatcactga tcaatcgaat

91 gacgtgtttg aagatgcagc aaaagcattc tctatgttta ctcgcagcga tgtctacaag gcgctggatg aaataccttt ctctgatgat

181 gcgatgcttc caatccctcc aactatatat acgaaaccat ctcacgattc atattattac attgatgctc taaaccgtgt gcgtcgcaaa

L1 B244-266

271 acatatcagg gccctgatga cgtgtacgta cctaattgtt ctattgttga attgctggag ccacatgaga ctctgacatc ttatgggcgg

361 ttgtccgagg ccatcgagaa tcgtgccaag gatggggaca gccaagccag aatcgccaca acgtatggta gaatcgctga atctcaagct

L1 T462-484

451 cgacagatta aggctccatt ggagaagttt gtgttggcac tattagtggc cgaagcaggg gggtctttat atgatccagt tttgcagaag

541 tatgatgaga ttccagatct atcgcataat tgccctttat ggtgttttag agagatctgt cgtcacatat ctggtccatt accagatcgg

631 gcaccttatc tttacttatc tgcaggggta ttctggttaa tgtcaccacg aatgacgtct gcaatccctc cgctactatc cgatcttgtt

721 aatttagcta ttttgcaaca aactgcgggt ttagatccat cattagtgaa attgggagta cagatatgcc ttcatgcagc agctagctca

L1 B781-803

811 agttattcat ggtttatctt aaagactaag tctatttttc ctcaaaacac gttgcacagt atgtatgaat ctctagaagg gggatactgt

901 cctaatcttg aatggttaga gcctagatca gactataagt tcatgtacat gggagtcatg ccattgtccg ctaagtatgc taggtcggcg

L1 T1019-1041

991 ccgtccaatg ataagaaagc gcgggaactt ggcgagaaat atggactgag ctcagtcgtc ggtgagcttc gtaaacggac aaagacgtat

1081 gttaaacatg actttgcttc agtgaggtac attcgtgacg ctatggcatg tactagcggt attttcttgg taagaacacc caccgaaacg

1171 gtattgcaag aatatacgca gagtccggag attaaggttc ccattcccca gaaagactgg acaggcccaa taggtgaaat cagaattcta

1261 aaagatacaa caagttccat cgcgcgttac ttatatagaa catggtactt ggcagcggcg agaatggcgg ctcaaccacg tacgtgggat

L1 B1328-1347

1351 ccattgtttc aagcgattat gagatctcaa tacgtgacag ctaggggtgg atctggcgca gactccgcga actctttgta tgcaatcaat

L1 T1517-1537

1441 gtgtcgttac ctgatttcaa gggcttacca gtgaaggcag caactaagat attccaggcg gcacaattag cgaacttgcc gttctcccac

1531 acatcagtgg ctatactagc tgacacttca atgggattgc gaaatcaggt gcagaggcgg ccacgatcca ttatgccatt aaatgtgccc

1621 cagcagcagg tttcggcgcc ccatacattg acagcggatt acattaacta ccacatgaat ctatcaccca cgtctggtag tgcggtcatt

1711 gagaaggtga ttcctttagg tgtatacgct tcgagccctc ctaaccagtc gatcaacatt gacatatctg cgtgtgacgc tagtattact

L1 B1733-1756

1801 tgggatttct ttctgtcagt gattatggcg gctatacacg aaggtgtcgc tagtagctcc attggaaaac catttatggg ggttcctgca

1891 tccattgtaa atgatgagtc tgtcgttgga gtgagagctg ctaggccgat atcgggaatg cagaacatga ttcagcatct atcgaaacta

L1 T2056-2078

1981 tataaacgtg gattttcata tagagtaaac gattcttttt ctccaggtaa cgattttact catatgacta ccactttccc gtcaggttca

2071 acagccacct ctactgagca tactgctaat aatagtacga tgatggaaac tttcctgaca gtatggggac ccgaacatac tgacgaccct

2161 gacgtcttac gtttaatgaa gtctttaact attcaaagga attacgtatg tcaaggtgat gatggattaa tgattatcga tgggactact

2251 gctggtaagg tgaacagtga aactattcag aacgatctag aattaatctc aaaatatggt gaggaattcg gatggaaata tgacatagcg

2341 tacgatggga ctgccgaata cttaaagcta tacttcatat ttggctgtcg aattccaaat cttagtcgcc atccaatcgt ggggaaagaa

L1 B2343-2366

2431 cgggcgaatt cttcagcaga ggagccatgg ccagcaattc tagatcagat tatgggtgtc ttctttaatg gtgttcatga tgggttacag

Primer C

2521 tggcagcggt ggatacgtta ttcatgggct ctatgctgtg ctttctcacg tcaaagaaca atgattggtg agagcgtggg ttaccttcaa

2611 tatcctatgt ggtcttttgt ctactgggga ttaccactgg ttaaagcgtt tgggtcagac ccatggatat tttcttggta catgcctact

2701 ggagatctgg gaatgtatag ttggattagc ttgatacgcc ctctgatgac aagatggatg gtggctaatg gttacgtaac tgacagatgc

Primer B

2791 tcaaccgtat tcgggaacgc agattatcgc aggtgtttca atgaacttaa actatatcaa ggttattata tggcacaatt gcccaggaat

2881 cctaagaagt ctggacgagc ggcctctcgg gaggtaagag aacaattcac tcaggcatta tccgactatc taatgcaaaa tccagagctg

L1 T2986-3007

2971 aagtcacgtg tgctacgtgg tcgtagtgag tgggagaaat atggagcggg gataattcac aatcctccgt cattattcga tgtgccccat

3061 aaatggtatc agggtgcgca agaggcagca atcgctacga gagaagagct ggcagaaatg gatgagacat taatgcgcgc tcgaaggcac

3151 agctattcga gcttttcaaa gttattagag gcgtatctgc tcgtgaaatg gcgaatgtgc gaggcccgcg aaccgtcggt tgatttgcga

3241 ttaccattat gtgcgggtat tgacccatta aactcagatc cttttctcaa gatggtaagc gttggaccaa tgctccagag tacgagaaag

3331 tactttgctc agacactatt catggcaaag acggtgtcgg gtcttgacgt taacgcgatt gatagcgcgt tattacgact gcgaacatta

L1 B3342-3365

L1 T3458-3478

3421 ggtgctgata agaaagcatt aacggcgcag ttattaatgg tggggcttca ggagtcagaa gcggacgcat tggccgggaa gataatgcta

3511 caggatgtga atactgtgca attagccaga gtggttaact tagctgtgcc agatacttgg atgtcgttag actttgactc tatgttcaaa

3601 caccacgtca agctgcttcc caaagatgga cgtcatctaa atactgatat tcctcctcga atgggatggt tacgggccat tttacgattc

3691 ttaggtgccg gaatggtaat gactgcgact ggagttgctg tcgacatcta tctggaggat atacatggcg gtggtcggtc acttggacag

3781 agattcatga cttggatgcg acaggaagga cggtcagcgt gagtctacca tgggtcgtgg tgcgtcaact catc 3' 3854

Primer D

Figure 5. T3D L1 gene sequence and the location of designed primers. The sequence of the T3D L1 gene was obtained from GenBank (Accession # M31058) and corrected (3854 nucleotides) (Wiener & Joklik 1989). The coding strand of the gene is shown 5' to 3'. Blue lines indicate where primers bind to the non-coding 3' to 5' strand. Red lines indicate where primers bind to the coding 5' to 3' strand. The codon in green marks the initiation codon. The codon in red marks the stop codon. The L1 gene primers are labelled by a letter designation indicative of which strand they bind to (T=top, B=bottom) and by numbers indicative of their location. Primers A, B, C, and D were created previously by Rashmi Goswami and in addition to sequencing, were used as described in section 2.10.3 to generate overlapping cDNA.

for 45 minutes. Samples were immediately transferred to an ice/water bath and snap-cooled by adding 63 µl of ice-cold DEPC-treated ddH_2O (double distilled water). Then, in order and without mixing, the following were added: 32U (0.8 µl of 40U/µl)of RNAse inhibitor (Boehringer), 0.1 µM (1 µl of 10 µM) of each an upstream and a downstream primer per strand, 5 µl each of 10 mM dATP, dCTP, dGTP, and dTTP, 20 µl of 5X 1st Strand Buffer (250 mM Tris-HCl, pH 8.3, 375 mM KCl, 15 mM $MgCl_2$), 0.001% BSA (Bovine serum albumin; Sigma)(1 µl of 10 mg/ml), 1 µM (1 µl of 100 µM) DTT, and 160U (0.8 µl of 200U/µl) of Superscript II reverse transcriptase enzyme (Gibco-BRL). The mixture was brought to a final volume of 100 µl with ddH_2O and then incubated at 42°C for 1.5-2 hours. Samples were immediately used for amplification as ssDNA is relatively unstable.

2.10.4. Amplification of L1 gene and purification of cDNA. The cDNA produced by reverse transcription as described in section 2.10.3 was amplified using the Expand™ Long Template PCR System according to the manufacturer's instructions (Boehringer Manheim). Briefly, to amplify one strand, 8 µl of cDNA was diluted to a final volume of 100 µl with ddH_2O with the following reagents at a final concentration of: 0.3 µM of an upstream and a downstream primer, 0.5 mM each of dATP, dGTP, dCTP, and dTTP, 0.75 mM $MgCl_2$, 1X Expand™ Long Template PCR buffer 3, and 2.5U of Expand™ Long Template enzyme mixture. PCR was performed on a GeneAmp PCR system 9700 (PE Applied Biosystems; Foster City, CA) for 5 cycles (94°C for 1.5 minutes to denature cDNA, 55°C for 1.5 minutes to allow primers to anneal, and 70°C for 3 min 10 seconds for elongation) followed by 31 cycles (92°C for 1.5 minutes to denature, 55°C for 1.5 minutes to anneal primers, and 70°C for 3 min 10 seconds to elongate) with a final elongation step of 70°C for 10 minutes. Samples were then cooled to 4°C and could be stored indefinitely.

To confirm amplified product, a small aliquot of sample diluted in DNA electrophoresis sample buffer was run on a 0.9% agarose horizontal slab gel in 0.5X TBE Buffer (45 mM Tris, 45 mM boric acid, 1 mM EDTA, pH 8.0), containing 0.1% ethidium bromide for later DNA visualization under UV, at 100V for ~1.5 hours. A 1 kilobase (kb) ladder (Boehringer Manheim) or purified virions were used as markers. Using a Gel Doc 2000 (BioRad) apparatus, a 2.75 kb and a 1.30 kb product were observed confirming successful amplification. Next, a large volume of sample was run on a larger 0.9% agarose gel prepared as described above. The resultant bands were excised using a sterile razor blade on top of a UV light box. The DNA was then extracted from the agarose using the QIAquick™ gel extraction kit (Qiagen, Germany) according to the manufacturer's instructions. The purification and quantity of product was determined (by visual comparison to a marker of predetermined amounts) on an agarose gel as described above.

2.10.5. Cycle sequencing. Cycle sequencing was carried out using the ABI PRISM® BigDye™ Terminator Cycle Sequencing Ready Reaction Kit (Perkin Elmer {PE} Applied Biosystems, Foster City, CA). Individual sequencing reactions were set up for each primer for both T3D and *tsD*357 which consisted of the following: 3.2 pmol of primer, 30-90ng of cDNA template, 4.0 - 8.0 µl BigDye™ Terminator Ready Reaction Mix (consisting of dye terminators, dNTP's, r*Tth* pyrophosphatase, $MgCl_2$, Tris-HCl buffer, pH 9.0, and the AmpliTaq DNA Polymerase, FS), and deionized water to a final volume of 20 µl. Cycle sequencing was performed on a GeneAmp PCR system 9700 for 1 cycle of 96°C for 1 minute 30 seconds, 55°C for 15 seconds, and 60°C for 4 minutes followed by 35 cycles of 96°C for 30 seconds, 55°C for 15 seconds, and 60°C for 3 minutes 10 seconds followed by cooling to

4°C. The products were then purified by two rounds of isopropanol precipitation (>15 minutes to not lose very short extension products and <24 hours to not increase the precipitation of unincorporated dye terminators), dried (on a lyophilizer or thermoblock), and resuspended in 22 µl template suppression reagent (ABI PRISM, Perkin Elmer) for 1 hour. Samples were then heated to 95°C for 2 minutes to denature the strands and immediately followed by snap cooling in ice-water. The ABI PRISM 310 Genetic Analyzer (PE Applied Biosystems Foster City, CA) was used to determine the sequence for each reaction. Chromas version 1.45 (McCarthy, 1998) was used to manually analyze sequences to ensure accuracy. EditSeq (DNASTAR Inc., Madison, WI) was used to construct the entire sequence of the gene and MegAlign (DNASTAR Inc., Madison, WI) was used for sequence comparison between T3D and *tsD*357.

2.11. Protein secondary structure analysis. The completed nucleotide sequences of the T3D and *tsD*357 L1 genes were converted to their respective sequence of amino acids using the program DNAClub (Ithaca, NY). The amino acid sequences were compared using MegAlign (DNASTAR Inc., Madison, WI) and the differences identified. The predicted protein secondary structure was calculated using various computer prediction programs: PSIPRED (version 2.0; Uxbridge, UK), SSpro 2 Prediction (http://promoter.ics.uci.edu/BRNN-PRED/), PredictProtein (Columbia University, New York, NY), and Protean (version 3.04b; DNASTAR Inc., Madison WI). The hydrophobic cluster analysis (HCA) plot was generated using the computational program DrawHCA via the Internet (http://www.lmcp.jussieu.fr/~soyer/www-hca/hca-form.html)(Gaboriaud *et al.*,

1987). The hydrophilicity plot was based on the Kyte-Doolittle algorithm (Protean). The antigenic index plot was based on the Jameson-Wolf algorithm (Protean). The σ3 X-ray crystallographic structure (Olland *et al.*, 2001) was manipulated and modified using the graphics visualization computer program RasMol 2.7.1. (Bernstein and Sons, Belport, NY).

2.12. Proteolytic digestion.

2.12.1. Generation of radio-labelled reovirus virions and cores. Purified virions were generated as described in section 2.3.1 and 2.3.2. Virions were labelled by adding >20 mCi ^{35}S-methionine (NEN-Mandel, Mississauga ON) per L of infection during the incubation period of amplification. Most of the ^{35}S-labelled virions were converted to cores by α-chymotrypsin digestion and purified as described in section 2.7. Labelled virions and cores were quantified by both UV spectroscopy and by scintillation counts.

2.12.2. Proteolytic digestion of virions and cores. Proteases (trypsin, α-chymotrypsin, pepsin, proteinase K, and staphylococcus V8 protease) were purchased from Sigma Chemicals and were resuspended in their appropriate buffers (either H_2O, D Buffer, pH 7.6, or Tris-HCl, pH 3.0) and stored at -20°C. Proteolytic digestions of virions (adjusted to pH of either 3.0, 4.5 or 7.6) or cores were carried out in 0.6 ml centrifuge tubes with a protein to enzyme ratio adjusted between 20:1 to 3000:1. Digestions were carried out over a time course at 37°C or 50°C. Aliquots from the digestion reaction were removed and the samples were inhibited with the addition of an enzyme inhibitor (PMSF), a pH change (0.1% TFA, trifluoroacetic acid, or 10 mM Tris pH 7.4) or by cooling on ice. Resultant peptide products were analysed by SDS-PAGE (described in sections 2.6 and 2.12.3) or MALDI-QqTOF mass spectrometry (described in section 2.12.4).

2.12.3. Analysis by fluorography and phosphor imaging. Viral proteins and proteolytic digestion peptide products were resolved by SDS-PAGE as previously described in section 2.6. After the gels were fixed, they were treated with Enlightening (DuPont Chemicals, Boston, MA), dried onto filter paper at 80°C for 2 hours on a Gel Dryer (Slab Gel Dryer, SGD4050, Savant) and fluorographed by exposure to Kodak X-AR sheet film (Kodak, Rochester, NY). Alternatively, dried gels were exposed to a Molecular Imager Fx Imaging screen (BioRad) for 12-24 hours at room temperature to generate a phosphor image. Images were then analysed by a Personal Molecular Imager® Fx (BioRad).

2.12.4. MALDI-QqTOF mass spectrometry.

2.12.4.1. Preparation of samples. T1L virion proteolytic digestion samples were prepared as described previously in section 2.12.2. To keep the intact virion stable, it was necessary to perform proteolytic digestions at high concentrations of salts (D-Buffer). The resulting products were then diluted with dH_2O 1 in 5 to reduce the salt concentrations to low levels favourable to the MALDI-QqTOF mass spectrometer.

Transcribing and non-transcribing cores were analysed. Optimal transcription by cores occurs when cores are maintained at low particle concentration. In addition to the high salt concentration cores are made up in (core buffer), a typical transcription reaction introduces more salts. To circumvent this problem, transcription conditions were modified. Cores were dialysed in 100 mM Tris pH 8.0 to remove core buffer and the 200 mM HEPES pH 8.0 in 2X TRB was substituted for 100 mM Tris pH 8.0. Furthermore, pyruvate kinase and phosphoenol pyruvate were removed from the transcription mixture. T1L and T3D cores in core buffer or 100 mM Tris, pH 8.0 buffer underwent transcription in a typical transcription reaction or under modified conditions. Both non-transcribing and transcribing cores were

then digested with trypsin at 37°C and equal aliquots were removed over time. As opposed to virion digest products, core peptide products were concentrated by evaporating the solvent, then re-suspending the samples in a smaller volume of dH_2O.

2.12.4.2. MS and MS/MS analysis. Samples were analysed on a prototype MALDI QqTOF mass spectrometer built at the University of Manitoba in collaboration with MDS Sciex (Concord, ON). The MALDI QqTOF mass spectrometer consists of a matrix-assisted laser desorption/ionization (MALDI) source coupled to a tandem quadrupole/time-of-flight (QqTOF) mass spectrometer by means of a collisional damping interface. A schematic diagram of the MALDI-QqTOF is shown in Figure 6. A matrix solution of 160 mg/ml DHB (2,5-dihydroxybenzoic acid, Sigma) was prepared in a 1:1 mixture of acetonitrile and water. Next, a 1:1 ratio of sample and matrix solution was prepared and 0.5 µl was placed onto a gold target probe. The probe is placed about 4 mm from the entrance of the quadrupole ion guide q0. Single MS (mass spectrometry) spectra were acquired by irradiating the samples with a nitrogen laser (Laser Science Inc.) model 337 ND at a repetition rate of 7 Hz for time intervals around one minute uninterrupted. Argon was used as the cooling gas in Q0. Tandem mass spectra (MS/MS) were acquired at a laser repetition rate of 9 Hz. Selected ions were fragmented using argon as the collision gas. The collision energy was set by applying the accelerating voltage by the rule 0.5 V/Da and then adjusted manually to obtain desirable fragmentation of the parent ion. Spectra data acquisition and analysis was performed using software developed in-house (Tofma). Calibration of the mass spectrometer was based on the quadratic equation and was typically calculated using two known mass peaks. To identify the peptide fragments, the m/z of monoisotopic ions were

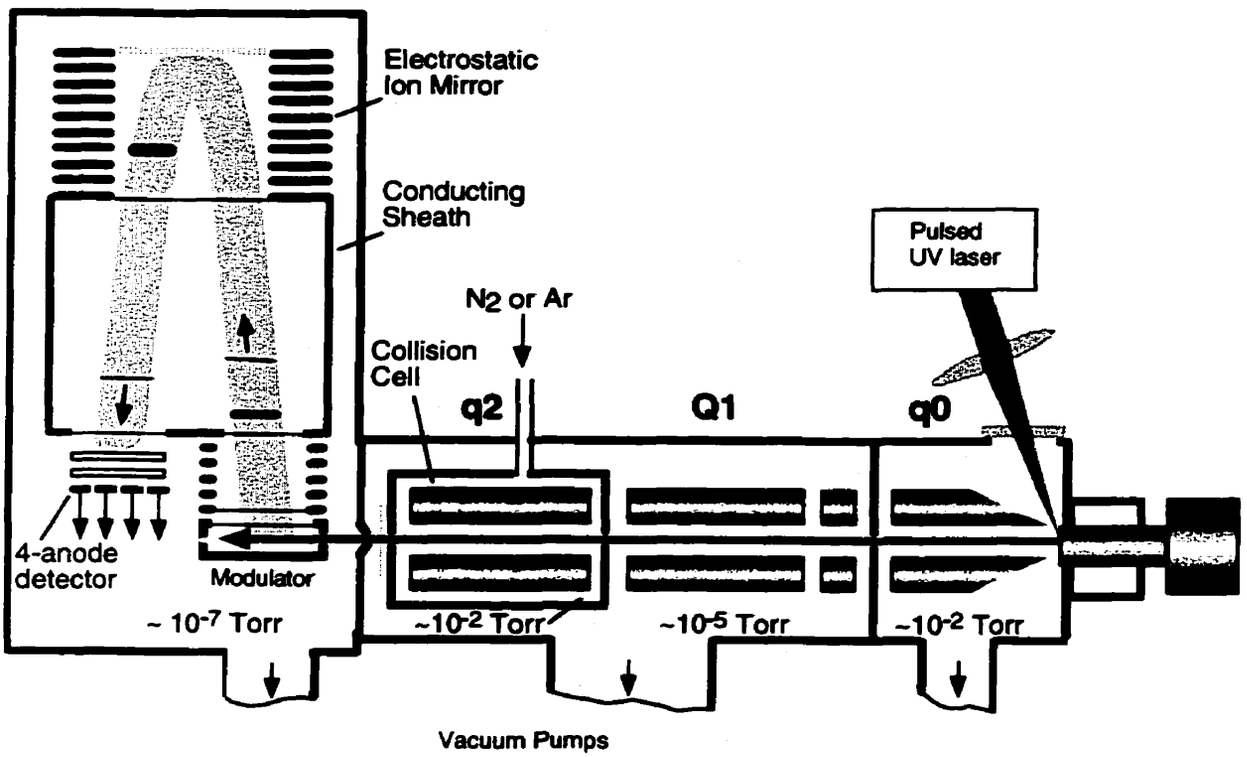
Electrostatic
Ion Mirror
Conducting
Sheath
Pulsed
UV laser
N2 or Ar
Collision
Cell
q2
Q1
q0
4-anode
detector
Modulator
~ 10-7 Torr
~10-2 Torr
~10-5 Torr
~10-2 Torr
Vacuum Pumps

Figure 6. A schematic cartoon of the MALDI QqTOF mass spectrometer (Shevchenko *et al.* 2000). The MALDI QqTOF mass spectrometer consists of a MALDI source coupled to a tandem quadrupole/time-of-flight (QqTOF) mass spectrometer by means of a collisional damping interface. A laser is pulsed at a repetition rate of 7Hz for single MS and 9Hz for tandem MS. The ions are cooled and accelerated through the quadrupoles. The ion beam is deflected and its time of flight is recorded once the beam hits the anode detector.

used to search databases using the computational program ProMac (Sciex, Concord, ON) or to search databases on the Internet by the MS-Tag and MS-Fit program (http://prospector.ucsf.edu/).

2.13. Statistical analyses. The nonparametric Wilcoxon rank sum test was used to determine the relative contribution of any single gene in reassortant mapping experiments (Hassard 1991). A minimum of two trials were carried out for all experiments. Where numerical values are obtained, the average was reported and the standard error of the mean calculated.

3. RESULTS

3.1. A comparative analysis of Freon substitutes in the purification of reovirus virions.

3.1.1. Comparison of organic solvents. Properties of an organic solvent are characterized by Hansen's three solubility parameters (D - dispersion energy, P - polar energy, and H - hydrogen bonding energy (Hansen & Beerbower 1971; Goldschmidt 1993)). The solubility parameters of Freon are shown in Table 1. In finding a replacement, solvents or solvent mixtures were selected that had solubility properties similar to those of Freon. Solvent mixtures were created by mixing two different solvents in various ratios. The resultant solubility parameters of the mixtures are theoretical values that were calculated manually and not emperically because of differential evaporation rates. Vertrel XF (1,1,1,2,3,4,4,5,5,5-decafluoropentane) is a Freon substitute developed by DuPont (Vertrel XF technical bulletin, 1999).

3.1.2. Purification of virions with Freon substitutes. Initially, hexane/1-chlorobutane (a 7:3 volume/volume mixture), isopentane/1-chlorobutane (7:3), toluene, and Vertrel® XF (Vertrel) were tested as suitable organic solvents. Other sets of solvents were also examined, either alone or in other mixture ratios, in case the proportion of the solvent in the mixture affected the results.

3.1.2.1. Purification of virions. To test the proposed solvents, basic viral purification procedures were performed with reovirus type 3 Dearing (T3D), as previously described for Freon extraction (Smith et al., 1969). Briefly, T3D-infected L929 cells were harvested, lysed with desoxycholate, and divided into equivalent aliquots. The samples then

Table 1. Solubility parameters of chosen solvents.

Solvent	Solubility Parameters					
	D[a]	P[a]	H[a]	MP[b] (°C)	BP[b] (°C)	Density[c] (g/cm^3)
Freon 113 (1,1,2-trichloro-1,2,2-trifluoroethane)	14.7	1.6	0.0	-36	48	1.56
Carbon tetrachloride	17.8	0.0	0.6	-23	77	1.59
1,2-dichloro-1,1,2,2-tetrafluoroethane	12.6	1.8	0.0	-94	4	> 1[d]
Hexane	14.9	0.0	0.0	-56	128	0.66
Isopentane	13.7	0.0	0.0	-56	30	0.62
1-chlorobutane	16.2	5.5	2.0	-123	78	0.89
Toluene	18.0	1.4	2.0	-95	110	0.87
Chloroform	17.8	3.1	5.7	-64	62	1.48
Isobutanol	15.1	5.7	15.9	-108	108	0.81
Vertrel® XF (1,1,1,2,3,4,4,5,5,5-decafluoropentane)	-[e]	-	-	-80	55	1.58
Hexane/1-chlorobutane (7:3)	15.3	1.7	0.6	-	-	0.73[f]
Isopentane/1-chlorobutane (7:3)	14.5	1.7	0.6	-	-	0.70[f]
Isopentane/1-chlorobutane (1:1)	15.0	2.8	1.0	-	-	0.76[f]
Chloroform/isobutanol (1:1)	16.5	4.4	10.8	-	-	1.15[f]

a: Hansen's solubility parameters where D = dispersion energy, P = polar energy, and H = hydrogen bonding energy (Barton, 1983).

b: MP, melting point; BP, boiling point (The Merck Index, 1983).

c: Density values of the liquid form at 24°C unless otherwise indicated by "d" (CRC Handbook, 1977).

d: Density of the gaseous form at room temperature.

e: Unknown.

f: Calculated and not emperically determined because of differential evaporation rates.

were emulsified with equal volumes of various solvents and centrifuged as previously described in Materials and Methods section 2.3.2. The location of the aqueous phase, which contains the virus, was dependent on the density of the organic solvents. Since Freon, Vertrel, chloroform, and chloroform/isobutanol (1:1) are denser than water, they produced a thick solid phase at the bottom of the tube which allowed for easy removal of the upper aqueous phase by pipetting. The other tested solvents and solvent mixtures formed a semi-solid phase above the aqueous phase whereas treatment with toluene resulted in a slurry consisting of a separation that yielded an extremely weak semi-solid phase on top. In such instances, extraction of the bottom aqueous phase required puncturing the solvent phase with a glass pipette, as plastic pipettes dissolved.

Gradient purification of Freon-extracted reovirus-infected cells resulted in two bands (indicated as V and T in Figure 8), which correspond to virus and *top component* respectively (Smith et al., 1969). Top component, or "empty virions", contain reduced to nil amounts of genomic material and may account for a large proportion of particles purified from infected cells (Smith *et al.*, 1969). With less genomic material, their densities will be less than full genome bearing virions and thus will not migrate as far as the denser virions. The derivation of these empty particles remains unknown. Most tested alternate solvents generated the same two bands (Figure 8). However, toluene-extracted samples consistently produced larger proportions of top component than of virus and treatment with chloroform/isobutanol (1:1) resulted in only a visible top component band. The resultant virus bands from each treatment appeared to be in the same regions of each gradient, and density measurements of each band, determined by refractive index measurements of appropriate gradient fractions, confirmed that all virus bands differed in density from each other by no more than 0.003g/ml. Similarly, all

Freon
Hexane/
1-Chlorobutane (7:3)
Isopentane/
1-Chlorobutane (7:3)
Toluene
Ventrel
Chloroform/
Isobutanol (1:1)
T
V

Figure 7. Buoyant density cesium chloride gradients of reovirus-infected cell lysates that had been extracted with the indicated solvents. Twice-extracted aqueous phases were layered onto 1.2-1.4g/ml cesium chloride gradients, centrifuged in a Beckman SW28 rotor at 25,000 rpm for 18 hours, and photographed. V = virions; T = top component. Three trials were carried out and the results shown are representative of all three.

top component bands differed from each other by no more than 0.002g/ml.

3.1.2.2. Confirmation of viral morphology.

3.1.2.2.1. Electron microscopic analysis of purified virions. To determine whether the method of extraction affected viral morphology, dialysed gradient-purified V and T band material were examined by negative stain transmission electron microscopy after drop method preparation as previously described in Materials and Methods section 2.9 (Hammond *et al.*, 1981; Hazelton & Coombs 1995). No difference was observed in the morphology of complete virions obtained by each of the purification methods (Figure 9). With the exception of chloroform/isobutanol (1:1) which did not yield a visible virus band from the T3D sample, complete virions comprised 95% of the particles in the virus fractions with all treatments. In each test, Freon and Vertrel treatments yielded equivalent apparent concentrations of virus, and much higher concentrations than hexane/1-chlorobutane (7:3), isopentane/1-chlorobutane (7:3), or toluene. Furthermore, the Freon and Vertrel treated purifications consistently contained little non-virion debris, while the remainder of the treatments contained comparatively large amounts (data not shown). Top component fractions were comprised primarily of genome deficient virions and outer shell structures, and complete virions consisted of only 10% or fewer of the particles observed for all treatments (Figure 9). As with the virus fractions, Freon and Vertrel treatments yielded equivalent amounts of particles with little cellular or viral debris, while hexane/chlorobutane (7:3), isopentane/chlorobutane (7:3), and toluene treatments yielded reduced quantities of top component and contained relatively larger levels of nonparticulate structures. Samples from other bands occasionally seen higher in some gradients were comprised primarily of debris,

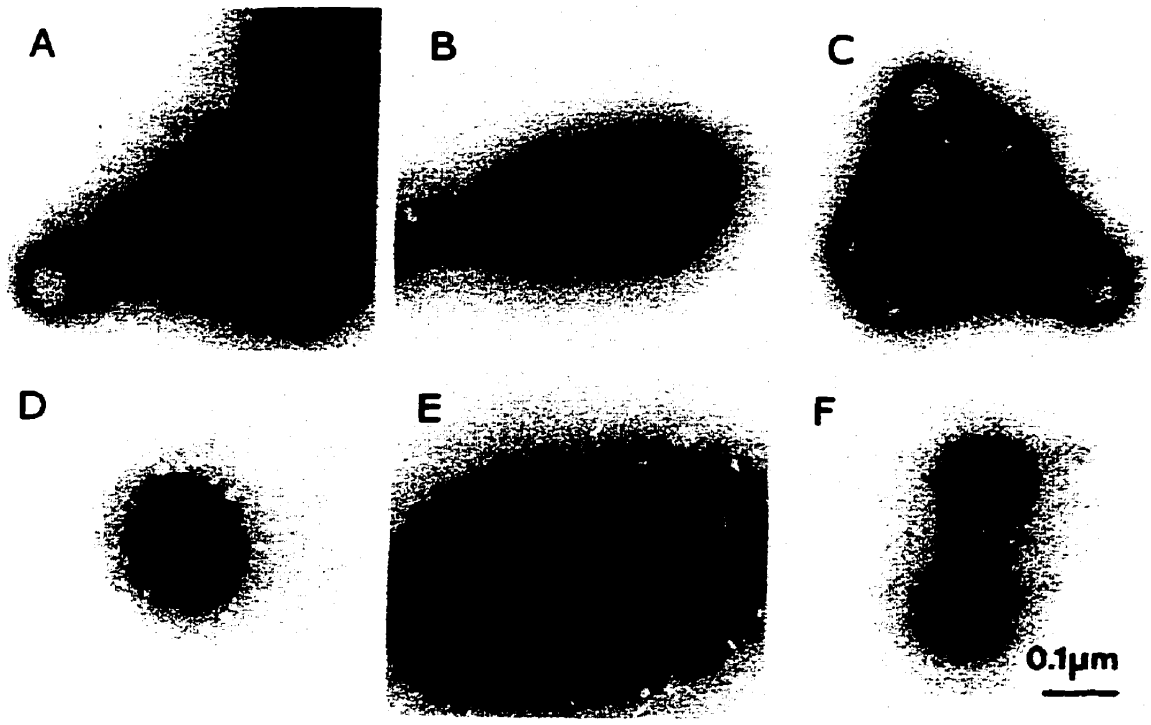
A
B
C
D
E
F
0.1µm

Figure 8. Morphology of gradient purified virion particles. Virus bands from gradients such as those depicted in Figure 8 were harvested, dialysed against dialysis buffer (150 mM NaCl, 15 mM $MgCl_2$, 10 mM Tris, pH 7.4) and aliquots diluted 100 fold with 0.1% glutaraldehyde in dialysis buffer to stabilize viral structures. Samples were mounted on 400-mesh formvar-coated copper grids by drop method, negatively stained with 1.2mM phosphotungstic acid, pH 7.0, and examined in a Philips model 201 transmission electron microscope as described (Hazelton & Coombs, 1995). A, Freon 113; B, Hexane/1-chlorobutane (7:3); C, Isopentane/1-chlorobutane (7:3); D, Toluene; E, Vertrel XF; F, Chloroform/Isobutanol (1:1). Bar represents 0.1μm.

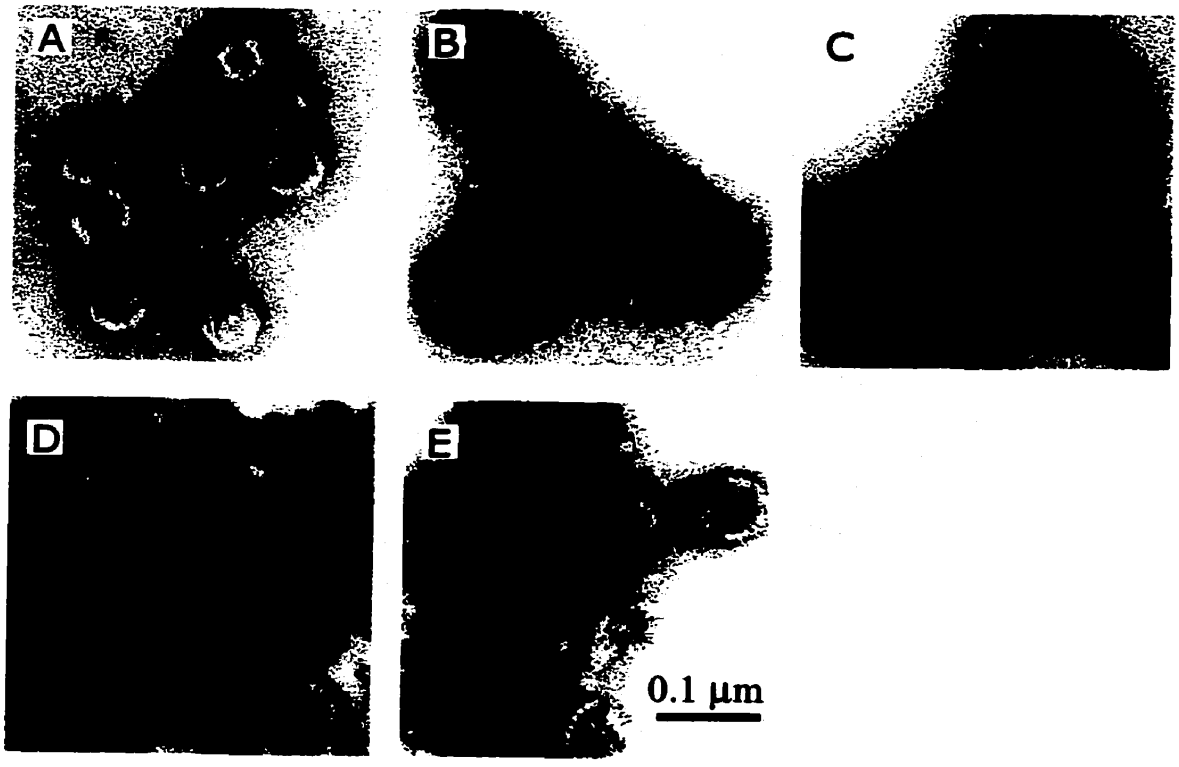
A
B
C
D
E
0.1 µm

Figure 9. Morphology of gradient purified top component particles. T bands from gradients such as those depicted in Figure 8 were harvested, dialysed against dialysis buffer (150 mM NaCl, 15 mM $MgCl_2$, 10 mM Tris, pH 7.4) and aliquots diluted 100 fold with 0.1% glutaraldehyde in dialysis buffer to stabilize viral structures. Samples were mounted on 400-mesh formvar-coated copper grids by drop method, negatively stained with 1.2mM phosphotungstic acid, pH 7.0, and examined in a Philips model 201 transmission electron microscope as described (Hazelton & Coombs, 1995). A, Freon 113; B, Hexane/1-chlorobutane (7:3); C, Isopentane/1-chlorobutane (7:3); D, Toluene; E, Vertrel XF. Bar represents 0.1μm.

with rare viral structures identified (data not shown). Similar experiments to those described above were also performed with type 1 Lang (T1L), another strain of reovirus. Results were similar to those described for T3D; however, chloroform/isobutanol (1:1) extraction and gradient purification revealed a faint virus band. Morphological examination showed few virus particles, and those observed appeared to have disrupted outer capsids (Figure 8F).

3.1.2.2.2. SDS-PAGE analysis of purified virions. To confirm the intactness of virus samples after various treatments, equivalent numbers of purified virions were dissolved in electrophoresis sample buffer and examined by SDS-PAGE as described in Materials and Methods section 2.6. With the exception of 1:1 chloroform:isobutanol treatment, resolution of genomic material in 10% SDS-PAGE from each of the treated samples revealed an equivalent amount of each of the 10 gene segments which indicates that none of the solvents had differential effects on the presence of genome (Figure 10). Even though equivalent amounts of virions as determined by UV spectroscopy were loaded, 1:1 chloroform:isobutanol treatment yielded very faint genomic bands (data not shown).

Viral proteins were resolved in 5-15% gradient SDS-PAGE and stained (Figure 11). The migration of the protein bands were not altered in any of the samples and there was no apparent difference in quantities of various proteins, supporting the morphologic evidence that the virions that were purified were unaffected structurally when compared to Freon treated samples. The hexane/1-chlorobutane (7:3) treated sample contained some contaminants near the bottom of the gel indicating that the purification was not as complete when compared to the other treatments.

3.1.2.3. Analysis of virions purified with Freon substitutes. As a more sensitive assay of the structural and functional integrity of each sample, virion specific

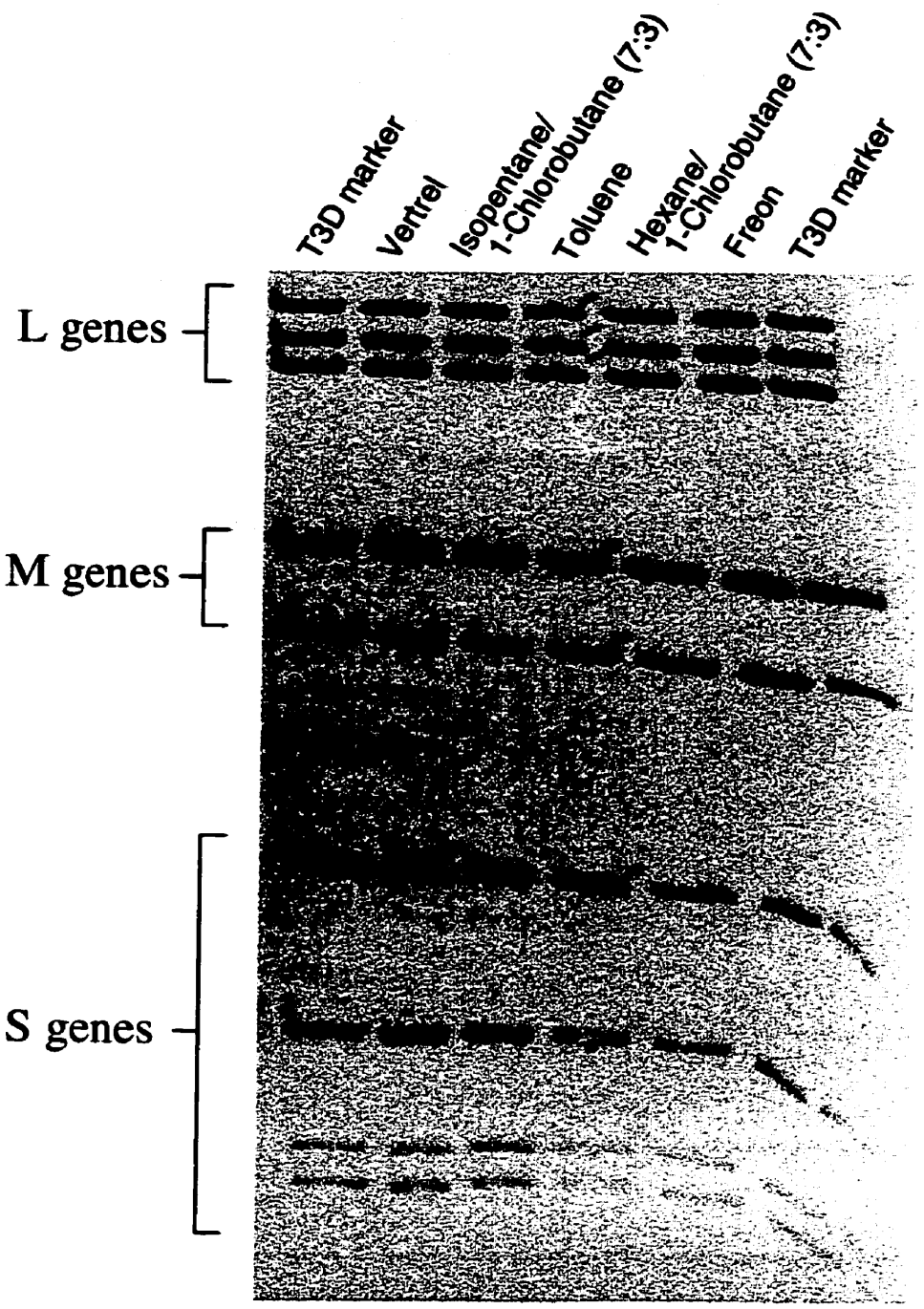
T3D marker
Vertrel
Isopentane/
1-Chlorobutane (7:3)
Toluene
Hexane/
1-Chlorobutane (7:3)
Freon
T3D marker
L genes
M genes
S genes

Figure 10. Electropherotype of virions purified with various solvents. Equal amounts of virus (harvested from gradients similar to those shown in Figure 8) were heated to 65°C for 5 minutes in electrophoresis sample buffer (0.24M Tris, pH6.8, 1.5% dithiothreitol, 1% SDS) and resolved in a 10% SDS-PAGE (16 x 16 x 0.1 cm) at 18 mA for 40 hours. The gel was then treated with 0.1% ethidium bromide, visualized under UV light using a Gel Doc 2000 (BioRad) apparatus. Solvent treatments are indicated above the lanes (with the exception of T3D marker; T3D virions previously purified with Freon). Locations of specific classes of reovirus genes are indicated on the left.

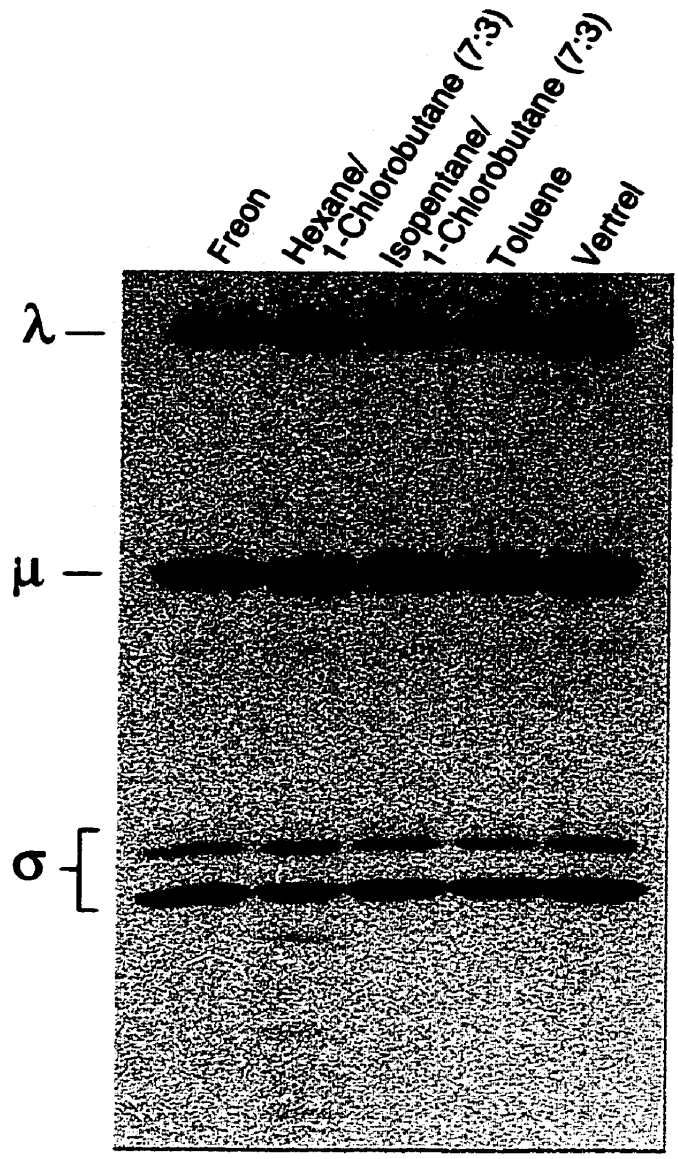
Freon
Hexane/
1-Chlorobutane (7:3)
Isopentane/
1-Chlorobutane (7:3)
Toluene
Ventrel
λ
μ
σ

Figure 11. Protein profile of virions purified with various solvents. Equal amounts of virus (harvested from gradients similar to those shown in Figure 8) were heated to 95°C for 5 minutes in electrophoresis sample buffer (0.24M Tris, pH6.8, 1.5% dithiothreitol, 1% SDS) and resolved on a 5-15% gradient SDS-PAGE (12 x 16 x 0.1 cm) at 5W for 4.2 hours. The gel was then fixed and stained with Coomassie Brilliant Blue R250. Solvent treatment are indicated above the lanes. Locations of specific classes of reovirus proteins are indicated on the left.

infectivities were also determined. Viral particle concentrations were determined by spectrophotometric analysis and virus titres were determined by plaque assay as described in Materials and Methods section 2.2.2 (Smith *et al.*, 1969; Coombs *et al.*, 1994). The total number of virus particles purified with each solvent was determined and compared to Freon (Table 2). Most extraction treatments resulted in recovery of fewer virus particles. Only extraction with Vertrel produced as much or more virus than extraction with Freon. Relative infectivity ratios were also determined by taking the ratio of particles/ml to PFUs/ml (Table 2). Only Vertrel and the isopentane/1-chlorobutane (7:3) solvent mixture had comparable ratios to that of Freon. Thus, treatment with other solvents led to both lesser amounts of virus and less infectious virus preparations. Similar results to those described above were also obtained when T1L was tested (data not shown). The above results have been published (Mendez *et al.*, 2000).

3.2. Use of temperature sensitive (*ts*) mutants to characterize capsid proteins.

*tsD*357 contains its *ts* mutation(s) in the L1 gene which encodes the 142-kDa minor core protein λ3, the RNA-dependent RNA polymerase (McCrae & Joklik, 1978; Ramig *et al.*, 1978). At non-permissive temperatures, *tsD*357-infected cells have been shown to produce viral particles devoid of any genomic material (Fields *et al.*, 1971). Furthermore, decreased amounts of ssRNA and protein (Cross & Fields 1972; Fields *et al.*, 1972) and less than 0.1% dsRNA (Cross & Fields 1972; Ito & Joklik 1972b) were found, all of which are suggestive of a defective polymerase. EOP profiles revealed that *tsD*357 virions appeared to be more stable than their wild-type parent T3D, as the *rate* of T3D viral titres dropped off sooner than *tsD*357 viral titres in response to increasing temperatures which suggests that *tsD*357 virions

Table 2. Summary of reovirus yield and specific infectivity for various solvent treatments.

Solvent	Relative total virus particles recovered[a] ± SEM[b] (%)	Specific infectivity (Particles/PFU[c]) ± SEM	Relative infectivity[d] ± SEM
Freon 113	100	176 ± 29	1.00
Hexane/1-chlorobutane (7:3)	56 ± 13	367 ±158	1.82 ± 0.43
Isopentane/1-chlorobutane (7:3)	77 ± 20	197 ± 64	1.24 ± 0.52
Toluene	58 ± 29	341 ±197	2.19 ± 1.58
Vertrel XF	163 ± 58	204 ± 21	1.19 ± 0.12

a: Determined by dividing the total number of virus particles recovered for each solvent in each replicate trial by the total amount of virus recovered after Freon extraction in the same trial. Values represent the averages of at least 3 experiments.

b: Standard error of the mean was calculated with a pooled estimate of error variance.

c: Plaque forming units determined from infectious titre.

d: Determined by dividing the specific infectivity of virus particles recovered for each solvent in each replicate trial by the specific infectivity of virus recovered after Freon extraction in the same trial. Values represent the averages of at least 3 experiments.

may have a certain level of thermal stability, despite having a *ts* characteristic. It is important to note that the *rate* of viral titre drop is not equal to the actual viral titres. Mutant *tsD*357's viral titres were still significantly lower than its wild-type parent T3D at non-permissive temperatures.

*tsG*453 contains three already identified point mutations in its S4 gene, one or all of which confer temperature sensitivity (Danis *et al.*, 1992; Shing & Coombs 1996). At the non-permissive temperature, *tsG*453 produces reduced amounts of protein and RNA (Cross & Fields 1972; Fields *et al.*, 1972; Danis *et al.*, 1992; Shing & Coombs 1996). Past experiments have also shown that at non-permissive temperatures, *tsG*453 infected cells fail to yield complete virions but instead produce large amounts of core-like particles (Morgan & Zweerink 1974; Danis *et al.*, 1992). It was concluded that outer capsid assembly required $\mu 1/\sigma 3$ interactions which were prevented by a misfolded $\sigma 3$ protein (Shing & Coombs 1996).

To be able to characterize these *ts* mutants first requires confirmation that a conditionally-lethal *ts* lesion exists in that particular gene. In order to confirm a *ts* lesion in a gene first requires the generation and identification of *ts* reassortants.

3.2.1. Identification of mammalian reovirus *ts* reassortants. Mixed infections between T1L and *tsD*357 and between T1L and *tsG*453 were carried out previously in the lab. T1L x *tsD*357 and T1L x *tsG*453 reassortants were identified by observing their electropherotype profiles in 10% SDS-PAGE as described in Materials and Methods section 2.6. Those clones that displayed genes from both parents were selected and amplified as described in Materials and Methods section 2.2.1. To test for temperature sensitivity, an EOP assay was carried out for each reassortant as described in Materials and Methods section 2.4. A *ts* mutant is defined as having an EOP value a minimum of one order of magnitude lower

than the wild-type virus EOP value. A non-*ts* mutant will typically have an EOP within one order of magnitude of the EOP value of wild-type. Due to random fluctuations, the EOP value of wild-type virus is usually 1 ± 10. EOP values of non-*ts* progeny virions can also fluctuate within an order of magnitude from their wild-type parent.

3.2.2. Reassortant mapping of *tsD*357 and *tsG*453. To confirm the gene segment that harbored the *ts* lesion in *tsD*357, reassortant mapping of *tsD*357 was performed. EOP assays were run in triplicate on different days (each initiated on a separate day) on all identified P_2 stocks of *tsD*357 x T1L reassortants. Progeny reassortants were divided into two separate panels: those that have the *ts* phenotype similar to mutant parent *tsD*357 and those that have the non-*ts* phenotype similar to wild-type parent T1L (Table 3). All progeny within their respective panel had an EOP value within one order of magnitude of the parent that falls within the range of that reassortant panel. The panel of reassortants that behaved like *tsD*357 all had their L1 gene come from *tsD*357, whereas the panel of reassortants that behaved like T1L all had their L1 gene come from T1L. There were no exceptions and all other genes were randomly distributed. This indicates that the *tsD*357 *ts* mutation or mutations resides in the L1 gene, with a probability of 0.05 (using the Wilcoxin rank sum test, (Hassard 1991)) which confirms previous mapping (Ramig *et al.*, 1978). The Wilcoxin prediction also indicate that the M2 gene may contain a lesion, with a probability of 0.05; however, the EOP value of the one exception, D21, is closer to wild-type parent T1L.

Repeated attempts by SDS-PAGE failed to resolve the S3 and S4 gene segments clearly in clone D36. It would have been helpful to know which parent these genes came from only if these genes were not already randomly distributed. However, as the genes are

randomly distributed, whichever parental S3 and S4 genes clone D36 contains has no bearing on the reassortant mapping results.

To confirm the gene segment that harbored the *ts* lesion in *tsG*453, reassortant mapping of *tsG*453 was performed. EOP assays were run in triplicate on different days (each initiated on a separate day) on all identified P_2 stocks of *tsG*453 x T1L reassortants. Progeny reassortants were divided into two clearly distinguishable panels: those that have the *ts* phenotype similar to mutant parent *tsG*453 and those that have the non-*ts* phenotype similar to wild-type parent T1L (Table 4). All progeny within their respective panel had an EOP value within 1.5 orders of magnitude of the wild-type parent whose EOP fell within the range of that reassortant panel. With the exception of clone LG113, the panel of reassortants that behaved like *tsG*453 all had their S4 gene come from *tsG*453. The panel of reassortants that behaved like T1L all had their S4 gene come from T1L. All other genes were randomly distributed which therefore indicates that the *tsG*453 *ts* mutation or mutations resides in the S4 gene, with a probability of 0.002, in agreement with past studies (Ramig *et al.*, 1978; Shing & Coombs 1996).

Occasionally, *ts* reassortants exhibit one or more anomalous gene segment migration patterns by SDS-PAGE. Viruses, especially RNA viruses, characteristically have an abnormally high mutation rate. Typical of all RNA viruses, including reovirus, spontaneous mutations may occur at a frequency of 1 in every 1000 bases during genomic replication and transcription. This is due to the fact that the viral polymerase, RNA-dependent RNA polymerase, lacks editing and proof-reading capabilities that prokaryotic and eukaryotic polymerases possess. There is no differentiation to whether mutations occur in conserved or non-conserved regions. However, mutations in non-conserved regions are more evident as

Table 3. Electropherotypes and EOPs of wild-type 1 Lang (T1L), tsD357, and T1L x tsD357 reassortants

Clone	Electropherotype[a]										EOP ± SEM[b]
	L1	L2	L3	M1	M2	M3	S1	S2	S3	S4	
T1L	**1**	1	1	1	1	1	1	1	1	1	0.585 ± 0.0932
tsD357	3	3	3	3	3	3	3	3	3	3	0.00424 ± 0.000860
D36	3	3	3	3	3	3	3	3	?	?	0.00109 ± 0.000110
D38	3	1	1	3	3	1	1	1	1	1	0.00201 ± 0.000710
D50	3	3	3	3	3	3	1	3	3	3	0.0142 ± 0.00445
D17	3	1	1	3	3	3	3	3	1	3	0.0101 ± 0.000995
D21	**1**	3	3	3	3	3	1	3	3	1	0.0760 ± 0.00205
D8	**1**	1	1	1	1	3	1	3	1	1	0.683 ± 0.0830
D52	**1**	3	1	1	1	3	1	1	3	3	0.781 ± 0.0405
D46	**1**	1	1	3	1	3	3	3	1	1	0.882 ± 0.102
D29	**1**	1	1	1	1	1	1	1	3	3	1.03 ± 0.155
Total exceptions	*0*	*5*	*3*	*2*	*1*	*5*	*3*	*4*	*4*	*3*	
Wilcoxin (p value)[c]											
0.05	+	-	-	-	+	-	-	-	-	-	

[a] Parental source for each gene: T1L = 1, tsD357 = 3

[b] Efficiency of plating determined by dividing viral titre at 39°C by viral titre at 33.5°C. Values represent the averages of at least two experiments ± standard error of the mean.

[c] The nonparametric Wilcoxon rank sum test was used to determine the relative contribution of any single gene in the reassortant map (Hassard 1991).

Table 4. Electropherotypes and EOPs of wild-type 1 Lang (T1L), tsG453, and T1L x tsG453 reassortants

Clone	Electropherotype[a]										EOP ± SEM[b]
	L1	L2	L3	M1	M2	M3	S1	S2	S3	S4	
T1L	1	1	1	1	1	1	1	1	1	1	0.514 ± 0.104
tsG453	3	3	3	3	3	3	3	3	3	3	0.000102 ± 0.0000216
LG 98	3	3	3	3	3	3	1	3	3	3	0.0000191 ± 0.0000113
LG 99	1	1	3	3	3	3	1	3	3	3	0.0000488 ± 0.0000357
LG 75	3	3	1	1	1	3	1	3	3	3	0.0000543 ± 0.0000384
LG 101	3	3	3	3	1	3	3	3	3	3	0.0000674 ± 0.0000297
LG 100	3	3	3	3	3	3	1	3	3	3	0.000122 ± 0.0000410
LG 118	1	3	3	3	3	3	3	3	3	3	0.000720 ± 0.000358
LG 113	3	3	1	3	1	1	1	1	1	1	0.00680 ± 0.00156
LG 122	1	3	3	3	3	1	1	1	1	1	0.215 ± 0.0938
LG 121	3	3	1	3	3	3	1	1	1	1	0.243 ± 0.148
LG 73	1	1	1	1	3	3	3	3	3	1	0.254 ± 0.113
LG 132	3	3	3	3	3	1	3	3	1	1	0.335 ± 0.168
LG 91	1	3	3	3	3	3	1	3	1	1	0.385 ± 0.0000500
LG 116	1	3	3	3	3	3	1	3	3	1	0.459 ± 0.0221
LG 126	1	1	1	3	1	3	1	1	1	1	0.490 ± 0.257
LG 74	3	3	1	3	3	3	3	3	3	1	0.537 ± 0.167
LG 112	3	3	3	3	3	3	1	1	3	1	0.573 ± 0.498
LG 96	1	1	1	1	1	3	1	3	1	1	0.575 ± 0.0675
Total exceptions	*6*	*9*	*7*	*9*	*12*	*9*	*9*	*7*	*5*	*1*	
Wilcoxin (p value)[c] 0.002	-	-	-	-	-	-	-	-	-	+	

[a] Parental source for each gene: T1L = 1, tsG453 = 3

[b] Efficiency of plating determined by dividing viral titre at 39°C by viral titre at 33.5°C. Values represent the averages of at least two experiments ± standard error of the mean.

[c] The nonparametric Wilcoxon rank sum test was used to determine the relative contribution of any single gene in the reassortant map (Hassard 1991).

mutations in conserved regions will usually have an adverse effect on the virus in which the mutation/virions would undergo negative selection. Mutations in non-conserved regions will usually have less of a detrimental effect. Furthermore, base changes within a gene have been shown to alter its molecular weight (Sharpe *et al.*, 1978). This may be the case for the observed S4 gene migration in LG113. Further tests with restriction endonucleases would confirm the parental origin of the gene. Regardless of the outcome, the reassortant map would not be affected.

3.2.3. Characterization of *tsD*357 and *tsG*453 virions and cores. To supplement what is currently known about *tsD*357 and *tsG*453, and to gain additional insight into how the protein affects function, *tsD*357 and *tsG*453 virions and cores were further characterized.

3.2.3.1. Heat-induced loss of infectivity of *tsD*357 and *tsG*453 virions. To measure the effect of heat on infectivity, purified T1L, T3D, *tsD*357 and *tsG*453 virions (all grown at permissive temperatures), generated as described in Materials and Methods section 2.3, were pre-heated at 50°C and 55°C for various periods of time and then immediately cooled on ice. L929 cell monolayers were infected with serial 1:10 dilutions of pre-heated virions and incubated at permissive temperatures as described in Materials and Methods section 2.2.2. Viral titres were determined and plotted against incubation times of pre-heating. Little difference in viral titres were observed in virions pre-heated at 50°C for up to 30 minutes (Figure 12A); however, a large difference was observed in virions pre-heated at 55°C (Figure 12B). Mutant *tsD*357 and T3D virions pre-heated for up to 30 minutes showed a negligible decrease in viral titres. On the other hand, *tsG*453 showed a dramatic drop of over 5 orders of magnitude when pre-heated at 55°C for 5 minutes. T1L viral titres decreased by one order of magnitude after 15 minutes of pre-heating, and by a further three

orders of magnitude after 30 minutes of pre-heating. These results suggest that *tsG*453 virions are sensitive to heat-induced loss of infectivity whereas *tsD*357 virions are not.

3.2.3.2. Heat-induced loss of transcriptase activity of *tsD*357 and *tsG*453 cores. To measure the effect of heat on transcriptase activity, purified T1L, T3D, *tsD*357 and *tsG*453 cores, generated as described in Materials and Methods section 2.7, were pre-heated at temperatures ranging from 50°C to 70°C for 15 minutes and then immediately cooled on ice. Pre-heated cores were then allowed to transcribe for one hour at 50°C as described in Materials and Methods section 2.8. The transcriptase activity of pre-heated cores was calculated as a percentage of the transcriptase activity of non-heated cores and plotted against different incubation temperatures (Figure 13). *tsD*357 pre-heated cores are more resistant to heat-induced loss of transcriptase activity than wild type parent T3D. This is largely noticeable at an incubation temperature of 60°C where *tsD*357 cores retained over 70% of its transcriptase activity whereas T3D retained less than 40% of its transcriptase activity. On the other hand, *tsG*453 lost 75% of its transcriptase capabilities after being pre-heated at 55°C whereas *tsD*357 and T3D lost less than 30% of their transcriptase activity. This indicates that *tsG*453 cores are more sensitive to heat-induced loss of transcriptase ability than T3D whereas *tsD*357 is more resistant.

3.2.3.3. Virion and core electron microscopic analyses of T3D, *tsD*357 and *tsG*453. To determine whether loss of infectivity or transcriptase activity is a function of structural damage to the capsid, equivalent numbers of pre-heated virions and cores, treated as described above, were visualized by negative stain transmission electron microscopy as described in Materials and Methods section 2.9.

A.

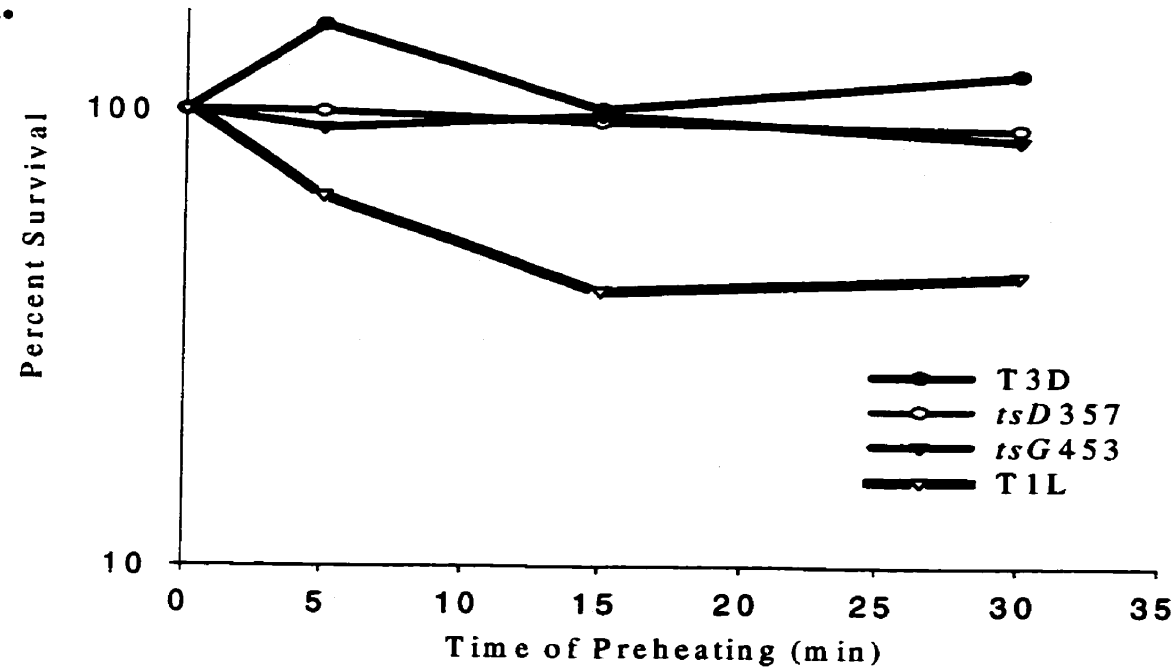
Percent Survival
100
10
0
5
10
15
20
25
30
35
Time of Preheating (min)
T3D
tsD357
tsG453
T1L

B.

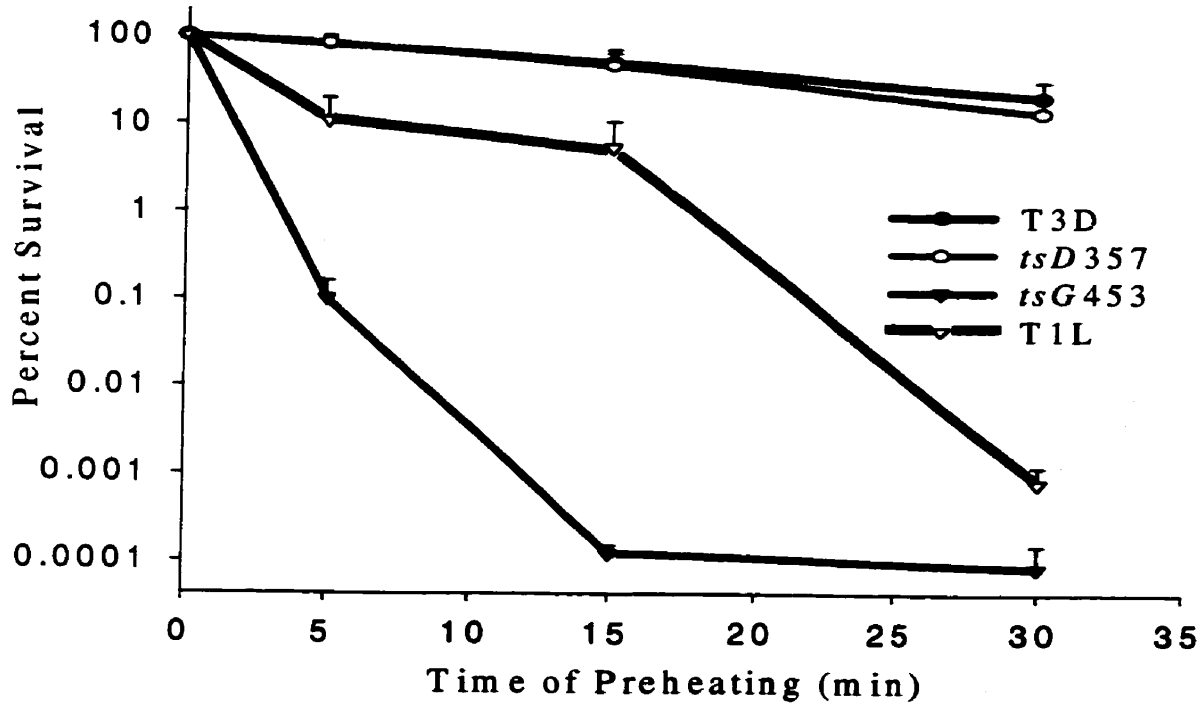
Percent Survival
100
10
1
0.1
0.01
0.001
0.0001
0
5
10
15
20
25
30
35
Time of Preheating (min)
T3D
tsD357
tsG453
T1L

Figure 12. Effects of preheating virions on their infectivity. Purified virions from T1L, T3D, *tsD*357 and *tsG*453 were preheated at 50°C (A) and at 55°C (B) for the various times indicated followed by immediate cooling on ice. Serial dilutions of preheated and non-preheated virions were used to infect L929 cell monolayers and incubated at permissive temperature. The percent survival was determined by dividing the titre of preheated virions by the titre of non-preheated virions multiplied by 100. Error bars shown represent the standard error of the mean from three separate trials done on different days.

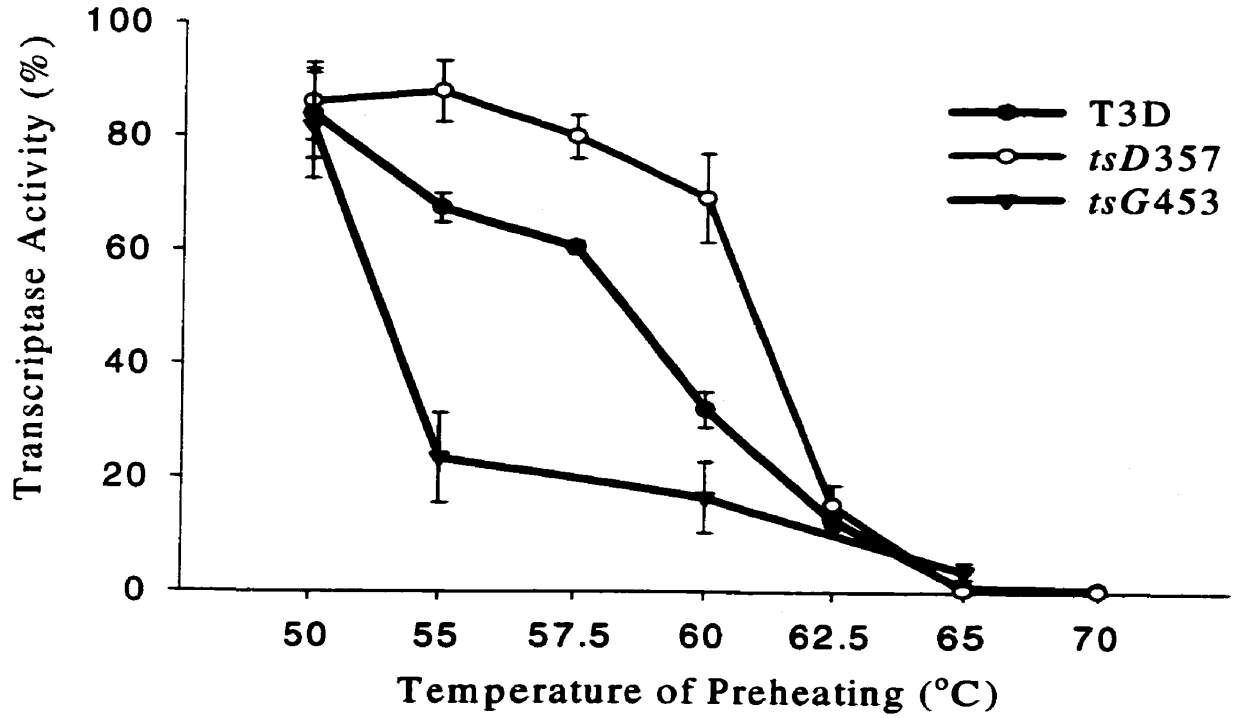
100
80
60
40
20
0
Transcriptase Activity (%)
50
55
57.5
60
62.5
65
70
Temperature of Preheating (°C)
T3D
tsD357
tsG453

Figure 13. Effects of preheating cores on their transcriptase activity. Purified cores from T3D, *tsD*357 and *tsG*453 were preheated at various indicated temperatures for 15 minutes followed by immediate cooling on ice. Preheated and non-preheated cores were then allowed to transcribe for one hour at 50°C. The amount of acid precipitated radio-labelled transcripts were used as a measure of transcriptase activity. The percent transcriptase activity was determined by dividing transcriptase activity of preheated cores by the transcriptase activity of non-preheated cores multiplied by 100. Error bars shown represent the standard error of the mean from five separate trials done on different days.

Examination of T3D and *tsD*357 virion samples pre-heated at 55°C for 15 minutes revealed >95% intact virions (Figure 14). Examination of *tsG*453 virions pre-heated at 55°C for 15 minutes did not yield the same results. Instead, 75% of the particles observed appeared to be virions with an outer capsid loosely connected but not completely disassociated. The other 25% of particles consisted of cores. This suggests that the loss of infectivity observed in *tsG*453 when pre-heated is a result of structural damage to the outer capsid.

Examination of *tsD*357 and *tsG*453 core samples pre-heated at 60°C for 15 minutes revealed >90% intact cores with spikes (Figure 14). Examination of T3D cores revealed intact cores as well, however about 75% of them formed aggregates and may have lost some genomic material. These aggregates were not observed in *tsD*357 and *tsG*453 core samples. A decrease in T3D transcriptase ability may be the result of interference from clumping, as the percentage of clumping is roughly similar to the percentage of loss of transcriptase activity. No structural changes appear evident in cores which suggests that the phenotypic differences observed are not a function of core structural disruption, but instead are a function of something less dramatic and perhaps internal in the core.

3.2.4. Reassortant mapping of phenotypic differences from *tsD*357 and *tsG*453. Reassortants were exploited to determine which gene or genes were responsible for the detected phenotypic differences.

Mutant *tsG*453 virions are more sensitive to heat-induced loss of infectivity than wild-type parent T3D. To map this phenotypic difference, selected representative T1L x *tsG*453 reassortants were amplified and purified as discussed in Materials and Methods section 2.3. Purified reassortant virions were then pre-heated at 55°C or left untreated, serial diluted 1:10, and used to infect L929 cell culture to determine viral titres as described in Materials and

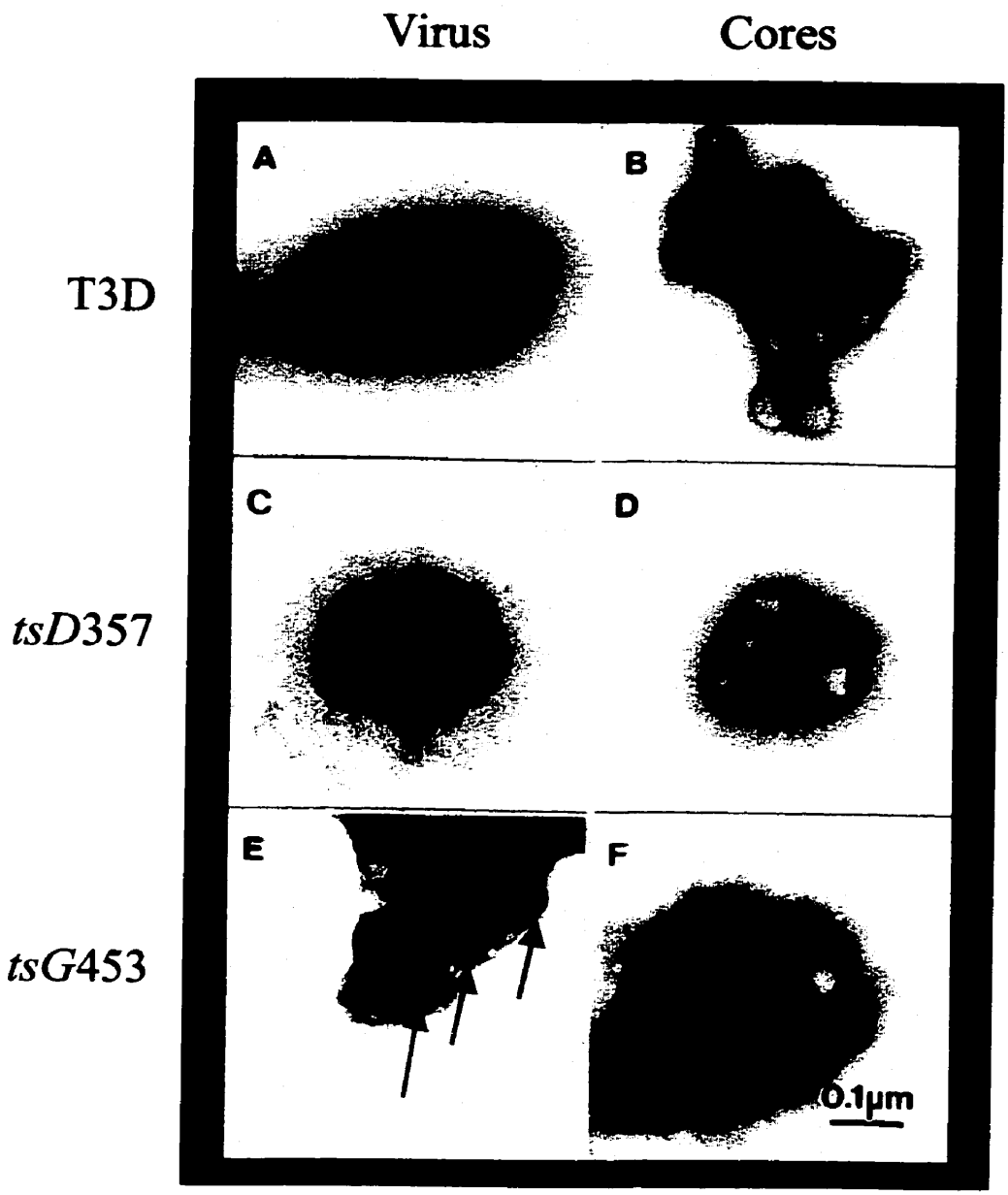
Virus
Cores
T3D
tsD357
tsG453
A
B
C
D
E
F
0.1μm

Figure 14. Electron micrographs of preheated virions and cores. Samples of purified virions (grown at the permissive temperature) or cores from T3D, *tsD*357 and *tsG*453 were preheated at 55°C (virions) or 60°C (cores) for 15 minutes followed by immediate cooling on ice. Samples were then mounted on 400-mesh formvar-coated copper grids by drop method, negatively stained with 1.2mM phosphotungstic acid, pH 7.0, and examined in a Philips model 201 transmission electron microscope as described (Hazelton & Coombs, 1995). Non-preheated samples served as control (not shown: virions appeared as in (A) and cores appeared as in (B) in morphology). A. T3D virions; B. T3D cores; C. *tsD*357 virions; D. *tsD*357 cores; E. *tsG*453 virions; F, *tsG*453 cores. Bar represents 0.1μm. Arrows indicate loosely associated outer capsid.

Methods section 2.2.2. Each reassortant's percent survival was calculated by dividing the titres from pre-heated samples by the titres of untreated samples. A minimum of two trials were carried out for each clone. Clones, including parent T1L, that exhibited a percent survival above 0.01 were placed into one panel, while those, including parent *tsG*453, that had a much lower percent survival were organized in a separate panel (Table 5). All of the genes are randomly distributed with the exception of the S4 gene. Without exception, the group with a percent survival above 0.01 had its S4 gene come from parent T1L, whereas the group with the lower percent survival had its S4 gene come from parent *tsG*453. These results suggest that the S4 gene is responsible for the phenotypic difference observed in *tsG*453, with a probability of 0.002.

Mutant *tsD*357 displayed higher tolerance to heat-induced loss of transcriptase activity than its wild type parent T3D, as discussed above. T1L x *tsD*357 reassortants were amplified and purified as discussed in Materials and Methods section 2.3. Sometimes, reassortants had to be passaged an extra time to achieve sufficiently high titres. Once a high concentration of purified virions was attained, they were converted to cores as described in Materials and Methods section 2.7. Purified reassortant core particles were then pre-heated at 60°C for 15 minutes and allowed to transcribe under identical conditions described in section 3.2.3.2. Non-preheated reassortant cores served as a control. An incubation temperature of 60°C was chosen as the phenotypic difference observed between *tsD*357 and T3D cores was highest at this temperature (see Figure 13). Trials were done at least three times and on different days to ensure statistical significance.

The percent of transcriptase activity reduction after heating when compared to non-heated samples was calculated (Figure 15). Reassortants can be divided into two

Table 5. Electropherotypes and percent survival of wild-type 1 Lang (T1L), tsG453, and T1L x tsG453 reassortants when pre-heated at 55°C

Clone	Electropherotype[a]										Percent Survival ± SEM[b]
	L1	L2	L3	M1	M2	M3	S1	S2	S3	S4	
T1L	1	1	1	1	1	1	1	1	1	1	19.4 ± 19.3
tsG453	3	3	3	3	3	3	3	3	3	3	0.000111 ± 0.000102
LG 75	3	3	1	1	1	3	1	3	3	3	0.0000549 ± 0.0000368
LG 118	1	3	3	3	3	3	3	3	3	3	0.0000726 ± 0.0000524
LG 101	3	3	3	3	1	3	3	3	3	3	0.000246 ± 0.000165
LG 45	1	3	3	3	3	3	3	1	3	3	0.000233 ± 0.000229
LG 38	3	3	3	3	3	3	1	3	3	3	0.000421 ± 0.000217
LG 122	1	3	3	3	3	1	1	1	1	1	0.0165 ± 0.0165
LG 66	3	3	3	3	1	3	3	3	3	1	0.626 ± 0.624
LG 23	1	3	1	3	1	3	3	3	3	1	3.57 ± 3.56
LG 91	1	3	3	3	3	3	1	3	1	1	5.84 ± 5.66
LG 112	3	3	3	3	3	3	1	1	3	1	7.48 ± 7.42
LG 96	1	1	1	1	1	3	1	3	1	1	10.5 ± 7.41
Total exceptions	*4*	*5*	*5*	*6*	*5*	*5*	*4*	*5*	*3*	*0*	
Wilcoxin (p value)[c]											
0.002	-	-	-	-	-	-	-	-	-	+	

[a] Parental source for each gene: T1L = 1, tsG453 = 3

[b] Percent survial determined by dividing titre of unheated virus by titre of virus pre-heated at 55°C x 100%. Values represent the averages of at least two experiments ± standard error of the mean.

[c] The nonparametric Wilcoxon rank sum test was used to determine the relative contribution of any single gene in the reassortant map (Hassard 1991).

non-overlapping groups: one group, which includes the parent *tsD*357, shows less than 40% transcriptase reduction whereas the other group, which contains the parent T1L, shows a greater than 55% reduction. All of the genes are randomly distributed with the exception of the L1 gene. The thermal-stable group all obtained their L1 gene from the *tsD*357 parent whereas the thermal-sensitive group derived their L1 gene from T1L. These results suggest that the L1 gene, with a probability of 0.02, is responsible for the phenotypic difference observed in *tsD*357. A probability of 0.05 was calculated for the S4 gene but it is unlikely to be the gene phenotypically responsible as it encodes a protein not present in the cores. However, as will be discussed below, the possibility that the S4 gene may play a secondary role can not be ignored.

Purified *tsG*453 cores, which lack σ3, transcribe less efficiently than their T3D parent. This observation suggests a previously unknown function of the S4 gene in transcription, or previously undetected lesions in another gene in this mutant. To map this paradoxical phenomenon, purified T1L x *tsG*453 reassortants were examined.

Representative T1L x *tsG*453 purified virions were converted to cores as described in Materials and Methods section 2.7. Purified reassortant core particles were then pre-heated at 55°C for 15 minutes and allowed to transcribe under identical conditions as described in section 3.2.3.2. Non-preheated reassortant cores served as a control. The transcriptase activity of pre-heated cores was calculated as a percentage of the transcriptase activity of non-heated cores. Reassortants were grouped into two panels: those that retained over 80% of their transcriptase activity (Figure 16: shaded in red and green) and those that retained less than 80% of their transcriptase activity (Figure 16: shaded in grey). This phenotypic difference mapped to three genes, S3 and S4 which encode non-core proteins and

A.

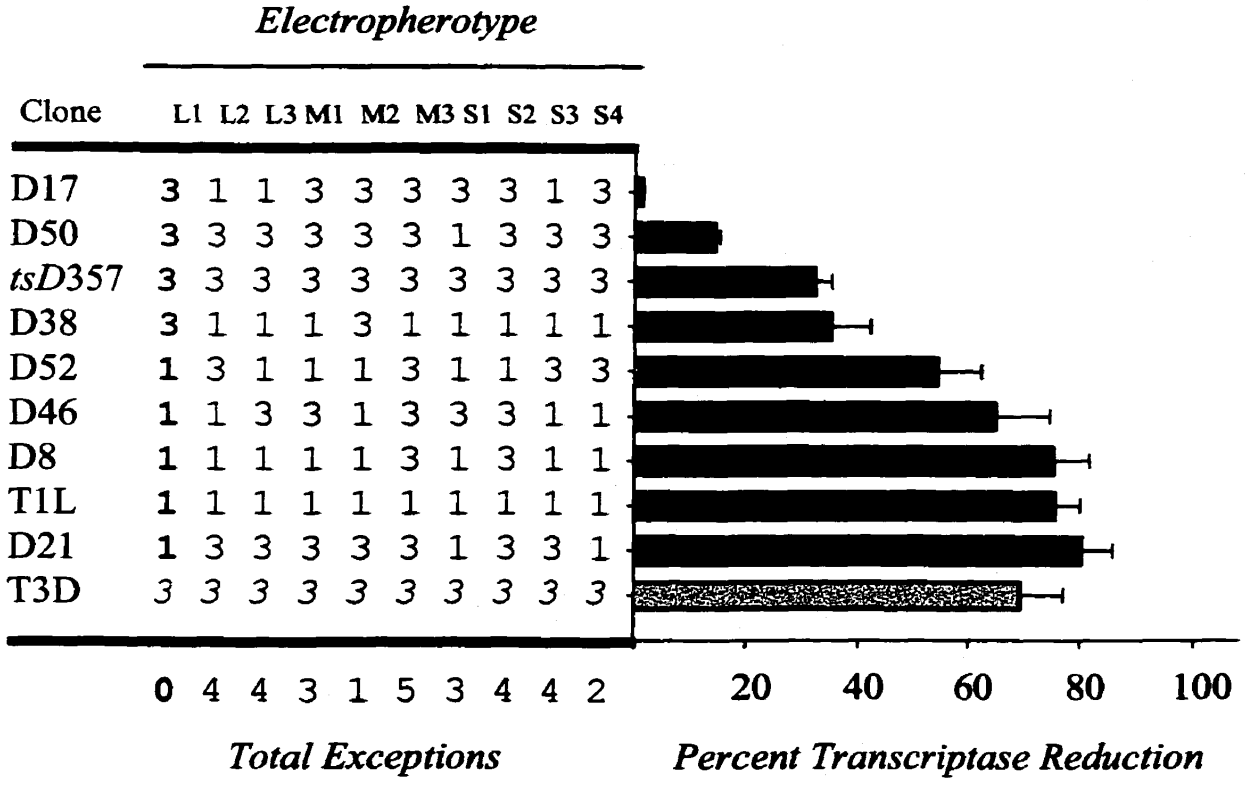

B.

Wilcoxin (P value)	L1	L2	L3	M1	M2	M3	S1	S2	S3	S4
p = 0.05	+	-	-	-	-	-	-	-	-	+
p = 0.02	+	-	-	-	-	-	-	-	-	-

Figure 15. Electropherotypes and percent transcriptase reduction of T1L, *tsD*357 and T1L x *tsD*357 reassortants. Purified T1L x *tsD*357 reassortant core particles were pre-heated at 60°C for 15 minutes and allowed to transcribe for one hour at 50°C. Non-preheated samples were used as control. **A.** The percent transcriptase reduction was calculated by dividing the transcriptase activity of preheated samples by the the transcriptase activity of non-preheated samples, then taking this value and subtracting it from 100. Error bars represent the standard error of the mean from a minimum of three trials executed on different days. The reassortants, and their corresponding electropherotypes, were then sorted by increasing percent transcriptase reduction. T3D was included for sake of comparison and was not involved in the sorting of the reassortants. **B.** The nonparametric Wilcoxon rank sum test was used to determine the relative contribution of any single gene in the reassortant map (Hassard 1991). T3D was omitted from these calculations.

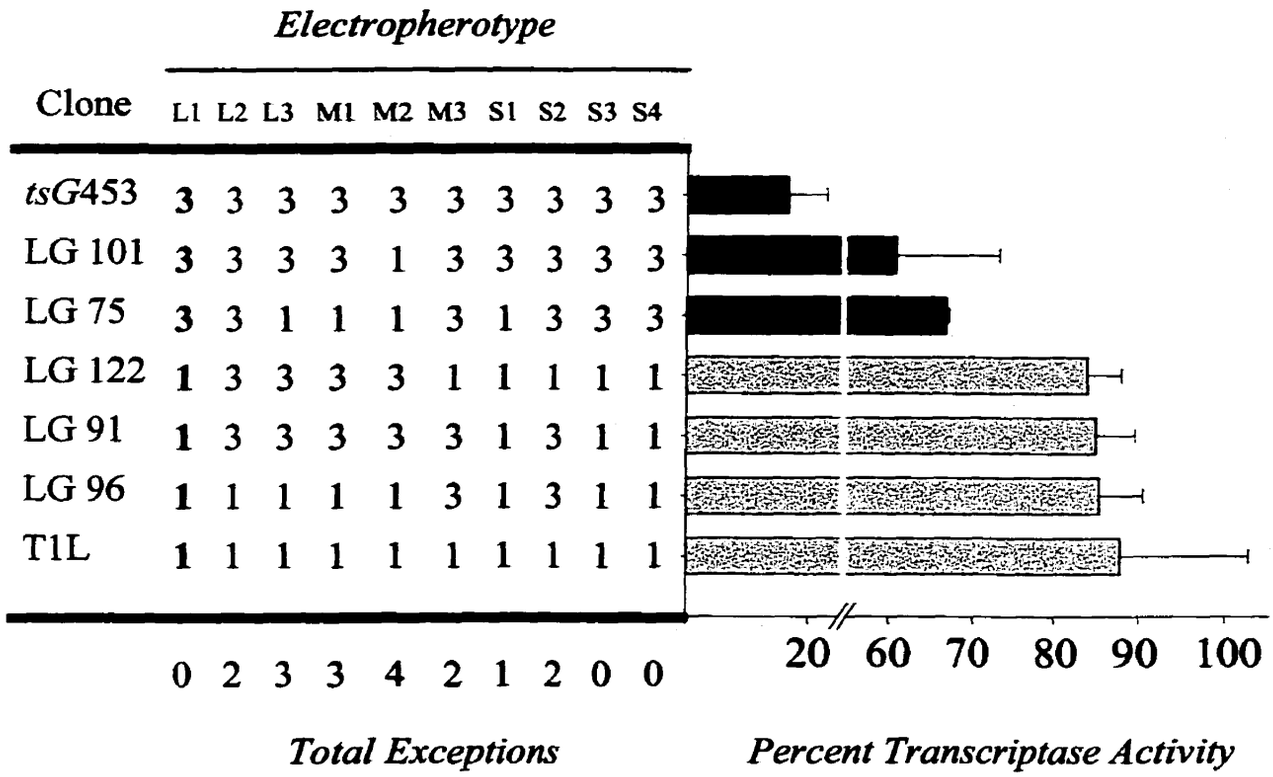
Electropherotype
Clone
L1 L2 L3 M1 M2 M3 S1 S2 S3 S4
tsG453 3 3 3 3 3 3 3 3 3 3
LG 101 3 3 3 3 1 3 3 3 3 3
LG 75 3 3 1 1 1 3 1 3 3 3
LG 122 1 3 3 3 3 1 1 1 1 1
LG 91 1 3 3 3 3 3 1 3 1 1
LG 96 1 1 1 1 1 3 1 3 1 1
T1L 1 1 1 1 1 1 1 1 1 1
0 2 3 3 4 2 1 2 0 0
Total Exceptions
20 60 70 80 90 100
Percent Transcriptase Activity

Figure 16. Electropherotypes and percent transcriptase reduction of T1L, *tsG*453 and T1L x *tsG*453 reassortants. Purified T1L x *tsG*453 reassortant core particles were pre-heated at 55°C for 15 minutes and allowed to transcribe for one hour at 50°C. Non-preheated samples were used as control. The percent transcriptase activity was calculated by dividing the transcriptase activity of preheated samples by the the transcriptase activity of non-preheated samples. Error bars represent the standard error of the mean from a minimum of three trials performed on different days. The reassortants, and their corresponding electropherotypes, were then sorted by increasing percent transcriptase activity.

L1 which, as stated earlier, encodes the minor core protein λ3. These results suggest that either one or more of these genes is responsible for the phenotypic difference observed in *tsG*453. It is important to note that of the reassortants that were in the same group as parent *tsG*453, their percent transcriptase activity was significantly higher than that of *tsG*453 (see Figure 16; reassortants shaded in green). This may suggest interference from secondary genes, possibly one or more of the L1, S3 and S4 genes there display no exceptions in the reassortant map. Whether these genes act alone or in concert can be determined if the panel of reassortants is expanded. Probabilities were not calculated due to the small size of the data set.

3.2.5. Analysis of the L1 gene sequence of *tsD*357.

3.2.5.1. Identification of *tsD*357 mutations. Results indicate that the L1 gene is phenotypically responsible for the thermal stability displayed by *tsD*357. To add supportive evidence to whether the temperature lesion affected the morphological nature of the protein requires the genomic sequence be known. The L1 gene segments from *tsD*357 and T3D were sequenced twice in either direction with regions of mutation sequenced at least three times as described in Materials and Methods section 2.10, and the resulting protein primary structures determined.

The T3D laboratory strain had few L1 gene sequence changes compared to the T3D strain L1 sequence reported in GenBank (accession number # M31058; Wiener & Joklik 1989). *tsD*357 was found to have three nucleotide base changes from laboratory sequenced T3D: a transversion at base number 1214 where thymine was replaced with guanine, a transition at base number 2967 where an adenine was replaced with a guanine, and a transition at base number 3161 where an adenine was replaced with a guanine (Table 6). The

second nucleotide base change is a silent mutation and no change in amino acid occurs. However, The first and the third nucleotide base changes result in the following T3D to *tsD*357 amino acid changes respectively: $isoleucine_{399}$ to $serine_{399}$, and $asparagine_{1048}$ to $serine_{1048}$.

Hydropathy is defined as a measure of attraction toward water, with positive being hydrophilic and negative being hydrophobic. All amino acids, based on their water-vapor transfer free energies and polarity, are assigned a relative hydropathy index value. Based on the hydropathy index of amino acids (Kyte & Doolittle 1982), the amino acid change at codon number 399 results in a decrease from 4.5 to -0.8 whereas the amino acid change at codon number 1048 results in an increase from -3.5 to -0.8.

Amino acids 399 and 983 are conserved among the three predominant reovirus strains (T1L, T2J, and T3D) while amino acid 1048 is not (Wiener & Joklik 1989). This suggests that amino acids 399 and 983 play important roles, more so than the non-conserved amino acid 1048. Amino acid 399 changed in *tsD*357 and seems to be the more relevant of the three changes; therefore it may be the amino acid responsible for a morphological change in the protein that results in the phenotypic difference.

3.2.5.2. Prediction of protein secondary structure. To assess any morphological change that may have occurred as a result of the amino acid changes in *tsD*357, the protein secondary structure was analysed. The predicted protein secondary structure was calculated using various computer prediction programs: PSIPRED (version 2.0; Uxbridge, UK), SSpro 2 Prediction (http://promoter.ics.uci.edu/BRNN-PRED/), PredictProtein (Columbia University, New York, NY), Protean (DNASTAR Inc., Madison WI)(Protean is a collection of several independent prediction algorithms), and DrawHCA

(http://www.lmcp.jussieu.fr/~soyer/www-hca/hca-form.html). Only three of the seven programs predict a minor insignificant change at amino acid 1048 whereas, the other four predicted no changes at all. However, six of the seven programs did predict a major structural change at amino acid 399 (AA^{399}) (Figure 17 and 18).

PredictProtein is a program that relies more heavily on prediction through other related known secondary structure sequence comparisons. The program was unable to find other related sequences; hence, it predicted no structural change to occur at AA^{399}. Protean, based on the Garnier-Robson algorithm whose method relies on statistics (Garnier *et al.*, 1978), predicted a change from a strand-turn to a strand-coil-turn within the area immediately surrounding AA^{399} (Figure 17). SS Pro and PSIPRED both predicted a strand to a coil morphological change as well (Figure 17). SS Pro reports an accuracy output of 78% but does not report individual confidence levels per amino acid. PSIPRED reports an accuracy output of 68% based on a single sequence and reports confidence levels per amino acid ranging from 1=low to 9=high. PSIPRED predicts a confidence level at AA^{399} of seven in T3D and of eight in *tsD*357.

The hydophilicity and hydrophobicity of the area surrounding AA^{399} was also measured. A hydophilicity plot was generated based on the Kyte-Doolittle system (Protean)(Kyte & Doolittle 1982). This method predicts regional hydropathy of proteins from their determined amino acid sequences. Known hydropathy values are assigned for all amino acids in the sequence and are then averaged over a user defined window. A value of nine residues to average was selected, as anything less than seven will display too much noise and anything above 11 will generally miss small hydropathic regions. The hydrophilicity plot shows a substantial increase in hydophilicity in the region surrounding AA^{399} (Figure 18). To

Table 6. Details of identified mutations in *tsD*357's L1 gene[a].

Base number	AA[b] number	Type of mutation	Codon change	AA change	Polarity change[c]
1214	399	transversion	ATT to AGT	I[d] to S[d]	-5.3 (+4.5 to -0.8)
2967	983	transition	GAA to GAG	E[d] to E	0
3161	1048	transition	AAC to AGC	N[d] to S	+2.7 (-3.5 to -0.8)

a: The sequence was obtained from GenBank (Accession # M31058) and corrected (Wiener & Joklik 1989)

b: AA = amino acid

c: Based on the hydropathy index of amino acids (Kyte & Doolittle 1982)

d: I = isoleucine; S = serine; E = glutamic acid; and N = asparagine

validate the strength of the prediction, the residues to average was changed from a range between seven to eleven and in all cases, the end result did not change (data not shown).

The hydrophobic nature of the region surrounding AA^{399} was measured through a hydrophobic cluster array (HCA) using the program HCADraw. This program, based on the hydrophobic values of an amino acid, will construct a 2-dimensional representation of the protein sequence, highlighting areas of hydrophobic clusters (Gaboriaud *et al.*, 1987). The HCA plot of T3D and *tsD*357 depicts a drop in hydrophobicity at AA^{399} when isoleucine (T3D) is changed to serine (*tsD*357) (Figure 18).

One further measure of the morphological change about AA^{399} involved an algorithm that measures the antigenic index (a maximum value of ±1.7) for one or more residues. The Jameson-Wolf algorithm (Protean) predicts antigenic determinants from an amino acid sequence based on hydophilicity values, surface probabilities, backbone chain flexibility, secondary structure prediction, and solvent accessibility factors (Jameson & Wolf 1988). This antigenic index increases substantially when isoleucine at AA^{399} in T3D is changed to a serine in *tsD*357 (Figure 18).

With the exception of one, the seven different algorithms applied all predict a similar structural change at AA^{399} providing strong collective evidence that the protein does undergo a morphological shift which may be responsible for the phenotypic difference observed in *tsD*357.

3.3. Structural orientation of viral capsid proteins.

Recent developments in mass spectrometry have made it an invaluable tool to characterise proteins, in particular viral proteins (Carneiro *et al.*, 2001; Loboda *et al.*, 2000;

	T3D	*tsD357*
PSIPRED → *confidence level*	coil – strand – coil (7/9)	coil – coil – coil (8/9)
		
SS PRO Prediction → *confidence level not reported*	coil – strand – coil	coil – coil – coil
		
Protean →	strand – turn	strand – coil - turn
		

PredictProtein → *no structural change predicted*

Figure 17. Secondary structure predictions of T3D and *tsD*357 λ3 proteins. The predicted protein secondary structure surrounding amino acid 399 from the λ3 amino acid sequence was calculated using various computer prediction programs: PSIPRED (version 2.0; Uxbridge, UK), SSpro 2 Prediction (http://promoter.ics.uci.edu/BRNN-PRED/), PredictProtein (Columbia University, New York, NY), and Protean (version 3.04b; DNASTAR Inc., Madison WI). Protean predictions are based on the Garnier-Robson algorithm (Garnier *et al.*, 1978). Only PSIPRED reports confidence levels of individual amino acids and the levels reported are of isoleucine$_{399}$ in T3D and of serine$_{399}$ in *tsD*357.

 = coil,  = strand, = turn/loop.

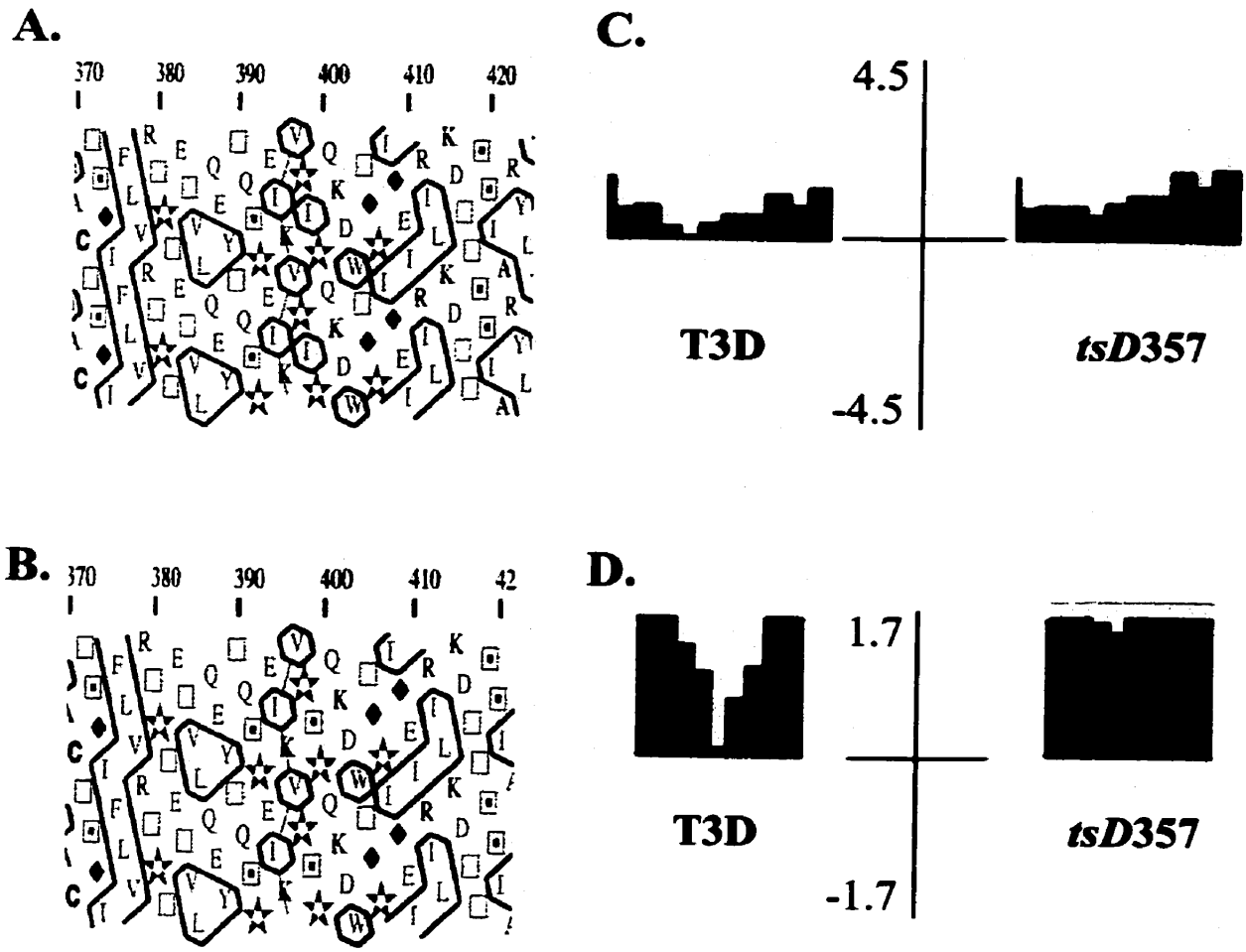
A.
370
380
390
400
410
420
B.
370
380
390
400
410
42
C.
4.5
T3D
tsD357
-4.5
D.
1.7
T3D
tsD357
-1.7

Figure 18. Polarity predictions of T3D and *tsD*357 λ3 proteins. A. Hydrophobic cluster analysis (HCA) plot of the region surrounding isoleucine$_{399}$ in T3D. Sets of adjacent hydrophobic residues are outlined and termed hydrophobic clusters. HCA plots were generated using the computational program DrawHCA via the Internet (http://www.lmcp.jussieu.fr/~soyer/www-hca/hca-form.html) (Gaboriaud *et al.*, 1987). Amino acids are labeled conventionally by their designated one letter codes except where the following symbols are used where ★ = proline, ● = glycine, □ = threonine, and ▣ = serine. **B.** HCA plot of the region surrounding serine$_{399}$ in *tsD*357. **C.** Hydophilicity plots for T3D and *tsD*357 of the region surrounding amino acid 399. Plots were generated based on the Kyte-Doolittle system using a value of nine residues to average (Protean)(Kyte & Doolittle 1982). **D.** The antigenic index (a maximum value of ±1.7) surrounding amino acid 399 in both T3D and *tsD*357 was measured based on the Jameson-Wolf algorithm (Protean)(Jameson & Wolf 1988).

Phinney *et al.*, 2000; Siuzdak 1998). MALDI QqTOF mass spectrometry was used to characterize the complexity and structural orientation of the proteins that make up the bi-layered capsid of reovirus.

3.3.1. MALDI QqTOF analyses of virion outer capsid proteins.

3.3.1.1. Identification of virion proteins. Purified T1L virions were digested with typsin at pH 7.4 at 37°C for 24 hours at a protein to enzyme ratio of 1000:1 (typical ratio for trypsin digestions) as described in Materials and Methods section 2.12.2. Samples were then diluted with dH_2O and prepared as described in Materials and Methods section 2.12.4.1, and were analysed by MALDI QqTOF mass spectrometry as described in Materials and Methods section 2.12.4.2. The overnight digestion in solution yielded enough peptides to identify several proteins of reovirus (Figure 19) by using the user defined sequence search program ProMac (Sciex, Concord, ON) or via the Internet using the programs MS-Fit and MS-Tag (http://prospector.ucsf.edu/). Individual peptide peak masses are checked against a database of proteins. Peptides from the protein database that have the same molecular mass as the unknown peptide are listed. The proteins identified were the major capsid proteins present in large numbers; outer capsid proteins σ3 and μ1 and inner capsid proteins λ1, λ2 and σ2. One major m/z peak, 2511.2, was unidentified as no peptides of this mass existed in the protein database.

3.3.1.2. σ3 is post-translationally modified. Peak 2511.2 was not detected in background controls that lack virions which suggests that the peak must correspond to a virion peptide. To identify this peak, MS/MS analysis was performed on this peak as described in Materials and Methods section 2.12.4.2. The fragmented daughter peptide peaks were analysed by MS-Tag. Measurements revealed that the peak of m/z 2511.2 corresponds

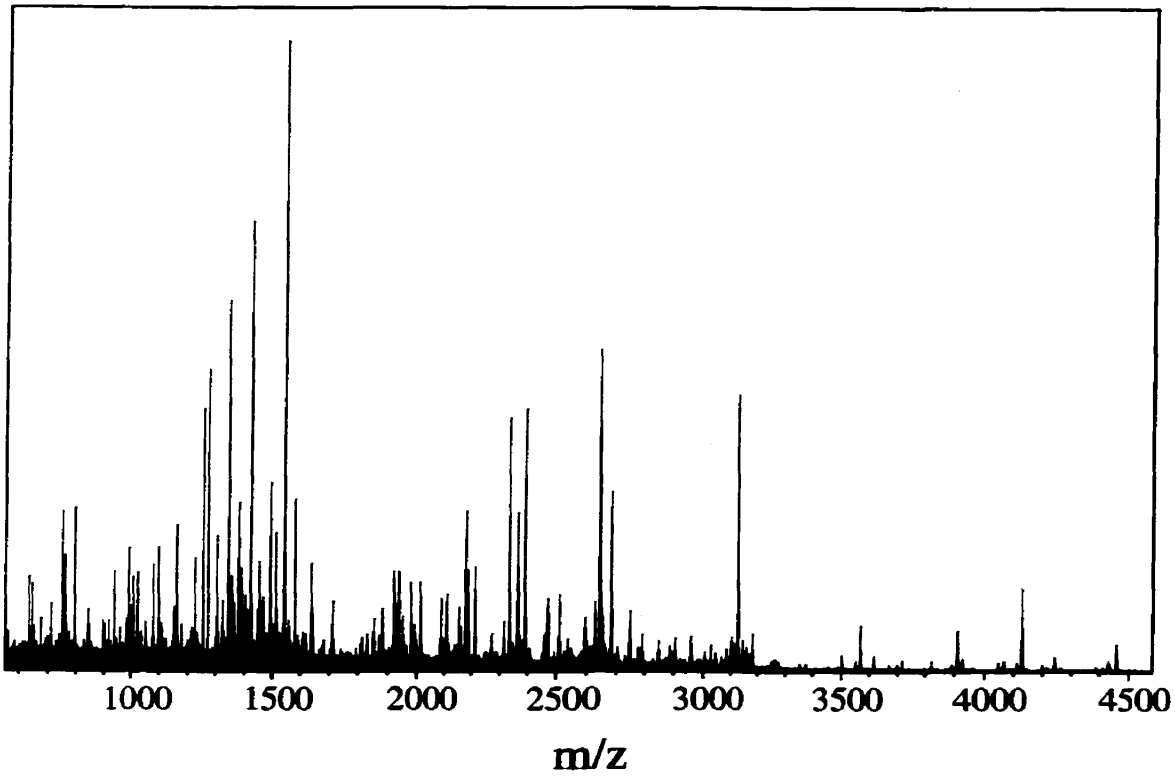
1000
1500
2000
2500
3000
3500
4000
4500
m/z

Figure 19. MS spectrum of an overnight trypsin T1L digestion. Purified T1L virions were digested with trypsin at 37°C for 24 hours at a viral protein to enzyme ration of 1000:1. An aliquot was prepared and then analysed by MALDI QqTOF mass spectrometry. The single MS (mass spectrometry) spectrum was acquired by irradiating the samples with a nitrogen laser at a repetition rate of 7 Hz for time intervals around one minute uninterrupted. Argon was used as the cooling gas. Spectra data acquisition and analysis was performed using software developed in-house (Tofma). Calibration of the mass spectrometer was based on two known mass peaks. An overnight trypsin digestion yields enough peptides to identify the main proteins of reovirus, outer capsid proteins σ3 and μ1, and inner capsid proteins λ1 and σ2, by MS-Fit and MS-Tag via the internet (http://prospector.ucsf.edu/).

to the amino terminus (N-terminus) fragment consisting of residues 1-22. The predicted mass of this peptide is 2469.2, a difference of an additional 42.0 which is indicative of an acetyl group and calculated to lie on the first amino acid, methionine (Figure 20). The actual mass of an acetate group is 43.0; however, two hydrogen molecules are lost during the bond formation, one from the acetate group and the other from the peptide amino terminal group. Therefore, this is the first evidence that shows acetylation of the σ3 N-terminus. Acetylation would be favourable on the amino group as there is no other freely available electron donor; a prerequisite to covalent bond formation.

3.3.1.3. Orientation and surface exposed regions of outer capsid virion proteins. For a more detailed examination of virion protein digestion, a more tightly controlled time course digestion with typsin was conducted. A large sample of purified virions was digested with trypsin at pH 7.4 and at 37°C with equivalent aliquots collected at different time points. TFA was added to the aliquots immediately to inhibit any further digestion. Samples were frozen at -20°C and then prepared for mass spectrometry. Peaks, and their corresponding peptides, were analysed for their order of appearance. The first peptide released is an eight residue peptide corresponding to the carboxy terminus (C-terminus) of major outer capsid protein μ1 (Figure 22). After that, σ3 is proteolytically digested followed by digestion of the remainder of μ1. Results are summarized in Table 7 and Figure 23. The first σ3 peptide corresponded to the amino acid fragment 214-236. Digestion then proceeded in either direction until σ3 was completely digested. Immediately after σ3 digestion, μ1 was proteolytically processed beginning at amino acid regions 235-243 and shortly thereafter at 507-537. Digestion then proceeded in both of these regions in either

A.

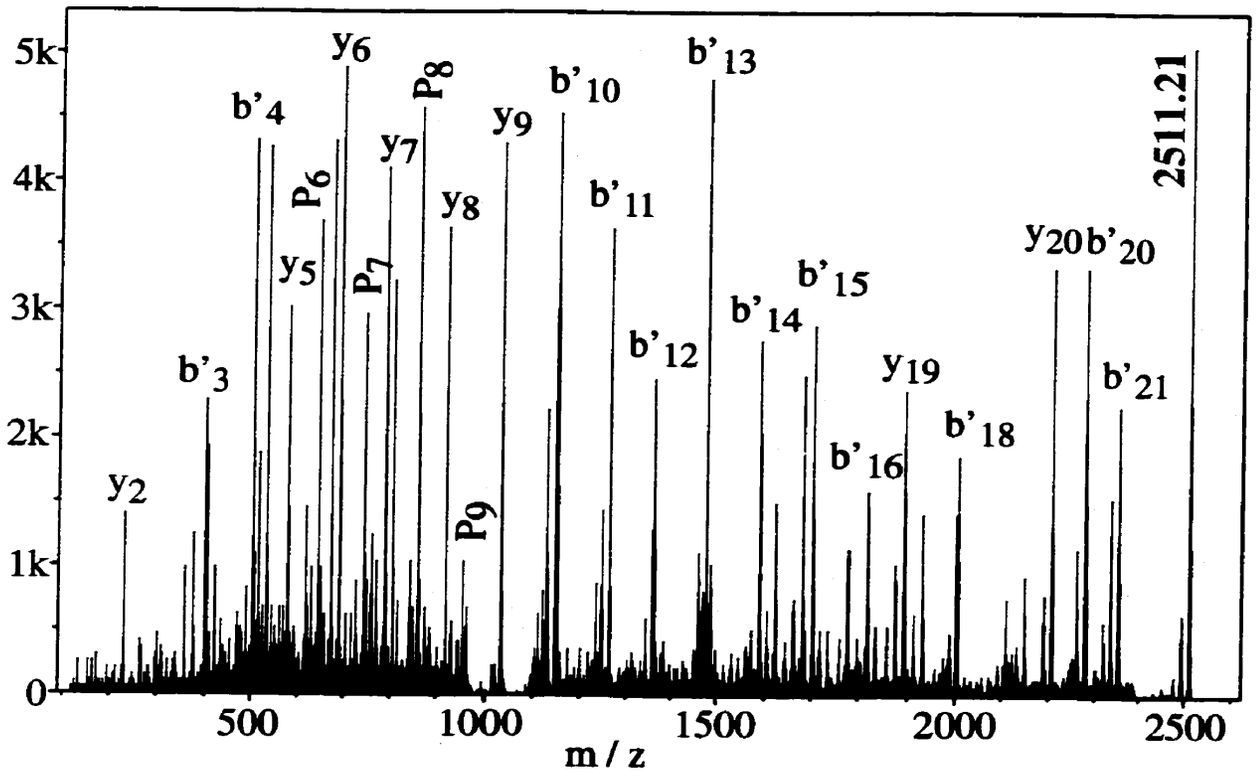

B.

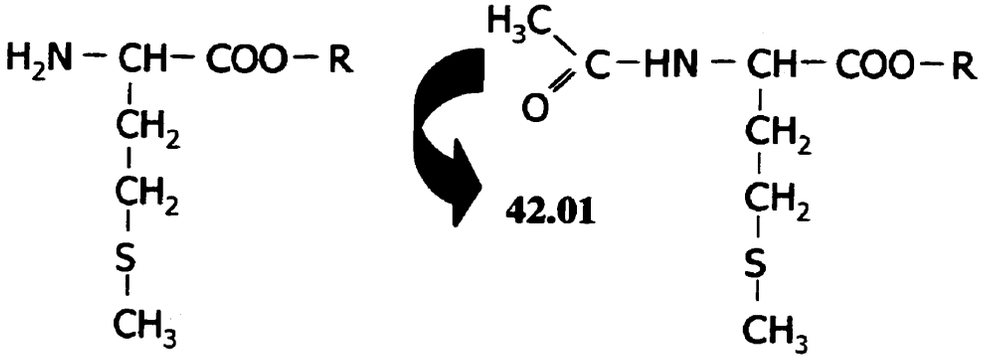

Predicted mass = 2469.20

Calculated mass = 2511.21

Figure 20. MS/MS spectrum of the tryptic ion at m/z 2511.2. A. The tandem mass spectra (MS/MS) of ion 2511.2 (labeled) was acquired at a laser repetition rate of 9 Hz. The ion was fragmented using argon as the collision gas. The collision energy was set by applying the accelerating voltage by the rule 0.5 V/Da and then adjusted manually to obtain desirable fragmentation of the parent ion. Spectra data acquisition and analysis was performed using software developed in-house (Tofma). Manual analysis indicates the N-terminal acetylation of σ3 peptide 1-22: Acetyl-MEVCLPNGHQIVDLINNAFEGR. Pn shows the internal proline fragments. y_n indicates fragments from the C-terminus; b'_n indicates fragments from the modified N-terminus. **B.** The structural formula and mass of the σ3 peptide fragment 1-22 in a non-acetylated and N-terminus acetylated form. R = amino acids 2-22: EVCLPNGHQIVDLINNAFEGR.

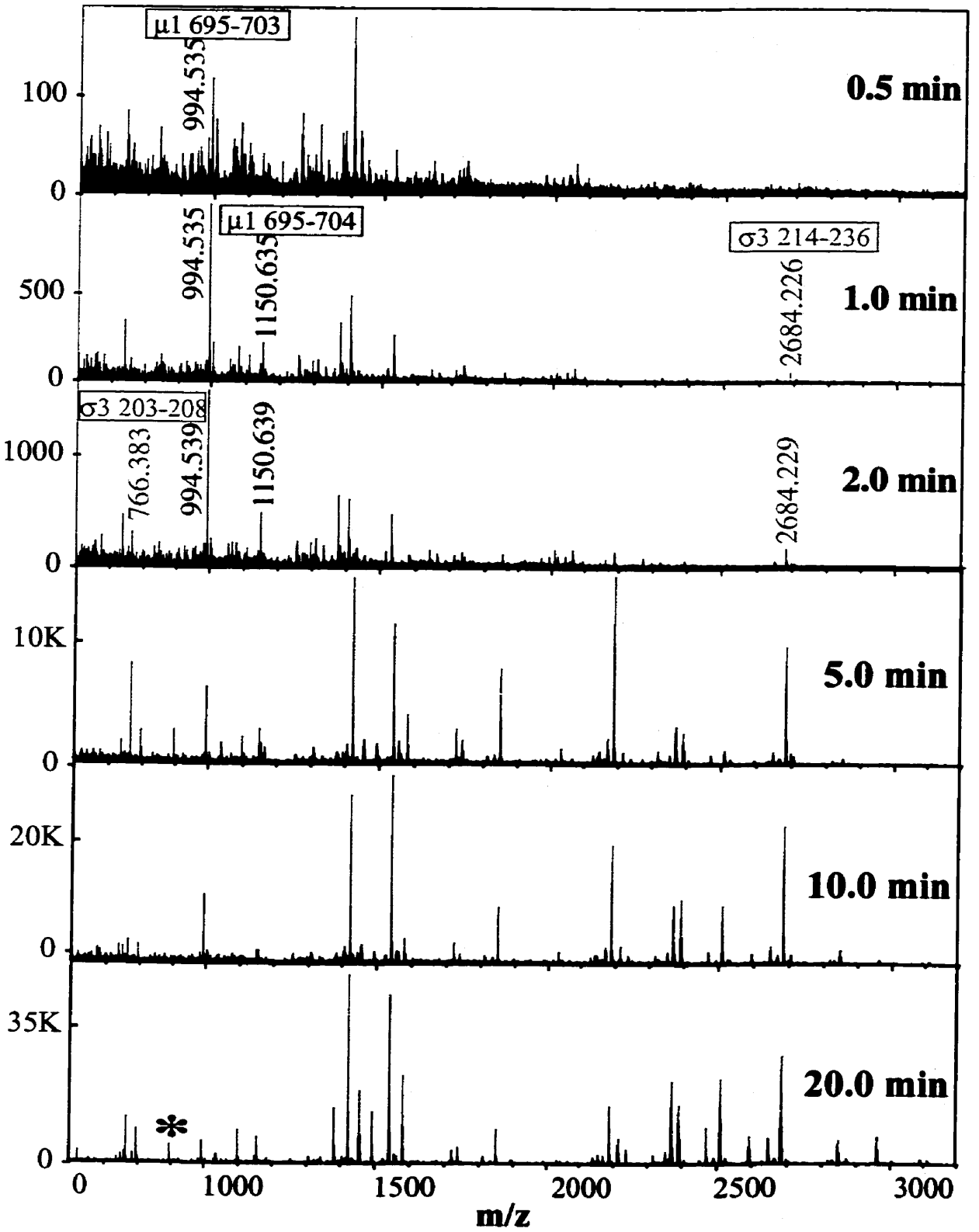
μ1 695-703
994.535
0.5 min
100
0
μ1 695-704
994.535
1150.635
σ3 214-236
2684.226
1.0 min
500
0
σ3 203-208
766.383
994.539
1150.639
2684.229
2.0 min
1000
0
10K
5.0 min
0
20K
10.0 min
0
35K
20.0 min
*
0
0
1000
1500
2000
2500
3000
m/z

Figure 21. Peptide mapping of tryptic T1L virion digests. Purified T1L virions were digested with trypsin at 37°C at a viral protein to enzyme ratio of 1000:1. At various time intervals, aliquots were removed and analysed by MALDI QqTOF mass spectroscopy. To identify the peptide fragments from the mass spectra, the m/z of monoisotopic ions were used to search a database of reovirus proteins using the computational program ProMac (Sciex, Concord, ON). Peptide peaks in green identify μ1 fragments; peptide peaks in red identify σ3 fragments. Initial peptides from both proteins are labeled. * = next μ1 peptide identified after total σ3 digestion.

direction. This order of identified peptides following digestion provides evidence to the structural orientation of the protein and identifies surface exposed regions.

To provide additional structural evidence, purified virions were also digested with V8 protease which gave a similar σ3 and μ1 pattern of digestion as trypsin processed virions did (Table 7 and Figure 22). However, one major difference between V8 protease and trypsin digestion was the fragment order of appearance. Despite μ1 cleavage initiating in two locations in a manner parallel to trypsin digestion, its digestion began before the complete digestion of σ3, where in trypsin digested virions, with the exception of the initial small C-terminus fragment, μ1 digestion did not re-initiate until σ3 was completely digested.

3.3.1.4. X-ray crystallographic analysis of σ3. The available X-ray crystallographic structure of the σ3 dimer (Olland *et al.*, 2001) was analysed and manipulated using the computer based program RasMol 2.7.1. (Bernstein and Sons, Belport, NY). RasMol was used to identify where the initial peptide from both trypsin and V8 protease digestion is situated in the σ3 monomer. The trypsin fragment 214-236 and the V8 protease fragment 199-217 are located on external surfaces of the protein (Figure 24). This suggests that this region of the protein is more accessible and surface exposed, away from the interior of the virion.

3.3.2. MALDI QqTOF analyses of core capsid proteins. Purified T1L and T3D virions were converted to cores as described in Materials and Methods section 2.7. Purified T1L cores were then digested with trypsin at pH 7.4 at 37°C for 24 hours. Cores, present at low concentrations, were then lyophilized and resuspended in dH_2O to concentrate peptides and were prepared as described in Materials and Methods section 2.12.4.1 for analysis by MALDI QqTOF mass spectrometry. This is contrary to the dilution of virion samples,

Table 7. Peptide products[a] from a time course protease digestion of σ3 and μ1 from T1L virions.

Time (min)	Trypsin		V8 Protease			Pepsin
	pH 7.4		pH 7.4		pH 4.5	pH 3.0
	σ3	μ1	σ3	μ1	σ3	σ3
0.5		695-703				
1.5	214-236					111-128
2.0	203-208					195-206
2.5				513-525		142-159
3.0	209-213 241-259					27-42 245-265 295-309 343-357
5.0	1-22 67-143 187-202 214-235 297-326		199-217		199-217	
10.0	23-63 144-162 327-365					Too many
20.0		235-241	228-241		228-241	
30.0			21-30	137-157	21-30	
50.0		507-537	3-20		3-20	
60.0		43-64 114-230 243-282 507-632		607-620 637-645		
120.0		367-377	176-198 301-309		176-198 301-309	

a: Peptides listed are either individual peptides or, in cases when numerous peptides were identified, they are listed as a range

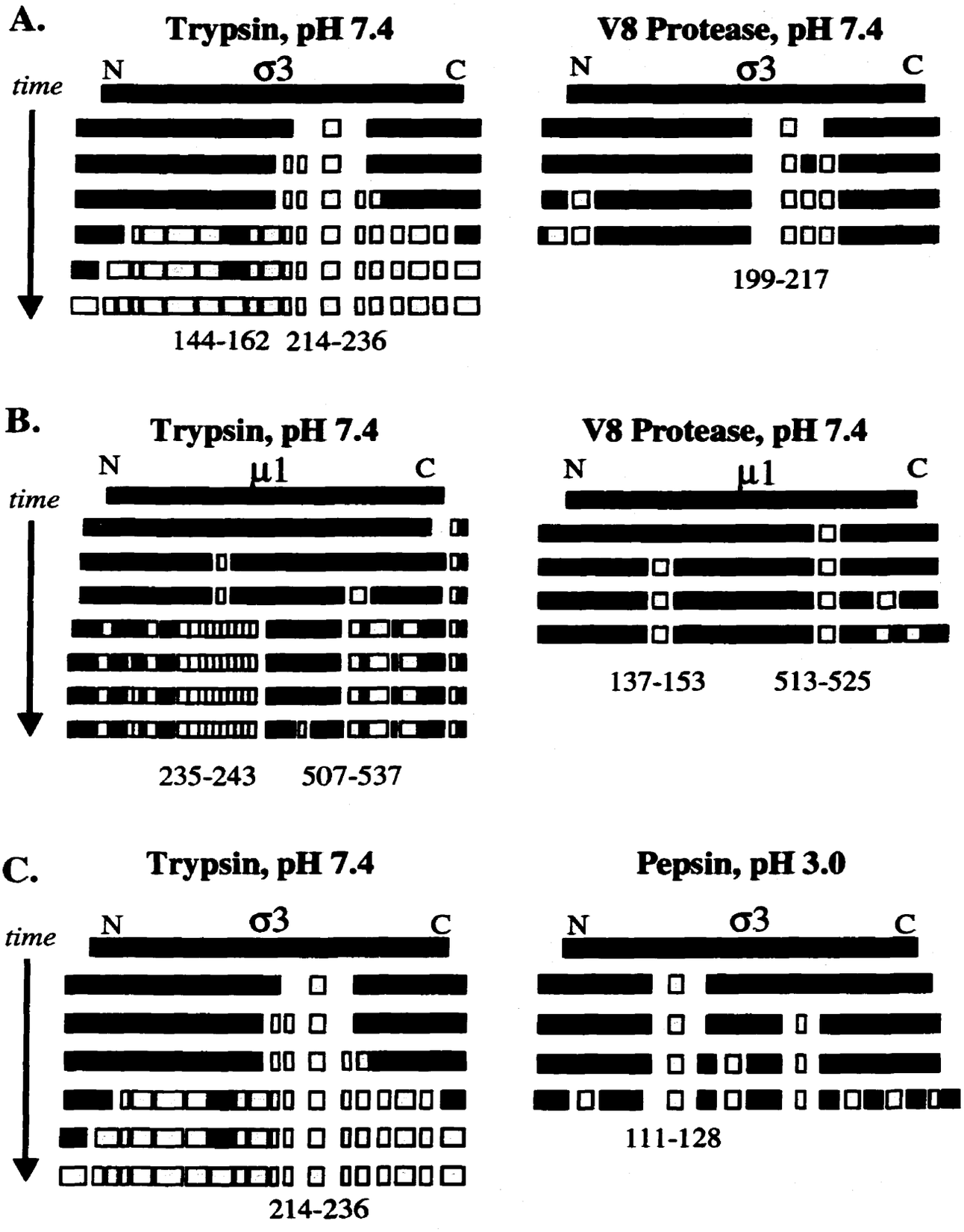
A.
Trypsin, pH 7.4
V8 Protease, pH 7.4
time
N
σ3
C
144-162 214-236
199-217
B.
Trypsin, pH 7.4
V8 Protease, pH 7.4
time
N
μ1
C
235-243 507-537
137-153 513-525
C.
Trypsin, pH 7.4
Pepsin, pH 3.0
time
N
σ3
C
214-236
111-128

Figure 22. Time course enzymatic digests of σ3 and μ1 outer capsid proteins. A. Time course digestion of T1L σ3 by trypsin and V8 protease at pH 7.4. **B.** Time course digestion of T1L μ1 by trypsin and V8 protease at pH 7.4. **C.** Time course digestion of T1L σ3 by pepsin at pH 3.0. Trypsin digestion is included for visual side-by-side comparison. Green = undigested protein, yellow = peptides identified by MS or MS/MS, red = non-identified peptides. Initial peptide cleaved is indicated with the exception of 144-162 in A (please see results discussion).

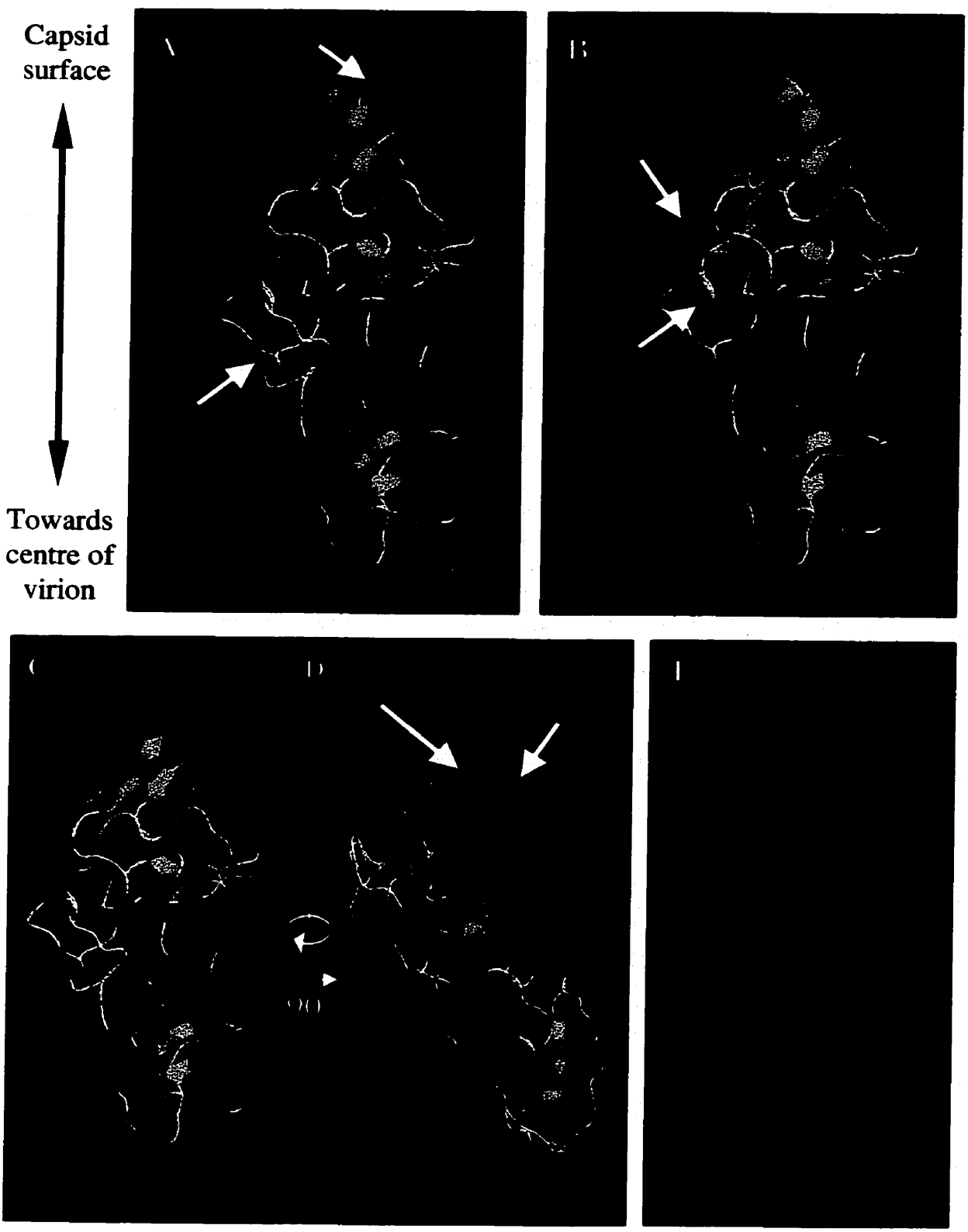
Capsid surface
Towards centre of virion

Figure 23. X-ray crystallographic structure of the σ3 monomer. The orientation of the σ3 monomer (adapted and modified from Olland *et al.*, 2001 using RasMol (Bernstein and Sons, Belport, NY)) is shown. With the exception of a selected region in blue or green or of (E); helices are in pink, β-sheets are in orange and turns are in grey. **A.** The selected region corresponds to residues 214-236, the initial tryptic fragment at pH 7.4. **B.** The selected region corresponds to residues 199-217, the initial V8 protease fragment at pH 7.4. **C & D.** The blue region corresponds to residues 214-236 from trypsin digestion at pH 7.4 and the green region corresponds to residues 111-128 from pepsin digestion at pH 3.0. In (D) the σ3 monomer is rotated 90° clockwise about the y-axis. **E.** Representation of a measure of the mobility/uncertainty of a given residue's position. High values, representative of higher mobility/uncertainty, are coloured in warmer (red) colours and lower values, representative of lower mobility/uncertainty, in colder (blue) colours.

because unlike cores, virions are at a higher particle concentration and at much higher salt concentrations, the latter of which adversely affects the mass spectrometer. Analysis of the resultant peptide peaks identified all five core proteins; λ1, λ2, λ3, μ2, and σ2.

3.3.2.1. Orientation of core capsid proteins. To determine the orientation of the core capsid proteins, a tightly controlled time course digestion was carried out. A large sample of T1L and T3D purified cores were digested with trypsin at pH 7.4 at 37°C. Equivalent aliquots were removed at various time intervals to which TCA was added immediately to inhibit further digestion. A summary of the initial peptide products is shown in Table 8 and Table 9. Unlike the sequential digestion of proteins observed in the virion capsid, core capsid proteins λ1, λ2 and σ2 were digested simultaneously. This agrees with previous structural organization evidence that suggests that within reovirus cores, λ1, λ2 and σ2 are surface proteins that are equally exposed (Dryden *et al.*, 1993; Reinisch *et al.*, 2000). The core spike protein λ2 is oriented in such a fashion that exposes numerous regions of itself as digestion was able to initiate in different locations throughout the protein. Major core capsid protein λ1 must be arranged such that its N-terminus is predominantly exposed as this is where digestion initiates. Major capsid protein σ2 on the other hand, which is thought to form an intricate lattice with λ1 (Dryden *et al.*, 1993; Reinisch *et al.*, 2000), is oriented such that its C-terminus is located towards the surface of the capsid as this is the site where digestion initiates.

A closer examination of the cleaved proteins from T1L and T3D reveal slight differences in the initial released peptides, either in terms of the order of appearance or in terms of the actual peptides themselves (Table 8). Differences are observed in all three major capsid proteins. For example, in T1L, the initial λ1 peptides in the N-terminus region that

corresponds to amino acids 55-64 and 64-84 whereas in T3D, the first peptides correspond to amino acids 38-54 and 55-64, a region located slightly upstream. As another example, in T1L, σ2 peptides 315-322 and 394-418 are seen before 370-377 whereas in T3D, peptides 378-393 and 394-418 are seen before 315-322. A similar example is seen in λ2, where peptide 549-556 does not appear simultaneously with 769-778 in T3D cores as it does in T1L cores. These peptide patterns provide evidence which suggests that, while not affecting the general orientation of the core proteins, there are subtle conformational differences between the two major reovirus strains T1L and T3D.

3.3.2.2. X-ray crystallographic analysis of the reovirus core. The X-ray crystallographic structure of the T3D core particle has been previously determined (Reinisch *et al.*, 2000). Using RasMol, a five protein subunit of the X-ray crystallographic T3D core structure was manipulated to show where the initial T1L and T3D peptides for each surface core protein were located (Figure 24 and Figure 28A). Although the X-ray crystallographic core structure is of T3D, T1L peptides were identified for the sake of comparison.

3.4. Structural conformational changes observed in virions and cores.

Despite maintaining high structural stability during the extracellular phases of their replicative cycles, viruses are significantly dynamic during other stages in their life cycle. In particular, previous experiments have shown that the protein capsids of reovirus virions and cores undergo conformational changes during key events in the reovirus life cycle (Dryden *et al.*, 1993; Fernandes *et al.*, 1994; Shepard *et al.*, 1995; Yeager *et al.*, 1996). These may occur during entry, or during biological events such as transcription, as suggested by cryoelectron microscopy (Yeager *et al.*, 1996).

Table 8. Peptide products from a limited time course tryptic digestion of T1L cores.

Time (min)	Non-transcribing Cores			Transcribing Cores		
	λ1	λ2	σ2	λ1	λ2	σ2
1.0	55-64 65-84 136-168	9-21		136-168		
1.5	32-54 112-135	549-556 769-778	315-322 394-418	38-54 55-64		
2.0				32-54 65-84 112-135	9-21 549-556 769-778	315-322 394-418
3.0		938-947				
5.0	12-37 23-54 109-135	326-349 350-371 508-548 1237-1241	370-377	23-54 109-135	350-371 417-443 508-548 938-947 1205-1236 1237-1241	

Table 9. Peptide products from a limited time course tryptic digestion of T3D cores.

Time (min)	Non-transcribing Cores			Transcribing Cores		
	λ1	λ2	σ2	λ1	λ2	σ2
1.0	38-54 55-64 136-168	9-21	378-393 394-418			
2.0				136-168	769-778	394-418
3.0		769-778				
5.0			315-322	38-54 55-64		315-322 378-393

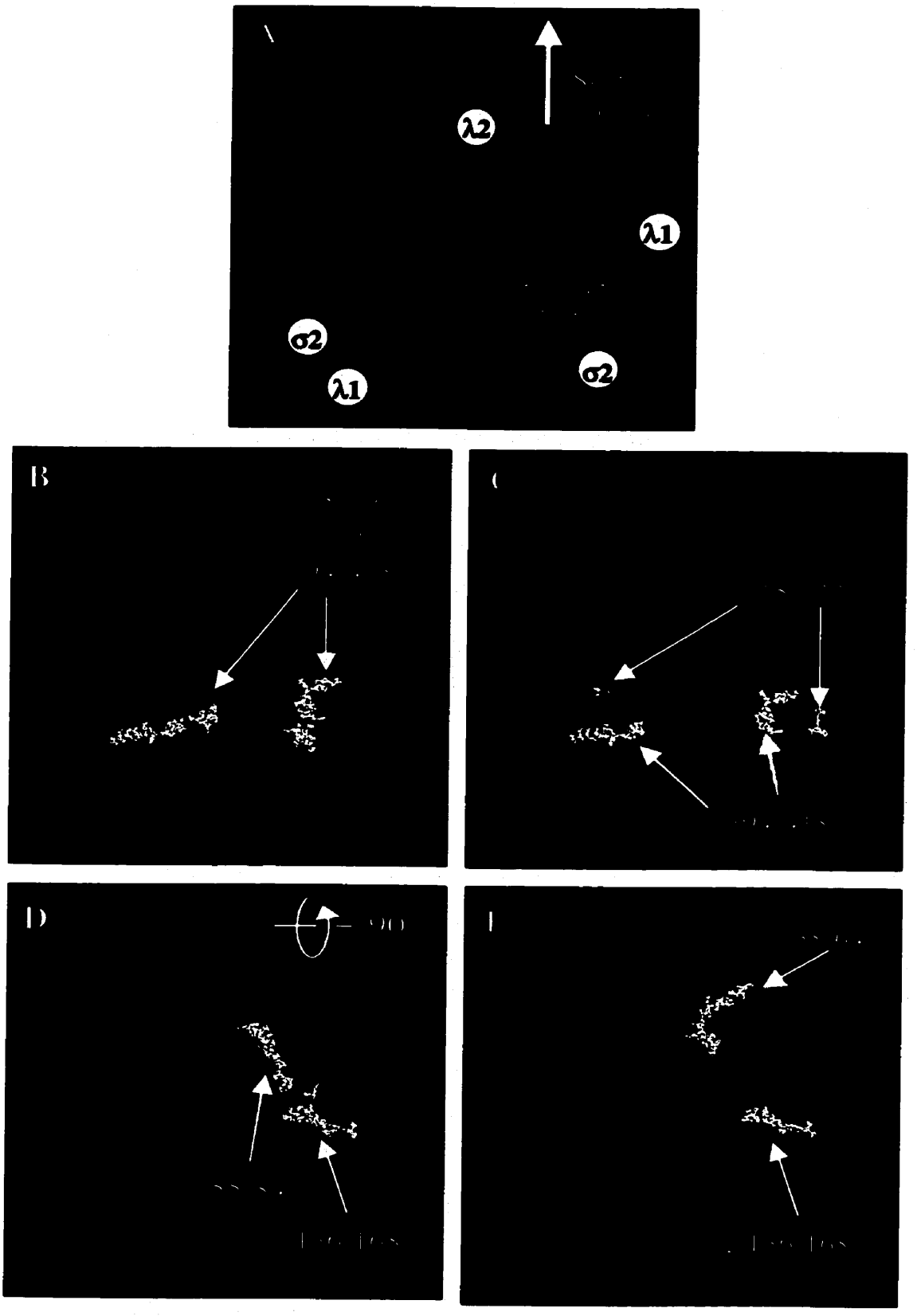
λ2
λ1
σ2
λ1
σ2

Figure 24. X-ray crystallographic structure of a five protein core complex: T1L and T3D comparison. The X-ray crystallographic structure (space-fill model) of a 5 protein complex was adapted and modified using RasMol (Bernstein and Sons, Belport, NY) from Reinisch *et al.*, 2000. Colours, indicate the different proteins and the initial peptides cleaved. **A.** Identification of the five proteins. **B.** The initial cleaved peptides from the σ2 proteins in T3D. **C.** The initial cleaved peptides from the σ2 proteins in T1L. **D & E.** The X-ray crystallographic structure is rotated 90 into the plane and towards the top of the paper to allow visualization of the initial cleaved λ1 peptides from T1L (D) and T3D (E).

3.4.1. Conformational changes observed in virions in response to pH change.

During the course of the reovirus life cycle, virions can experience low pH conditions within a host in two different locations. During a gastro-intestinal infection, the virion must go through the stomach and endure an acidic pH that can be as low as 0.82 (Vander *et al.*, 1994). During cellular infection, viruses are adsorbed via receptor-mediated endocytosis into endosomes which then fuse with lysosomes where the pH can drop below 4.0. To investigate whether conformational changes occur in virions in response to a decrease in pH, as past evidence suggests (Fernandes *et al.*, 1994), virions were digested at low pH values.

A sample of purified T1L virions were adjusted to pH 3.0 or 4.5 and then digested with pepsin or V8 protease respectively at 37°C. Tryspin was not used as it is inactive at such acidic pH's. Equivalent aliquots were removed at various time points ranging from 0.5 minutes to 24 hours. Digestion was inhibited with the immediate addition of 10 mM Tris pH 7.4 to pepsin digested samples or by the addition of 0.1% TCA to V8 protease digested samples. Following inhibition, samples were frozen at -20°C and then prepared for analysis by MALDI QqTOF as described in Materials and Methods section 2.12.4. All V8 protease peptides were identified using the program ProMac whereas MS/MS had to be performed on all pepsin fragments due to its non-specific cleavage. Results are summarized in Table 8 and Figure 22. The first initial peak identified corresponds to amino acids 199-217 when digested with V8 protease. However, the first identified peptide from pepsin digestion corresponded to amino acids 111-128. This pepsin digest fragment is about 100 residues closer to the N-terminus than where trypsin originally cleaved which indicates a different surface exposed region (Figure 22).

To examine whether the observed peptides were a result of viral protein disassociation due to a decrease in pH, purified virions were adjusted to pH 3.0 and maintained as such for up to one hour followed by observation via electron microscopy. Electron micrographs revealed fully intact virions (data not shown). This suggests the resultant peptides are not a result of acid-induced viral capsid disassociation. These observations provide evidence that the virion can undergo a conformational change during low pH exposure while retaining its integral state. Such observations have been shown in other viruses; for example, Sindbis virus, where low pH exposure alters the conformation of its membrane glycoproteins without disruption of the virus envelope (Phinney *et al.*, 2000).

The initial pepsin digest peptide 111-128 was identified on the X-ray crystallographic structure of the σ3 monomer using RasMol (Figure 23). Amino acids 111-128 are situated on an external face of the protein. Examining the flexibility of σ3 using RasMol, through a measure of the mobility/uncertainty of a given residue's position, reveals that the pepsin and trypsin cleaved peptides exist in a region of higher flexibility (Figure 23). This provides supportive evidence and adds credence to the fact that a conformational change occurs in virions in response to a change in pH.

3.4.2. Conformational changes observed between transcribing and non-transcribing cores. As discussed earlier in the Introduction, once virions are processed to their core form within the cell, being transcriptionally competent, they are able to undergo transcription of their viral genome. Cryoelectron microscopic analysis of transcribing and non-transcribing cores in a previous study suggests that conformational differences exist between the two (Yeager *et al.*, 1996).

3.4.2.1. Fluorography and phosphor imaging analysis. To determine whether possible conformational differences do exist between non-transcribing (NTS) and transcribing (TS) cores, T3D cores were examined by fluorography. Briefly, samples of purified ^{35}S-labelled cores, prepared as described in Materials and Methods section 2.12.1, were digested with various proteases at 37°C for 90 minutes. Core conditions were identical with the exception of the ingredient 2X TRB. The addition of 2X TRB allows for transcription, therefore cores in the presence of 2X TRB were TS and cores in which 2X TRB was replaced with 200mM HEPES pH 8.0 (2X TRB without NTP's, enzyme, and enzyme substrate) were NTS. TS cores were allowed to transcribe at 50°C for 10 seconds or at 37°C for 30 seconds before the addition of protease. NTS cores were also pre-incubated at 37°C for 30 seconds before protease addition. Conditions were such that the final protein to enzyme ratio was 3:2. Digestion was arrested by cooling the samples on ice. Samples were then analysed by SDS-PAGE and fluorographed as described in Materials and Methods section 2.12.3.

Fluorography revealed a difference in the peptides present between NTS and TS cores (Figure 25) which is suggestive of a conformational difference between the two forms of cores. This difference was not a function of the temperature of pre-incubation as the differences were identical in cores that underwent transcription at 37°C or at 50°C. Another experiment was run in which NTS and TS cores were digested with trypsin for 1, 5 and 15 minutes at 37°C at a protein to enzyme ration of 2000:1. Peptide products were then analysed by phosphor imaging analysis as described in Materials and Methods section 2.12.3. The three major bands (two λ and one σ band) from each time points were analysed for intensity and corresponding bands were compared to one another (Figure 26). The second

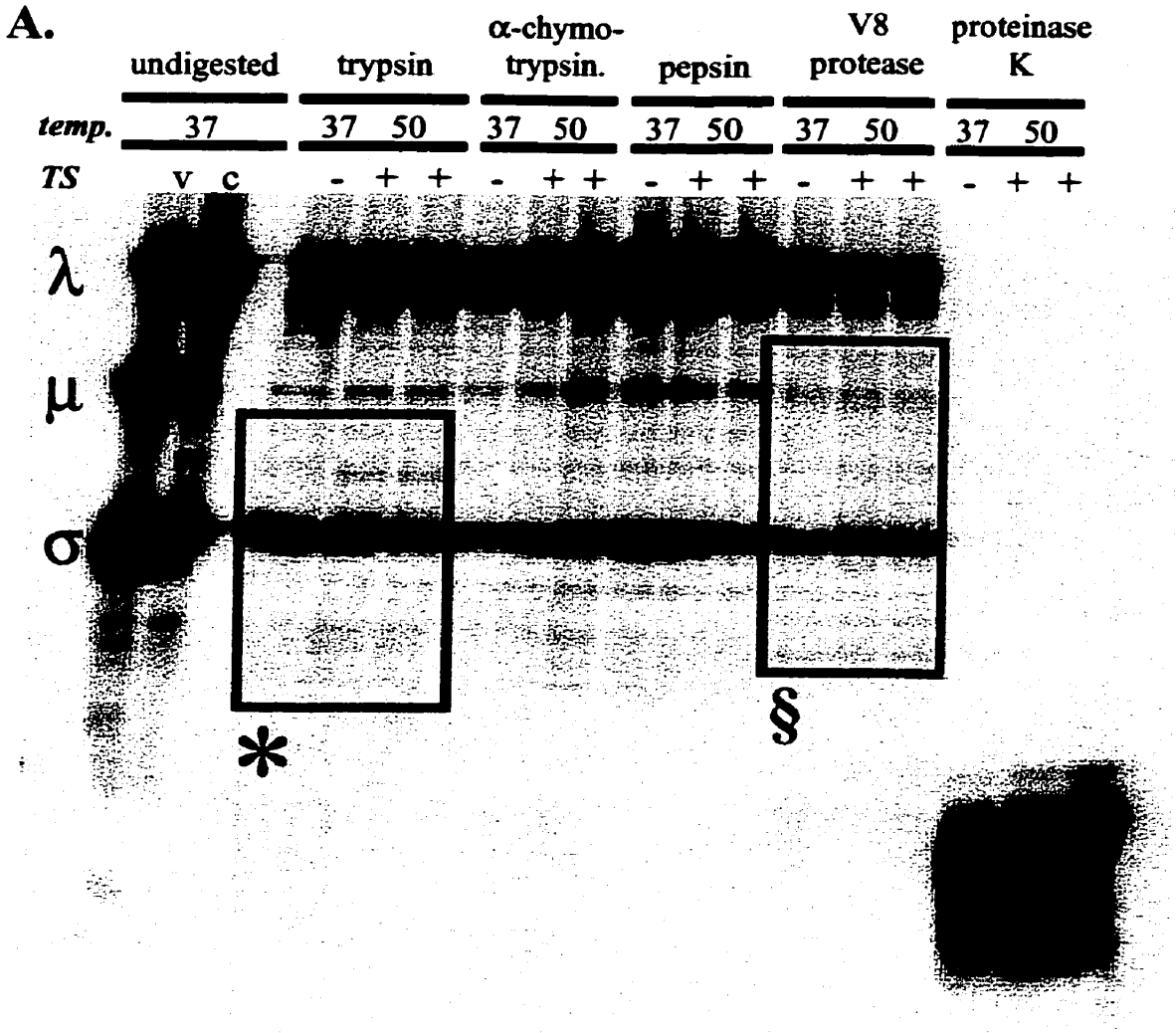
A.
undigested
trypsin
α-chymo-trypsin.
pepsin
V8 protease
proteinase K
temp.
37
37 50
37 50
37 50
37 50
37 50
TS
v c
- + +
- + +
- + +
- + +
- + +
λ
μ
σ
*
§

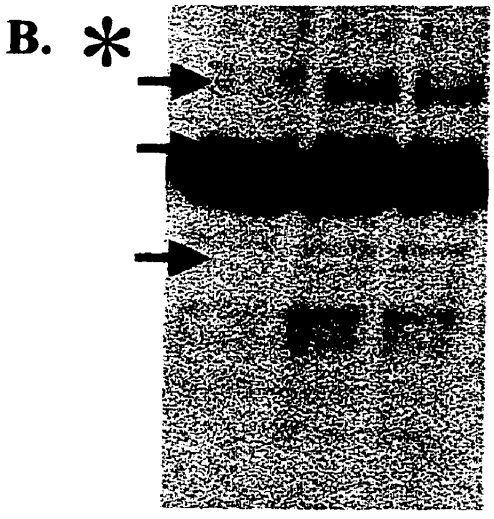
B. *

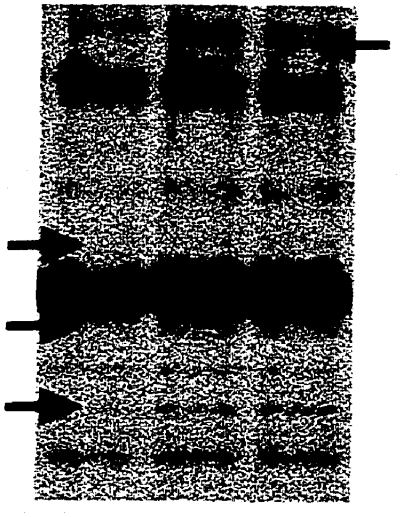
C. §

Figure 25. Fluorography of transcribing and non-transcribing cores digested with various proteases. A. Non-transcribing (TS -) and transcribing (TS +) T3D radio-labeled cores were digested with various indicated proteases for 90 minutes at 37°C. Cores underwent transcription at 37°C for 30 seconds or 50°C for 10 seconds (as labeled) before addition of protease. Protease was added at a viral protein to enzyme ratio of 3:2. After digestion, equivalent aliquots of peptide products from each sample were resolved by SDS polyacrylamide gel electrophoresis and the results fluorographed. Undigested virions (v) and cores (c) were used as markers. Sets of viral protein bands are labeled as such. **B & C.** Images of the outlined squares in (A) were blown up: * (B) and § (C). Arrows denote band differences between transcribing and non-transcribing samples.

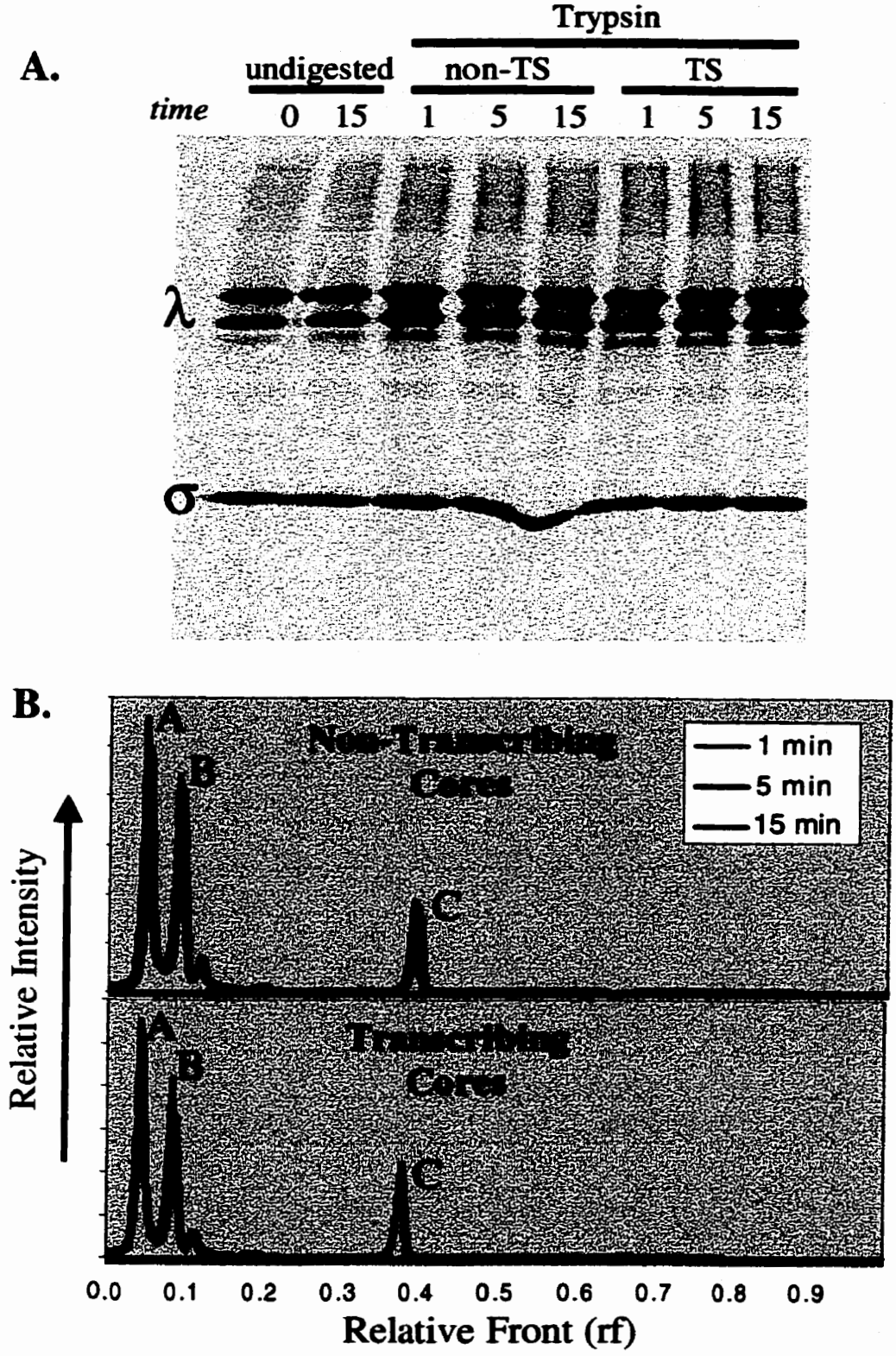
A.
Trypsin
undigested
non-TS
TS
time
0 15 1 5 15 1 5 15
λ
σ
B.
A
B
C
Non-Translating Core
Translating Core
1 min
5 min
15 min
Relative Intensity
0.0 0.1 0.2 0.3 0.4 0.5 0.6 0.7 0.8 0.9
Relative Front (rf)

Figure 26. Phosphor imaging analysis of transcribing and non-transcribing core peptide products. A. T3D non-transcribing and transcribing cores were digested with trypsin at 37°C at a viral protein to protease ratio of 2000:1. Equivalent aliquots were removed at 1, 5 and 15 minutes. Digestion was inhibited by immediate cooling on ice. Samples were then resolved by SDS-PAGE. Undigested cores were heated at 37°C for 0 and 15 minutes and were used as controls. Core proteins are labelled as such. **B.** Phosphor imaging analysis of the gel in (A). A corresponds to the top λ band in (A); B corresponds to the bottom λ band in (A); and C corresponds to the σ band in (A).

λ band had decreased in intensity by ~16% in NTS cores and by ~55%, or three times as much, in TS cores. These results provide further evidence that a different pattern of digestion occurs between NTS and TS cores, suggestive of possible conformational differences between the two. Fluorography and phosphor imaging analysis are valuable to obtain preliminary data yet are less sensitive than other means. Therefore to further investigate these findings, NTS and TS core samples were analysed by mass spectrometry.

3.4.2.2. MALDI QqTOF analysis. Purified T1L and T3D cores were incubated at 50°C for 30 seconds with or without 2X TRB under unmodified or modified transcriptional conditions as described in Materials and Methods section 2.12.4.1. Cores were then digested with typsin at pH 7.4 at 37°C at a protein to enzyme ratio of 1000:1. At selected time points, equivalent aliquots were removed and the digestion was inhibited by the immediate addition of TCA. Samples were then concentrated and prepared as described in Materials and Methods section 2.12.4.1 and analysed by MALDI QqTOF mass spectrometry. Results are summarized in Table 8 and Figure 27. Close inspection shows minor variations visible in these cores after transcription. Although two regions (38-64 and 136-168) in λ1 are exposed in the NTS cores from both strains, only one of them (136-168) is initially exposed in the TS cores. When digestion of λ2 is compared, fragment 769-778 in TS T3D cores is the first peptide cleaved by trypsin whereas peptide 9-21 is cleaved first in NTS T3D cores. In T1L, the order of peptide fragments from λ2 does not change, instead it is the rate of appearance that does. Parallel types of variations are also found in the digestive pattern of the σ2 protein. The evidence provided here suggests that conformational changes occur in cores when switching from a non-transcribing state to a transcribing one.

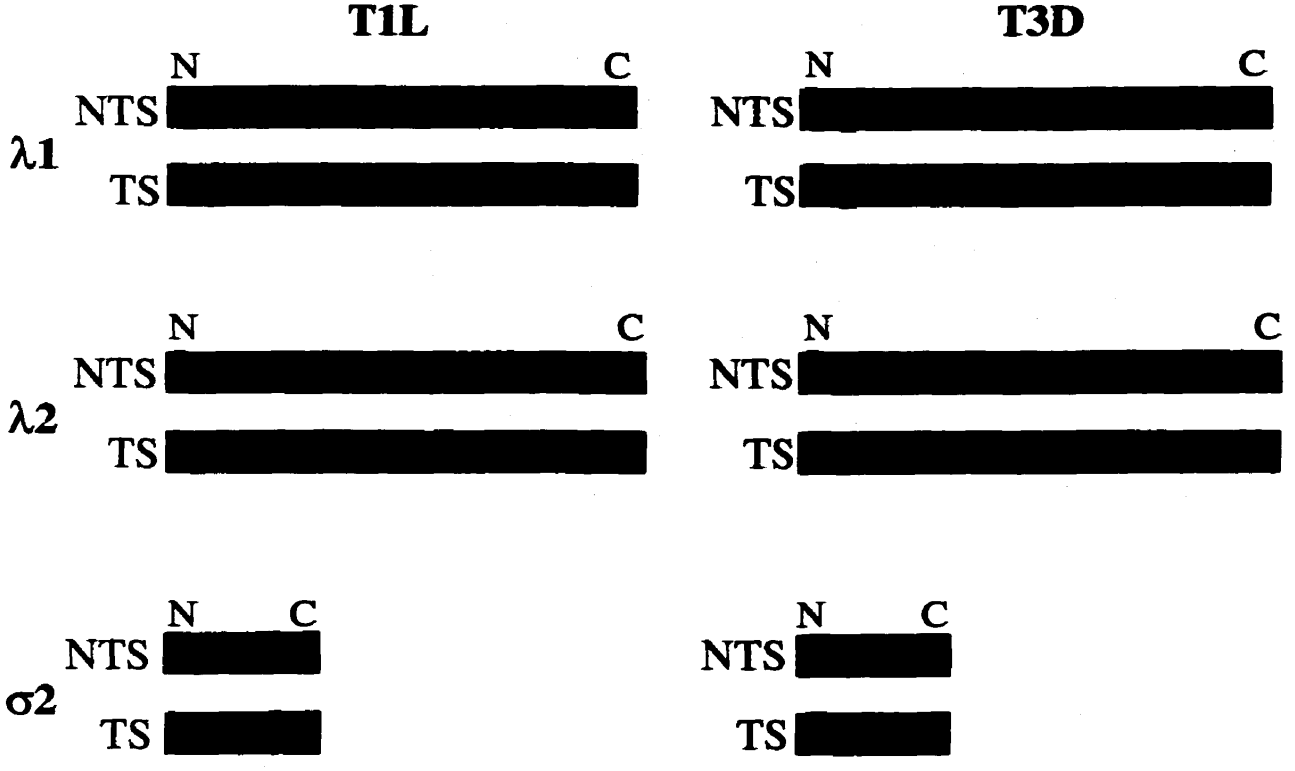
T1L
T3D
N
C
NTS
TS
λ1
λ2
σ2

Figure 27. Initial exposed regions in reovirus core proteins. Initial trypsin digested peptides (red) in reovirus non-transcribing and transcribing core proteins (green) of T1L and T3D. The length of the bar corresponds to the relative size of the protein. NTS = non-transcribing cores; TS = transcribing cores.

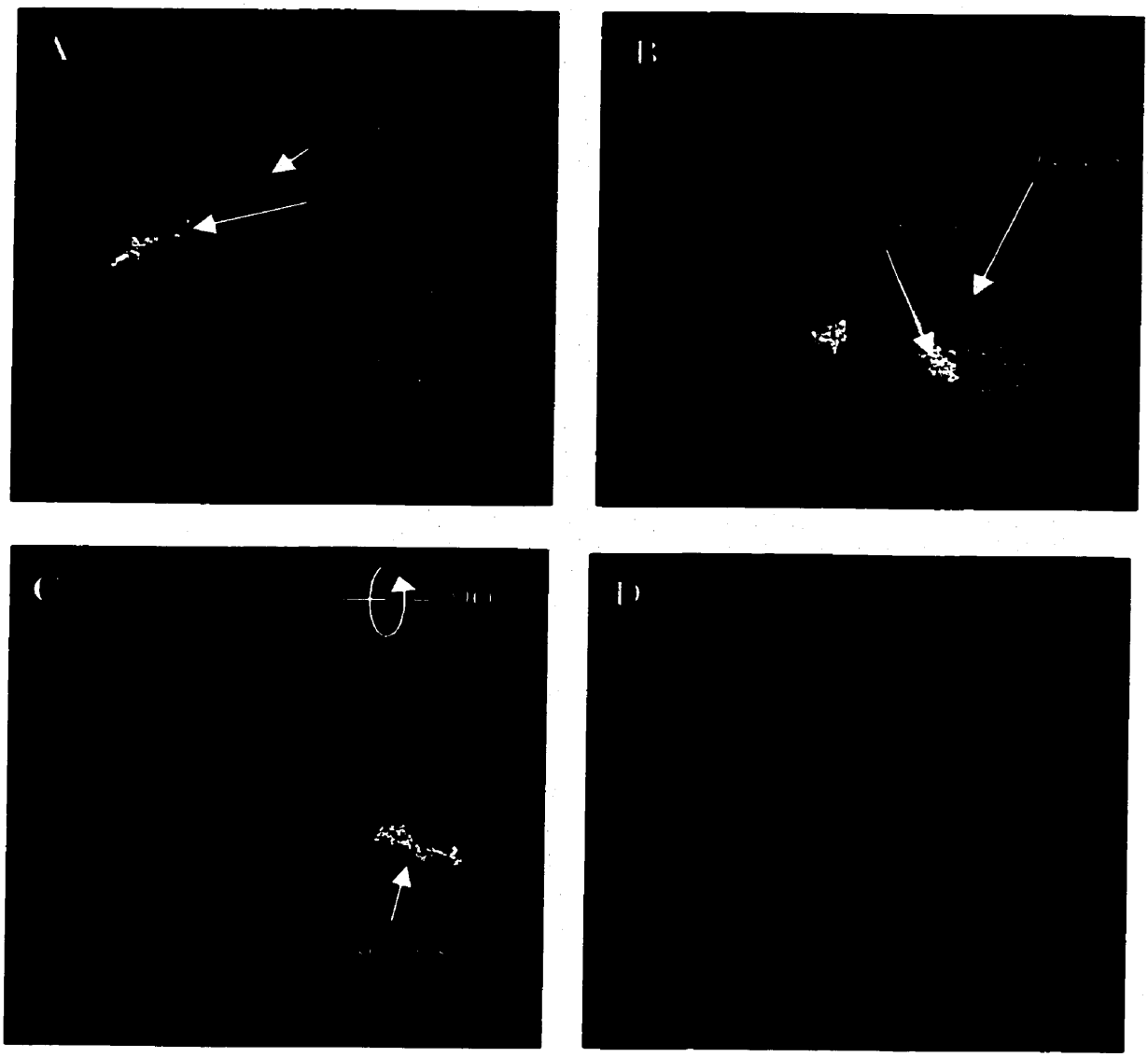

Figure 28. X-ray crystallographic structure of a five protein core complex: transcribing and non-transcribing comparison. The X-ray crystallographic structure (space-fill model) of a 5 protein complex from was adapted and modified using RasMol (Bernstein and Sons, Belport, NY) from Reinisch *et al.*, 2000. Colours, indicate the different proteins and the initial peptides as in Figure 24A. **A.** The initial cleaved peptides in λ2: 9-21 in non-transcribing T3D cores, and 768-778 in transcribing T3D cores. **B.** The initial cleaved peptides from the σ2 proteins: 378-393 and 394-418 in non-transcribing T3D cores, and 394-418 only in transcribing T3D cores. **C.** The X-ray crystallographic structure is rotated 90 into the plane and towards the top of the paper to allow visualization of the initial cleaved λ1 peptides from transcribing T3D cores (for the initial peptides released in non-transcribing T3D cores, please see Figure 24E). **D.** A representative measure of the mobility/uncertainty of a given residue's position. High values are coloured in warmer (red) colours and lower values in colder (blue) colours.

For further analysis, the initial peptides from the three surface core proteins from NTS and TS cores were identified on the five protein subunit of the X-ray crystallographic T3D core structure using RasMol (Figure 28 and Figure 24 D and E). Examining the flexibility of the five protein subunit using RasMol, through a measure of the mobility/uncertainty of a given residue's position, reveals that the trypsin cleaved peptides exist in a region of high flexibility, particularly in spike protein λ2 (Figure 28). This provides further testimony that the core proteins can undergo a conformational shift that does not disrupt their capsid integrity.

4. DISCUSSION

A virus, such as reovirus, maintains high structural stability during the extracellular portion of their replicative cycle, yet are significantly dynamic during other stages in their life cycle, namely during cell attachment (Fernandes *et al.*, 1994), uncoating (Dryden *et al.*, 1993) and transcription (Yeager *et al.*, 1996). Despite the extensive studies that have characterized the various structural proteins found within the capsid layers of reovirus, little is known with regards to the proteins within it and to the overall dynamics of the virus particles. Furthermore, little is known with regards to the enzymatic proteins located inside the capsid, specifically with respect to λ3, the RdRp, and how it functionally carries out transcription. This study serves to further characterize the interior core protein λ3, and the structural proteins that make up the capsids. The morphology of the virion and core capsids were examined under various environmental conditions by mass spectrometry, a technique not so far applied to reovirus.

Results shown here provide evidence that different strains of reovirus are morphologically different and have the capacity to undergo extensive conformational changes. Furthermore, mutations within the catalytic portion of the RdRp which lead to a major change in secondary structure, may serve to facilitate transcription but not replication. In addition, the environmentally safe compound Vertrel XF was identified as a suitable substitute for the organic solvent Freon 113, extensively used in virus purification.

Combined evidence provided in these studies shed new light on the dynamics of reovirus during the course of an infection, evidence which can be extrapolated to all other RNA and DNA viruses.

4.1. A comparative analysis of organic solvent Freon substitutes in the purification of reovirus virions.

Purification of viruses from infected cell lysates is an important first step in many biochemical and structural studies. In the case of many non-enveloped viruses such as mammalian reovirus, separation of virus from infected cell debris is accomplished by organic solvent extraction. Freon 113 (1,1,2-trichloro-1,2,2-trifluoroethane)(Freon)(DuPont, Wilmington, DE) is one such organic compound which for decades has been a key component of some viral purification methods (Gomatos & Tamm 1963; Gschwender & Traub 1978; Berman *et al.*, 1981; Richt *et al.*, 1993; Liebermann & Mentel 1994). Due to its unique physical and chemical properties, this fluorinated hydrocarbon compound has been ideal in extracting lipids and lipid bilayers without extracting proteinaceous (and hence polar) material such as non-enveloped viruses. The extracted viral particles can then be concentrated and purified in ultra-centrifugation gradients and used in biochemical and structural studies. However, because Freon has been implicated in ozone layer depletion and because of rising environmental concerns, its use has been progressively eliminated and eventually will be prohibited (Taylor 1996). The future unavailability of Freon would remove an essential step in virus purification. A logical solution to this obstacle is to substitute it with another solvent that behaves like it, yet has low toxicity and environmental hazards.

In attempts to identify a suitable Freon substitute, the capacities of different organic solvents to purify cultivable reovirus from tissue culture were tested. As stated earlier, the properties of an organic solvent can be characterized by Hansen's three solubility parameters (D - dispersion energy, P - polar energy, and H - hydrogen bonding energy (Hansen & Beerbower 1971; Goldschmidt 1993). In finding a replacement, we concentrated on selecting

solvents that have solubility properties similar to those of Freon. A few alternate halogenated hydrocarbons have solubility parameters similar to those of Freon, but other properties make them unsuitable for use (examples include: 1,2-dichloro-1,1,2,2-tetrafluoroethane with a boiling point of 4°C and carbon tetrachloride with its high toxicity). Many other organic compounds, such as hexane and 1-chlorobutane, have some parameters similar to those of Freon, but differ substantially in other parameters. By combining some of these compounds in various ratios, solvent mixtures were created that closely matched Freon's solubility parameters. Initially, hexane/1-chlorobutane (a 7:3 volume/volume mixture), isopentane/1-chlorobutane (7:3), toluene, and Vertrel® XF (Vertrel) were tested as suitable solvents. Vertrel (1,1,1,2,3,4,4,5,5,5-decafluoropentane) is a Freon substitute developed by DuPont which is not implicated in ozone depletion (Vertrel XF technical bulletin, 1999).

Results indicate that both Vertrel XF and a 7:3 mixture of isopentane/1-chlorobutane serve as suitable substitutes for Freon 113 in the purification of reovirus virions. Although most of the other solvents tested were partially effective in purifying virus, the quantity of virus recovered was smaller and preparations had higher levels of contamination. It was found that a 1:1 mixture of chloroform/isobutanol was a poor choice for purification of intact reovirus virions due to the lack of genomic material observed under SDS-PAGE, disrupted viral morphology and low levels of infectivity. The poor results obtained from chloroform/isobutanol (1:1) may be explained by its different solubility parameter values. Compared to Freon, Vertrel, and isopentane/1-chlorobutane (7:3), chloroform/isobutanol (1:1) has a similar D value, a slightly higher P value, and a significantly larger H value. A higher H value would result in larger hydrogen bonding energies which would serve to promote interaction between solvent and both polar and nonpolar molecules. Therefore, the

solubility properties of chloroform/isobutanol (1:1) may be such that it does not extract intact virions away from cellular debris as well as the other solvents or may have a detrimental effect on the virions. Although both Vertrel and the 7:3 mixture of isopentane/1-chlorobutane appeared to be the best substitutes for Freon 113, other considerations suggest the former to be the better choice. Sample emulsification with Vertrel consistently gave larger amounts of purer and more infectious virus than the other tested solvents. In addition, 1-chlorobutane, isopentane, and hexane are all flammable and volatile liquids which are monitored by the Environmental Protection Agency (EPA). Because of their flammability, they are not recommended for use in any type of centrifugation process (an integral part of viral purification), as vapours may be ignited by exposure to electrical contacts. Furthermore Vertrel appears to be a more attractive solvent substitute due to its compatibility with most plastic pipettes (for example, polystyrene and polypropylene), low toxicity, chemical and thermal stability (up to 300°C), non flammability (no reported flash point), and reported lack of ozone depletion properties (Vertrel XF technical bulletin, 1999). Vertrel is also accepted as a substitute for ozone-depleting substances and is exempted from classification as a volatile organic compound by the EPA.

Extraction with Freon has also been a key step used in medical virology for purification of viral nucleic acids from non-enveloped fastidious agents found in clinical samples (Atmar *et al.*, 1995; Le-Guyader *et al.*, 1996; Traore *et al.*, 1998). The purification of calicivirus nucleic acid from stool samples using selected solvents was also examined (Mendez *et al*, 2000). Combined results have indicated that Vertrel was the ideal Freon substitute for the purification of calicivirus nucleic acid and of reovirus (Mendez *et al*, 2000). Vertrel is now the adopted choice of organic solvent in the laboratory for all necessary

purifications of non-enveloped viruses, an imperative step required when studying purified virions or cores.

4.2. Phenotypic differences observed in *temperature sensitive* mutants *tsD*357 and *tsG*453.

The genetic system of reovirus has allowed for the creation and manipulation of a panel of conditionally-lethal temperature sensitive (*ts*) mutants. *ts* mutants have been assigned to ten groups that represent the ten different gene segments (Coombs 1996; Fields & Joklik 1969; Ramig & Fields 1979). These *ts* mutants and reassortant analyses have proven to be vital tools in studies that have led to characterizing DNA and RNA metabolism, protein-folding pathways, viral assembly pathways, and viral pathogenesis and structure (Drayna & Fields 1982a; Drayna & Fields 1982b; Keroack & Fields 1986; Bodkin & Fields 1989; Coombs 1996; Shing & Coombs 1996; Yin *et al.* 1996; Hazelton & Coombs 1999; Becker *et al.*, 2001). The generation of *ts* reassortants allows us to assign a particular phenotype to a gene and consequently to its corresponding protein. Purified *ts* mutants *tsD*357 and *tsG*453 are an invaluable tool which though extended studies, will help characterize viral proteins.

At the non-permissive temperature, *tsD*357 has been shown to produce empty virions (Fields *et al.*, 1971), reduced amounts of single-stranded RNA and protein (Cross & Fields 1972; Fields *et al.*, 1972), and nearly undetectable amounts of progeny dsRNA in infected cells (Cross & Fields 1972; Ito & Joklik 1972a). A panel of reassortants were generated by crossing *tsD*357 with the wild-type parent T1L. The reassortants were subsequently analysed and through an EOP assay, a conditionally lethal lesion was mapped to the L1 gene which encodes the RdRp, (Drayna & Fields 1982a; Koonin *et al.*, 1989; Morozov 1989; Starnes &

Joklik 1993).

*tsG*453 is another *ts* mutant that produces core-like structures that have the full complement of genome but fails to produce ISVP-like particles or mature virions at the non-permissive temperature (Morgan & Zweerink 1974; Danis *et al.*, 1992). Other reassortant mapping studies confirmed the lesion in *tsG*453 to be in the S4 gene (Mustoe *et al.*, 1978a; Shing & Coombs 1996). The failure to produce mature virions in a restrictively infected cell is caused by the failure of μ1 to form complexes (required for the condensation of the outer capsid onto nascent cores) with mature σ3 which is misfolded (Shing & Coombs 1996). A second panel of reassortants were generated by crossing the *ts* mutant *tsG*453 with the wild-type parent T1L. An extensive EOP assay mapped the *ts* lesion to the S4 gene.

Through pre-incubation at high temperatures as described in Results section 3.2.3.1., purified virions from *tsD*357 and *tsG*453 were examined for any heat-induced decrease in viral titres. *tsD*357 viral titres were not affected when the virions were pre-heated at 55°C prior to infection whereas *tsG*453 were extremely susceptible, with viral titres dropping over five orders of magnitudes. This suggests that *tsD*357, despite being a *ts* mutant, is as thermal stable a virion as its parent T3D. These experiments also help answer the question whether the *ts* nature of the virion, i.e. the impairment of its replication at non-permissive temperatures, was due to structural disruption of a particular protein in response to elevated temperatures. *tsD*357 clearly displays its *ts* nature at a temperature of 39°C. Purified *tsD*357 virions were preheated at 55°C, which is far higher than the non-permissive temperature of 39°C. Therefore if the virions are able to withstand these extreme temperatures and not have them affect their infectious nature, then its *ts* characteristic is not a function of virion disruption, verified by examination under the electron microscope.

On the other hand, *tsG*453 showed remarkable susceptibility to heat-induced loss of infectivity when preheated at 55°C but not when preheated at 50°C. A selection of T1L x *tsG*453 reassortants, representative of diverse reassortment, were amplified and purified. Purified reassortants were then preheated at 55°C for 15 minutes and their viral titres were compared to both parents. Based on the percent survival of the virions, reassortants were organized into two panels which revealed the S4 gene to be responsible for this phenotypic observation. The S4 gene encodes the outer capsid protein σ3. The fact that pre-incubation at high temperatures disrupted levels of infectivity is highly suggestive of a structural failure within the virion. To examine for any aberrations in the virion, a sample of purified *tsG*453 virions preheated at 55°C for 15 minutes was examined by negative stain transmission electron microscopy. Electron micrographs clearly reveal a structural anomaly within virion particles. Up to 75% of the sample consisted of a virion-like particle which appeared to have a loosely associated outer shell when compared to untreated virions. Furthermore, the remaining 25% of the sample consisted of core particles. Exposure to extreme temperatures had disassociated the outer capsid either partially or completely to yield either abnormal virions or intact cores respectively. Therefore, the lesions in the S4 gene produce a structurally unstable protein that is able to assemble onto the inner capsid at permissive temperatures but is weak, generally or specific at the μ1-σ3 interaction, when exposed to elevated temperatures. Past studies have shown that the misfolded σ3 protein fails to form complexes with μ1, a pre-requisite to outer capsid assembly (Shing & Coombs 1996). A possible reason for the loose association of the outer shell is a weakened μ1-σ3 bond. This suggests that the μ1-σ3 interaction is negatively affected by the *ts* mutation(s), in accordance with previous observations (Shing & Coombs 1996). It is important to note however that the

decrease in infectivity was observed at 55°C but not at 50°C indicative of a threshold of tolerance higher than wild-type parent that must be surpassed for viral disruption. This threshold observed is a function of temperature as the time is held constant. However, time of incubation may play a role if the temperature was held constant. Further experiments where virions are preheated at lower temperatures over longer periods would answer this. 50°C is above the non-permissive temperature of 39°C where the mutant's *ts* trait is observed. Therefore this structural aberration is not responsible for the *ts* nature of the virus. This is suggestive of a weaker μ1-σ3 interaction due to a misfolded σ3 protein. Three non-silent mutations in the S4 gene segment that result in three amino acid changes have already been identified (Danis *et al.*, 1992; Shing & Coombs 1996). To further our understanding of the protein-protein interaction, it would be beneficial to examine protein secondary structure predictions to see if there are any dramatic changes in conformation. Moreover, mass spectrometric analysis, as discussed below, would confirm the presence of any major conformational change in σ3.

If the outer capsid is removed to yield the core particle, will the core retain structural stability comparable to virions in response to elevated temperatures? Or is the outer capsid vital to particle stability? Furthermore, what affects does heat have, if not on structure, than on enzymatic function? The next set of experiments helped resolve such questions and at the same time produce more questions.

*tsD*357 and *tsG*453 virions were converted to cores and purified. Cores were then preheated at various high temperatures, cooled on ice, and then examined for transcriptase activity as described in Results section 3.2.4. Two surprising observations were made in which *tsD*357 was revealed to be more resistant to, whereas *tsG*453 was more susceptible to,

heat induced loss of transcriptase activity than wild-type parent T3D, a finding similar to past observations (Cross & Fields 1972). Both results warrant a more in-depth analysis.

Although replication by *tsD*357 virions is impaired at elevated temperatures, purified *tsD*357 cores are less susceptible to heat-induced loss of transcriptase activity than T3D cores. To determine whether this phenotypic difference may be structurally related, an equivalent number of pre-heated *tsD*357 and T3D core samples were examined by electron microscopy to determine whether any visible structural alterations were present. Electron micrographs revealed the core particles from both clones to be structurally intact. However, electron microscopic visualization will not tell us whether major structural changes occurred to proteins found inside of the core particle. Results also revealed that 75% of the T3D core particles aggregated after they were heated; however, no such observations were made when examining *tsD*357. It could be possible that pre-incubation at high temperatures affected the surface properties of T3D such that resultant aggregation restricted transcription. To determine whether this may be the case, reassortants were exploited to determine which gene was phenotypically responsible. A gene encoding a core surface protein would add credence to the above probability.

T1L x *tsD*357 reassortants were amplified and purified to map this phenotypic difference. Reassortant cores were pre-incubated at a high temperature, cooled and then allowed to transcribe. Their transcriptase activities were compared to the transcriptase activities of non-preheated core samples. Reassortants were organized into two panels which revealed a phenotypic map to the L1 gene with no exceptions. These results suggest that a mutation or mutations in the L1 gene encode an altered RdRp that can either stabilize or facilitate transcription more so than the RdRp found in wild-type parent T3D. No gene that

encodes a major core surface protein was responsible. This observation then does not support the theory that aggregation was responsible for the decrease in transcriptase activity. Further electron microscopic observations of T1L x *tsD*357 reassortant preheated cores would either refute or support this conclusion as well as an increase in the panel size of reassortants to solidify the gene responsible. The current panel of tested reassortants suggests that the L1 gene is responsible. The logical next step would be to sequence the gene to learn what effects a mutation or mutations would have on the secondary structure of the encoded protein.

The L1 genes from both *tsD*357 and T3D were sequenced. One silent mutation and two non-silent mutations were found in the *tsD*357 L1 gene when compared to the T3D L1 gene sequence. The two non-silent mutations resulted in the following T3D to *tsD*357 amino acid changes: isoleucine to serine at codon location 399, and asparagine to serine at codon location 1048. Various prediction programs were then used to predict the resulting protein secondary structure. No prediction program alone can offer enough confidence to a single prediction; therefore, many programs were chosen that yielded a prediction based on different algorithms to strengthen the probability of the overall prediction. A few of the programs predicted a minor change at amino acid number 1048 whereas six of the seven programs predicted a major change at amino acid number 399. The six programs provide concerted predictions that show an $isoleucine_{399}$ to $serine_{399}$ residue change results in an increase in the hydrophilic nature of the region surrounding amino acid 399 as well as a strand to coil morphological change.

Protein λ3 has been shown to consist of multiple domains (Tao *et al.*, 2000). Amino acids 2-380 form a structural domain dedicated to stability. Amino acids 381-890 form the

highly conserved characteristic finger/palm/thumb domain found in all RNA polymerases. The remaining amino acids, 891-1265, form an overlying ringlet/bracelet that is believed to serve primarily as support. It would seem logical that a mutation in the middle domain may have more of a profound effect as it is in the catalytic heart of the enzyme and is more conserved than the other domains. The mutation at codon 399, where a major structural change is predicted to occur, lies in this catalytic portion of the enzyme. Thus, one would expect a definite effect when an amino acid in a conserved region is mutated such that there is a large change in polarity. In this case, the effect is increased particle stability as the mutated L1 gene encodes an RdRp that is less sensitive to heat-induced loss of transcriptase activity. These observations together with the reassortant analysis, suggests that the L1 gene contains a key amino acid change at number 399 that results in increased stability of the RdRp.

The underlying question still remains: if transcription is stable in cores after being exposed to high temperatures, then what explains the *ts* nature of the clone and why are empty virion particles produced and only low levels of RNA detected, a possible sign of impaired transcription? These experiments suggest that the *ts* lesion encodes a misfolded protein that can only be packaged at more tolerant permissive temperatures. Once it is packaged, it is "locked" into place and can function at all temperatures. However nascent misfolded protein has a difficult time becoming packaged at non-permissive temperatures but not at permissive temperatures. The low levels of dsRNA and ssRNA observed at the non-permissive temperature would then be from the initial virions only. If nascent core-like particles were effectively assembled, as found at permissive temperatures, the levels of dsRNA and ssRNA would increase as these particles also undergo transcription.

Furthermore, it appears as though the replicase nature of the mutated protein is also adversely affected. Unpackaged or free-floating misfolded RdRp does not function at non-permissive temperature when newly produced. However, it would function if produced at permissive temperatures, assembled, and then allowed to carry out its enzymatic functions at the non-permissive temperature. The identified mutations in the L1 gene actually serve to promote RdRp stability once effectively packaged.

One final question which remains unanswered is whether these mutations affect the rate of transcription, or the integrity of the RdRp itself. This can be answered through electron microscopic observation of transcribing cores that have been preheated. If electron micrographs reveal mRNA being equally extruded through the λ2 spikes in both *tsD*357 and T3D cores that were preheated, this would suggest then that the *rate* of transcription must be affected by the mutations. The actual synthesis would not be affected as the total amount or mRNA in T3D is less than in *tsD*357. Synthesis of mRNA is indicative of a structurally sound polymerase. If the electron micrographs instead reveal that not all T3D cores are synthesizing mRNA, then the observed decrease in T3D's transcriptase activity is a result of a less structurally stable RdRp and a more structurally stable one in *tsD*357.

Another possibility to explore is that the mutation may impair replicase ability and not transcriptase activity of the RdRp, evident through cores that are able to transcribe as efficiently as their wild-type parent. The past observations of less ssRNA, dsRNA and protein production by *tsD*357 at the non-permissive temperature support a plausible theory. Before a nascent core-like replicase particle can carry out transcription to synthesize ssRNA transcripts, its encapsidated mRNA genes must first be replicated (for a review, please refer to Introduction section 1.3.2). If no replication occurs, no ssRNA can be generated and

subsequently a decreased amount of protein will be present as no transcripts are available for translation. Therefore the lack of RNA and protein production is not a function of transcriptional impairment but rather of dysfunctional replication. Core functional studies presented here show that transcription may not be responsible. Instead, the impediment is at the replication level. Such a theory cannot be challenged accurately, as to date, an effective *in vitro* replication assay for reovirus has yet to be developed.

Contrary to *tsD*357, *tsG*453 purified cores are more susceptible to heat-induced loss of transcriptase activity, a phenotype which emerges when preheated at 55°C for 15 minutes. When examined by electron microscopy to determine if any structural alterations exist, core particles were intact and no abnormalities in the integrity of the cores were visible at a magnification of 100,000X. Like *tsD*357, this does not imply that no structural change has occurred within the core particle in non visible proteins. To help investigate why *tsG*453 cores are more susceptible than their wild type parent T3D to a dramatic decrease in transcriptase activity when exposed to heat, selected purified T1L x *tsG*453 reassortants were converted to cores and purified. These cores were then preheated at 60°C for 15 minutes, and their transcriptase activities were compared to their non-preheated counterparts. The reassortant map indicates either the L1, S3 and/or the S4 gene are responsible for the phenotypic difference.

The S3 and S4 genes encode non-structural protein σNS and outer capsid protein σ3 respectively, both of which are absent from core particles. By reason of elimination, the L1 gene which encoded the RdRp may be phenotypically responsible. However, to strengthen L1's involvement requires that the panel of reassortants be expanded. Confirmation of L1 gene involvement would imply that *tsG*453 contains a previously undetected lesion in its L1

gene. This would then re-classify *tsG*453 as a double mutant. To determine what effect the lesion has on the secondary structure of the protein requires future sequencing of the gene. Once the sequence is determined, computer based programs can predict any change in the protein's secondary structure.

It would be premature to exclude the S3 and S4 gene completely, as possible contributing factors. Perhaps the L1 gene is not responsible, and instead either or both of S3 and S4 are. However unlikely it may seem, if the latter case is true, then this suggests a previously unknown function of the S3 and/or S4 gene itself in transcription. Perhaps there are previously undetected transcriptional sequence signals within the gene(s) that are recognized by the RdRp, the μ1 polymerase cofactor, or any other core protein implicated in transcription. These signals may have been affected by possible mutations. Evidence of such signals would be a novel finding in reovirus. Only by expanding the panel of reassortants will such questions be answered.

Reovirus *ts* mutants still prove to be an invaluable tool to characterise viral proteins. They provide a molecular understanding and basis to what affect mutations may have on the virion and virion life cycle. However, *ts* mutants have their limitation in the ability to provide *whole* structural information of a protein but instead serve to provide *regional* structural information of a protein and functional phenotyping. Therefore to broaden our structural understanding of proteins as a whole, the use of more sensitive techniques were adopted. A recently refined method used to characterise proteins involves mass spectrometry (Loboda *et al.*, 2000; Shevchenko *et al.*, 2000), the driving force behind the focus of the next several sections.

4.3. Orientation of viral capsid proteins.

To date, there has been only limited evidence to the exact placement of viral proteins within the bi-layered capsids of reovirus. Analysis of purified virions and cores by limited proteolysis and mass spectrometry has furthered this understanding and has provided strong evidence to the nature of viral proteins in terms of structure and orientation. However, a major obstacle when analysing virion or core samples presented itself, one that had to be initially addressed. Both particles are suspended in high concentrations of salts to retain the particle's integrity. High salts, unfavourable to mass spectrometry, can substantially increase background noise and generate salt ions for each peptide. To circumvent this problem, it was necessary to dilute virion samples after digestion with dH_2O. As the concentration of virions was high to begin with, the dilution of peptides would not significantly affect their detection because MALDI QqTOF can measure peptides at attomolar (10^{-18}) concentrations (Loboda *et al.*, 2000; Shevchenko *et al.*, 2000). On the other hand, cores are present in lower concentrations, a necessity for optimal transcription. Therefore, diluting the resulting peptides did decrease their abundance and would have allowed for missed detection of certain peptides. Therefore, to avoid dilution, samples were concentrated first by lyophilizing to remove standing buffer, then resuspended in a smaller volume of dH_2O. This proved far more effective and allowed for subsequent detection of peptides.

Digestion with trypsin and V8 protease at pH 7.4 revealed a sequential digestion of outer capsid proteins σ3 followed by μ1. Furthermore, digestion by both proteases revealed a similar pattern. Protein σ3 digestion initiated within a protease hyper-sensitive region, suggesting that this region is located on the external surface of the virion. An interesting observation occurred with the time of appearance of tryptic peptide fragment 144-162.

Protein σ3 was digested on either side of this region, yet this peptide fragment did not appear until later in the digestion. This perhaps suggests that the peptide may have been particle bound, and it may be within this region where σ3 interacts with underlying μ1. The release of the peptide did not occur until σ3 was completely digested. Perhaps with the removal of the entire σ3 protein, μ1 which was initially bound in such a manner by the interaction with σ3, may have undergone some form of conformational change. This change would then cause a weak association with the peptide fragment which would allow it to disassociate and hence, be detected. This interesting result was not detected with V8 protease. This is probably due to the fact that there are far fewer cleavage sites for V8 protease than there are for trypsin which could result in the lack of detection of such a fragment.

Protein μ1's cleavage pattern differed from that of σ3. Whereas σ3 digestion initiated within one centralized location, there were two sites of initiation in μ1. This suggests that μ1 is folded in such a way that there are two surface exposed regions or lobes that face the external surface. A schematic model of protein orientation is shown in Figure 29. These surface exposed regions may function as binding sites for the overlaying σ3 protein. The middle portion of μ1 is the last to be cleaved during trypsin digestion which may suggest that it is the region that is buried deep and functions as the interactive site with the underlying capsid protein λ1 and σ2. It may be possible that μ1 is no longer in its σ3-bound state, and may undergo a conformational shift in the absence of σ3-induced constraints (once σ3 is digested away) to reveal the μ1 peptide profile observed. If this is the case, then the two primary points of digestion may or may not be the σ3 binding sites.

Two other interesting observations were made with regards to μ1 digestion. During trypsin digestion, immediately preceding σ3 digestion, a short fragment of eight residues

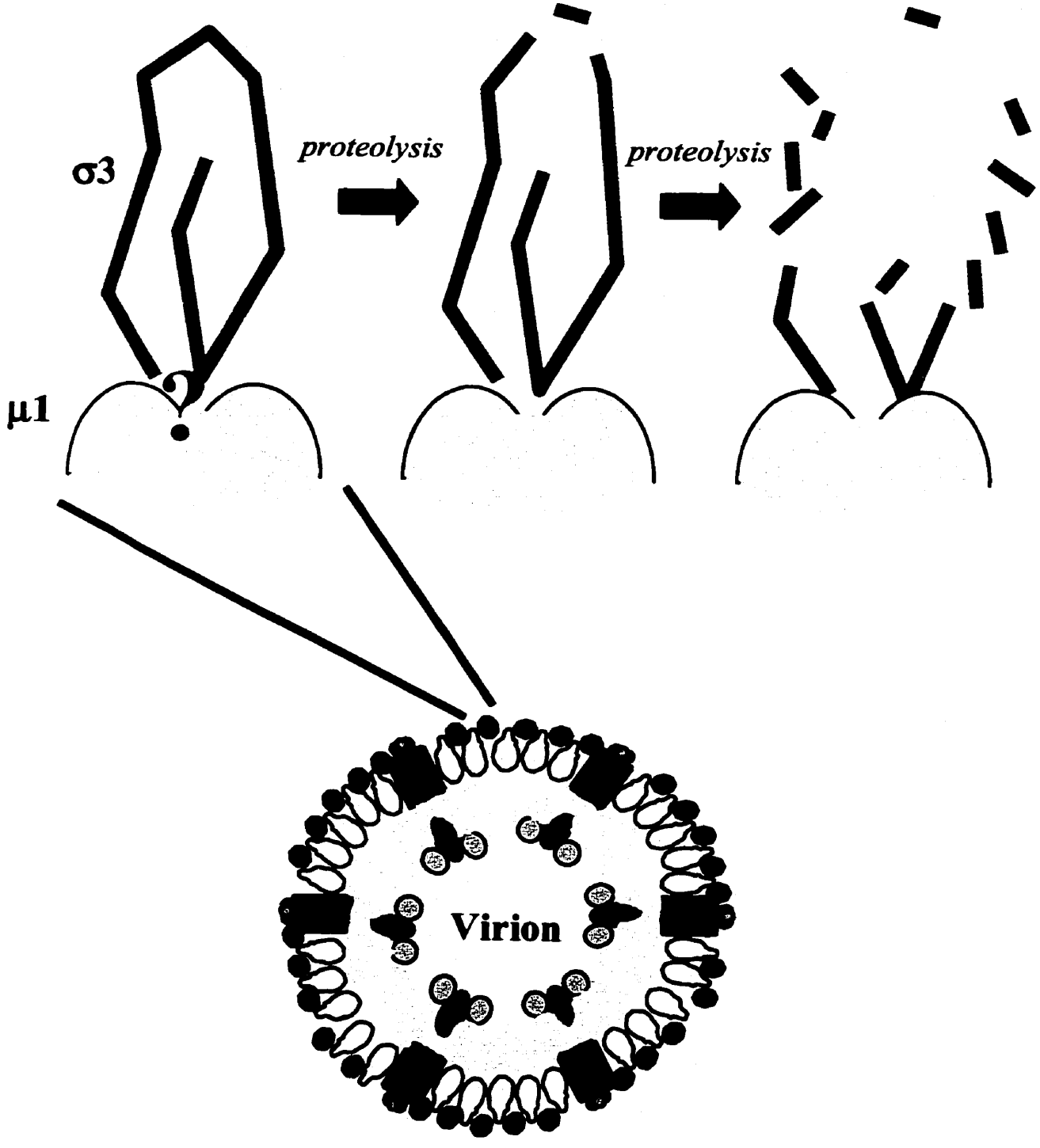
σ3
proteolysis
proteolysis
μ1
Virion

Figure 29. Schematic model of virion capsid protein orientation and digestion. A section of the virion outer capsid (σ3 and part of μ1) is enlarged. σ3 is drawn such that an internal region is shown to interact with underlying μ1. (?) indicates that the basis of this interaction is unknown. Proteolysis of σ3 results in digestion initiating in a protease sensitive region located on the most external surface exposed area of the protein. μ1 is drawn as a bi-lobed structure indicating that there are two surface exposed regions within the protein. These regions, being more external, are potential σ3 binding sites that become susceptible to proteolytic digestion once the entire σ3 protein is removed.

which corresponds to the extreme C-terminus of μ1, is released. This is surprising as it is generally believed that the μ1 protein is not surface exposed. However, the appearance of this fragment is suggestive that the C-terminus of μ1 is accessible to trypsin. If this is the case, this would then suggest that the C-terminus portion of μ1 may be slightly exposed to the surface. Based on the X-ray crystallographic structure, and on the cryoelectron microscopic image of the virion, there is ample room for trypsin to access the μ1 protein. σ3 monomers are arranged in non-interacting clusters of six (Figure 1C). Trypsin may have access to a surface exposed region of an arm of μ1 either within the centre of these clusters or in the area between them. If a single arm of μ1 is indeed protruding, possibly serving as some sort of anchor to σ3, then methods such as cryoelectron microscopy and X-ray crystallographic imaging may not detect it. Perhaps, the arm of μ1 intertwines within the overlaying σ3 protein with its C-terminus exposed but the rest of the arm buried. Schematic models depicting possible renderings of this phenomena are shown in Figure 30. This would then provide the first real evidence of surface exposure of μ1, a theory which could not have been supported until now.

Tandem MS has also identified a post-translational modification of σ3. An additional mass of 42.0 is indicative of an acetyl group and upon close calculations of the data, it is the first amino acid, methionine which bears the acetyl group. This would provide the first evidence of an N-terminal modification to σ3. Current studies in another laboratory, under the supervision of Terry Dermody, have shown the inability to detect the N-terminus fragment of σ3 from an acrylamide gel (personal communication). The inability to detect a peptide fragment from the gel is suggestive of an interfering modification that causes a tight association with the acrylamide polymer, and in this case, may be attributed to the acetyl

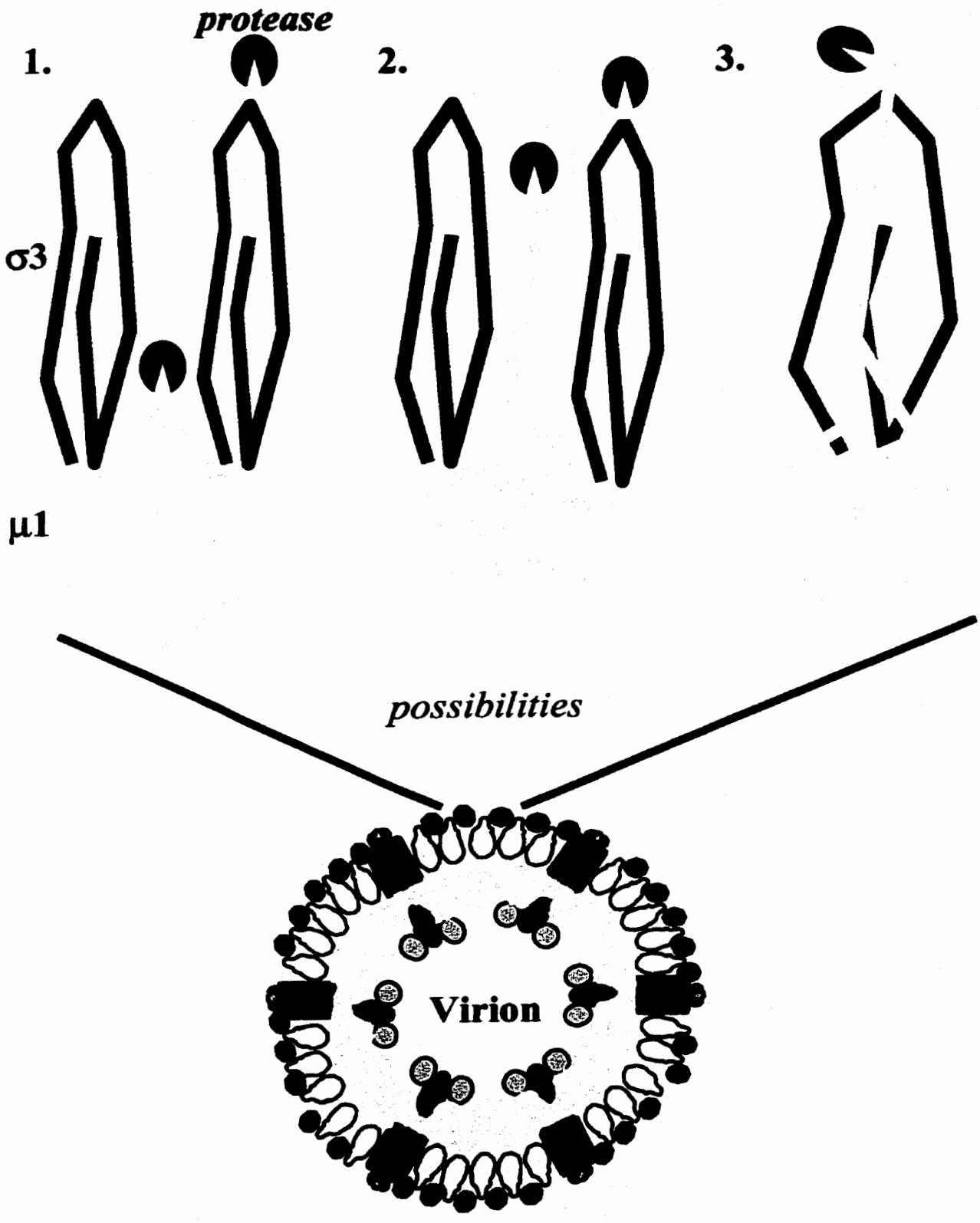
protease
1.
2.
3.
σ3
μ1
possibilities
Virion

Figure 30. Possible models depicting various σ3 and μ1 interactions. A section of the virion outer capsid (two σ3's and one μ1) is enlarged. Three possible models are illustrated to explain the appearance of the initial C-terminus μ1 fragment. 1. Non-interacting σ3 monomers are spaced far enough to allow for protease digestion of μ1 between them. This could occur within the centre of a cluster of six monomers, or in the area between neighbouring clusters (for a review of σ3 orientation on the outer capsid, please refer to discussion and Figure 1C). **B.** Protease may have access to the C-terminus "arm" of μ1 which may extend outwards. This extended arm may occur within σ3 clusters, between adjacent clusters, or between neighbouring σ3 monomers. **C.** The interaction between μ1 and σ3 may be more intricate in nature such that an arm of μ1 weaves through σ3, possible serving as a σ3 anchor. After proteolytic digestion of the initial μ1 fragment, the remainder of the protein may be protected by σ3 such that its exposure to protease does not occur until after complete digestion σ3.

group. Furthermore, not knowing that the N-terminus was acetylated, the investigators would not know which fragment to look for. This would not be the first reovirus protein identified with a post-translational modification. Outer capsid protein μ1 has been shown to contain a myristoyl group at its N-terminus (Nibert *et al.*, 1991). The function of an acetyl group at the N-terminus of σ3 is unknown but based on other acetylated molecules, may serve to provide structural support and possibly function as an energy provider for ligand binding. Another possibility is that the acetylation of its N-terminus may be required to differentiate the role σ3 plays during the virus life cycle (for a review, please see Introduction section 1.3.1). Through its ability to bind dsRNA, a feat considered to occur only upon dimerization (Olland *et al.*, 2001), σ3 is thought to counteract the reovirus induced host antiviral defence mechanism (Yue & Shatkin 1997). Protein σ3 also has the capacity to bind ssRNA and may play a role in the assortment complex during particle assembly (Antczak & Joklik 1992). Furthermore, past studies have shown that the efficiency of cellular translation is determined by the cytoplasmic level of σ3 that is not complexed with μ1 (Schmechel *et al.*, 1997). It would seem necessary that there must exist some level of regulation that would dictate in which of the numerous roles σ3 would function. One possible means of control is through μ1 binding, which would effectively remove freely available σ3 protein. Another regulatory role has been postulated to occur upon σ3 dimerization (Olland *et al.*, 2001). These studies provide evidence that perhaps a third level of regulatory control exists; acetylation of σ3 monomers. Acetylation would presumably direct either μ1 binding or σ3's role in assembly as the version of σ3 present in virions is one that is acetylated. To provide support to such a hypothesis, one could test the capacity of non-acetylated and acetylated forms of σ3 to bind to protein μ1.

There is the possibility that acetylation of σ3 may have been the result of either sample preparation or mass spectrometry. However, four separate observations suggest that neither is the case. Firstly, the N-terminus of the other outer capsid protein μ1 is not acetylated. Secondly, the N-terminus of σ3 is not surface exposed based on the observed peptide profiles. Thirdly, different samples pulsed at different laser frequencies did not affect the findings and the acetylated N-terminus of σ3 was present in every repeated trial. Fourth, no other peptide fragments have their N-terminus acetylated. Therefore, although not impossible, acetylation induced by methodology is unlikely the case. The X-ray crystallographic structure of a σ3 dimer does not reveal detectable N-terminus acetylation (Olland *et al.*, 2001). However, it is important to note that the purified protein was baculovirus expressed and its post-translational modification may require other viral proteins during an *in vivo* infection or expression in cell lines typical for a reovirus infection. Perhaps dimerization only occurs in the absence of N-terminus acetylation, providing additional credence to the aforesaid possibility of N-terminus-directed role differentiation.

Cores were also digested with trypsin to yield peptide profiles. Unlike the sequential digestion observed with virion particles, core capsid proteins were digested simultaneously. This is indicative of equally accessible surface exposed regions of the proteins. Core spike protein λ2 digestion initiated at different locations which would be expected as the spike, made up of five λ2 monomers, is a protruding structure that is predominantly exposed. On the other hand, major core capsid proteins λ1 and σ2 are digested initially from their N-terminus and C-terminus respectively. The orientation of these proteins is arranged such that the N-terminus of λ1 and the C-terminus of σ2 are surface exposed and both equally accessible. The λ1 digestion evidence contradicts the current X-ray crystallographic core

structure of the T3D core particle. The initial fragment, according to this crystal structure, is located towards the interior of the capsid. If the core crystal structure is correct, then how can trypsin cleave at a site that is inside the core capsid? There are two possible explanations. First, perhaps the cores were disassociated before digestion with protease and would thus allow access to the entire surface regions of the core proteins. However, electron microscopic analysis shows that these core particles were not disassociated. A second plausible solution is that the X-ray crystallographic rendering of the core particle does not accurately represent core particles in nature. There may be a misrepresentation of the position of the λ1 proteins. The crystal structure has it such that each λ1 protein is situated in the identical manner. However, it may very well be possible that the λ1 proteins may alternate in their orientation. This would then allow for N-terminus exposure on only some λ1 proteins. If this was the case, then we should have seen digestion initiation from more than one location, which we do not. The crystallographic structure presents a rigid representation of the virus. Most cell structures are flexible and it would not be unreasonable to propose flexibility in proteins; therefore, the crystal structure is correct but changes occur in the liquid state. Therefore I propose, since mass spectrometry, like x-ray crystallography, is a highly accurate and sensitive means of measurement, that certain λ1 protein domains, crystallographically determined as being internal, can be transiently exposed on the capsid surface. Past mass spectrometry studies with flock house virus offers precedent as certain solvent-accessible domains, defined as being internal to the capsid by X-ray crystallography (Fisher and Johnson, 1993), were also transiently present on the viral surface (Bothner *et al.*, 1998). In yet other studies, poliovirus was shown to be capable of translocation of its internal proteins to the exterior viral surface (Li *et al.*, 1994). Such a model may be the case in

reovirus as well. One further fact that must be mentioned is that the actual reovirus core X-ray crystallographic structure is not of the reported T3D, but instead of a reassortant (communication with the author). This may or may not have a negative bearing on the structure, but the possibility that it may should not be ignored.

When the digestion pattern of T1L and T3D cores are compared, slight differences can be observed in the order of peptide appearance. The location of the T1L initial fragments was also identified on the core crystal structure of *T3D* as T1L cores have not yet been successfully crystallized, a phenotype attributed to the L2 gene (λ2) (Coombs *et al.*, 1990). One would not expect that the two core particles would be 100% identical as sequence divergence between the two strains, although not high for most genes, would encode related proteins that had amino acid differences. The differences in the digestion pattern provides evidence that subtle conformational variance exists in core particles between the two strains. To answer whether a significant structural difference exists in λ2 that is responsible for the ability of cores to crystallize, a longer time course digestion and a more detailed analysis between the two strains is required.

4.4. Conformation changes within viral capsids.

Binding of the virion to the cellular receptor has been shown to lead to a conformational change in the viral capsid as cell-bound virions are more resistant to pepsin digestion than unbound virions (Fernandes *et al.*, 1994). Furthermore, this conformational change is totally reversible as bound virions reverted back to their pepsin sensitive state when released from the cell surface. An altered conformational state may be necessary for viral entry and subsequent uncoating; whether this conformational change occurs and is maintained

by receptor binding or through other means during endocytosis remains to be answered.

Mass spectrometry has been used in the past to provide evidence of conformational changes in other viruses such as in flock house virus (Bothner *et al.*, 1998), human rhinovirus (Lewis *et al.*, 1998a), and in Sindbis virus (Phinney *et al.*, 2000). Flock house virus capsids underwent a change in conformation when treated with different solvents (Bothner *et al.*, 1998). Human rhinovirus, when bound to antiviral agents, was shown to undergo localized conformational changes that stabilized the viral capsid (Lewis *et al.*, 1998). Low pH exposure caused conformational changes in the membrane glycoproteins of Sindbis virus (Phinney *et al.*, 2000). MALDI QqTOF mass spectrometric analysis of purified reovirus virions provides evidence that T1L virions undergo a conformational change in their protein structure when exposed to acidic pH. Past evidence had alluded to this fact, however, this provides the first real evidence that clearly demonstrates a shift in the primary exposed surface region of σ3. Pepsin digestion is non-specific; it will cleave a protein on the most exposed surface. Trypsin works in the same way but is limited by its amino acid specificity. The region which is cleaved by pepsin at low pH does contain trypsin cleavage sites. Had this region been more accessible at the higher pH, it would have been cleaved initially by trypsin. The same can be said with regards to pepsin proteolytic digestion; had the virion retained its form from high pH to low pH, then pepsin would have cleaved in the region where trypsin had. However as this is clearly not the case, this highly suggests that the σ3 protein changes in either orientation or conformation when exposed to a low pH. This morphological change does not affect the integrity of the virion as particles retained their form for at least an hour at pH 3.0 as revealed by electron microscopic analysis. These results are consistent with past studies that have shown the remarkable stability of virions as they were able to maintain their

morphology at pH's as low as 2.0 while still maintaining infectivity (Stanley 1967; Fields & Eagle 1973). Upon analysis of the X-ray crystallographic structure of the σ3 monomer, the sites initially cleaved at both pH's reside in an area of higher flexibility. This would add confidence to the notion that the protein is able to shift in form without becoming disassociated or without jeopardizing the virion particle's integrity. Therefore, reovirus virions are not as structurally rigid as previously thought but instead have the capacity to undergo a conformational change while preserving the particle as a whole. This phenomenon is referred to as viral *breathing* and has been observed in other viruses such as the common cold virus, human rhinovirus, (Lewis *et al.*, 1998a; Phinney *et al.*, 2000).

Despite strong evidence of a conformational change at a low pH, V8 protease, a protease capable of proteolytic activity at both acidic and neutral pH's, does not reveal evidence that a conformational shift has occurred. In fact, initial observation of the data would suggest no such alterations took place as the peptide profile at both pH 4.5 and pH 7.4 are identical. However, the V8 protease characteristics are highly dependent on reaction conditions which will define which sites are accessible. Furthermore, V8 protease is not as enzymatically active as trypsin is. The area that should have been targeted at pH 4.5 is not targeted at pH 7.4 either. Therefore, the lack of an obvious change in peptide digestion is not a reflection that a conformational change did or did not occur.

Previous findings have indicated that virions undergo a conformational change when they bind to cellular receptors and whether this change is necessary for viral capsid disassembly remains unknown (Fernandes *et al.*, 1994; Shepard *et al.*, 1995). The evidence provided here shows that the virions undergo a change in conformation at low pH exposure, a condition virions experience early in the course of a cellular infection. It is not known

whether this change is similar to the change observed during receptor binding but if it is, then a virus that allows for a sustained conformational change may require it for viral capsid disassembly. On the other hand, if the conformational changes are different, then there possibly is no significance to the earlier conformational change, except to perhaps allow for the virion to maintain its integrity. Furthermore, the flexibility may function to tolerate other changes such as when the cell attachment protein participates in protein:protein binding.

Cryoelectron microscopic images of transcriptionally active and inactive cores has suggested that cores can undergo a conformational change (Yeager *et al.*, 1996). The limitation of the data obtained from such studies is that it cannot accurately pinpoint areas of conformational changes. Instead, it suggests a general picture of conformational change within the core particles. Analysis of transcribing and non-transcribing cores by mass spectrometry allowed us to overcome such limitations. Both T1L and T3D cores experience a change in their conformational state. Changes are predominant in the core spike protein λ2. However, less noticeable changes occur in the core capsid proteins λ1 and σ2, changes that would be imperceptible by cryoelectron microscopy due to resolution limitations. Furthermore, electron microscopic analysis reveals that the cores do retain their integrity in both states indicating that this shift in conformation is not detrimental to the core particles. One would expect that λ2 would be the protein to experience the highest level of conformational change as this is the protein through which NTP's are thought to enter, and mRNA is extruded, i.e. a highly functional protein (Gillies, *et al.*, 1971; Bartlett *et al.*, 1974). When these proteins were examined for their flexibility using the program Rasmol, λ2 was shown to have the highest. The core spike is made up of five λ2 monomers that form a channel that is 70 Å diameter at its widest and 15 Å diameter at the top (Reinisch *et al.*,

2000). This channel has a total volume capacity of 2×10^5 Å^3, large enough to accommodate up to 300 nucleotides of nascent mRNA. It remains unknown whether this conformational change is due to either the availability and entrance of substrates, the generation of mRNA, or both. It also remains to be determined whether the changes in the core capsid proteins are a result of a λ2 shift that would affect the remainder of the capsid shell, and hence the core capsid proteins, or whether this shift is due to enzymatic proteins within the core that may change in response to a transcription supportive environment.

Core capsid protein, λ1, has recently been shown to possess NTPase/helicase activity (Bisaillon *et al.*, 1997; Bisaillon & Lemay 1997a; Bisaillon & Lemay 1997b) and can bind nucleic acids nonspecifically (Lemay & Danis 1994). This protein may play an integral role in providing the energy for the necessary unwinding of the RNA duplexes for transcription. Therefore, it is possible that a change in its conformation occurs while providing enzymatic activity yet maintaining its structural role during transcription. This change in state may be responsible for the difference in the observed peptide digest profiles for λ1.

One important issue to address is whether the order of peptides seen in transcribing cores are simply the result of a slower digestion rate due to mRNA interference. The answer to this is no, as close inspection of the peptides reveals that such a situation is not possible. Had mRNA interfered in some way with digestion, i.e. by covering and hence protecting external surfaces of the protein, then one would see a decrease in the peptides observed when in fact there are actually more initial peptides identified in transcribing than in non-transcribing cores, which have no mRNA.

These of experiments describe a virus that is dynamically intact which undergoes conformational changes at the virion and core level while maintaining integrity of the particle.

It remains to be seen whether these conformational changes are reversible or if the virion or core particle becomes locked into place once morphologically changed. Based on evidence from other viruses, chances are that reovirus is capable of fluctuating between different states and that changes in conformation are reversible. The fact that a certain level of flexibility exists in proteins, and that they are able to undergo a change in state while preserving their structure, supports this probability (Fernandes *et al.*, 1994; Shepard *et al.*, 1995; Bothner *et al.*, 1998; Lewis *et al.*, 1998a; Phinney *et al.*, 2000). Mass spectrometric analyses of virions and cores exposed to an environment that would induce a conformational shift and then brought back to original conditions would lay this issue to rest.

4.5. Future directions.

The experiments described here only begin to scratch the surface of what remains to be explored. It is useful to employ various techniques and methodologies to understand a protein's characteristics, whether examining its functionality or its structural aspects. No single method can stand alone when attempting to provide an in-depth analysis of a protein or proteins. It is imperative that methodologies are brought together as each will have something different to offer. Combined contributions are what solidify theories and allow for hypothesis testing.

The studies outlined in this work bring together old and new methodologies to characterise and further our understanding of reovirus proteins. The use of temperature sensitive mutants have long proven successful in relating functionality to a protein. To study the inner capsid protein λ3, *tsD*357 and *tsG*453 were looked at more closely. Identification of a phenotypic difference in transcriptase activities within these mutants helps to understand

the protein in question. In *tsD*357, sequencing of the *ts* lesion bearing gene, L1, has identified three mutations; one of which is proposed to be the significant factor responsible for conferring increased enzymatic stability. This mutation, although beneficial for transcription, can at the same time be detrimental to the virion's life cycle within the cell. Therefore it is evidently possible that a single mutation, falling in the highly conserved catalytically active region of the RdRp, can both positively and negatively affects an enzyme's capabilities.

On the other hand, *tsG*453 appears to be a double mutant in that there are possibly two lesion affected genes, L1 and S4, in which only one of them, S4, is responsible for conferring temperature sensitivity. The *tsG*453 story is far from complete. As heat-inactivation experiments have revealed a weak interaction between the outer capsid protein σ3 and the underlying protein μ1, analysis by mass spectrometry would help identify how the structure and interaction have been affected. Mass spectrometry has been used in other viruses to identify mutant strains of a virus (Lewis *et al.*, 1998b) and the effects of point mutations (Lewis *et al.*, 1998c) and would serve to benefit reovirus *ts* mutant studies. Secondly, the reassortant panel used to identify the transcriptase phenotype must be extended to confirm that the L1 gene is phenotypically responsible. Sequencing of the gene will allow one to predict what protein secondary changes have occurred and what they mean.

Applying mass spectrometric analysis to virions and cores have revealed an abundant amount of information and has provided strong evidence to post-translational modification of σ3, orientation of proteins, and conformational changes. These experiments can be extended by examining digestion of T3D virions and drawing comparisons between the two strains. In fact, examining any strain will help immediately identify whether they are structurally distinct.

Past data have suggested a defined cascade of proteolytic digestion of σ3 degradation leading to the virion-to-ISVP transition (Miller & Samuel 1992; Virgin *et al.*, 1994; Shepard *et al.*, 1995). It is also believed that this digestion is necessary to allow the underlying μ1 proteins to assist reovirus particle penetration of the cellular membrane (Nibert & Fields 1992; Lucia-Jandris *et al.*, 1993; Tosteson *et al.*, 1993; Hazelton & Coombs 1995; Hooper & Fields 1996). Virions, with the absence of proteases in the cell media, are able to still infect cell cultures, offering counter evidence that σ3 must be digested extracellularly. However, σ3 digestion does occur within lysosomes. It is within the lysosomes that perhaps the role of μ1-membrane interactions become important. However, virions must be digested completely to core particles to allow for transcription to occur, questioning the necessary role of μ1. Conceivably μ1 initiates membrane interactions that will facilitate core release prior to further digestion of the core particle itself. It would be important to localize what regions of σ3 must be lost prior to membrane penetration mediated by μ1. Using tightly controlled limited proteolysis and mass spectrometry, such questions can and will be answered in the future.

Furthermore, one can isolate the λ3 protein from T1L, T3D, and the two *ts* mutants studied by gel extraction and then carry out mass spectrometric analysis on them. Such experiments will help elucidate structural properties of the enzyme. However, one must take into consideration that the isolated protein may be denatured and not truly representative of its state *in vivo*.

Mass spectrometry analyses with the use of relevant cellular proteases such as cathepsins, which are present in lysosomes, would also shed new light to their function and how digestion actually proceeds during the entry portion of the reovirus life cycle. Such

evidence and the evidence provided here have helped further our knowledge of reovirus protein structure and function. These studies have paved the way for future findings. Correlations from these significant findings using reovirus as a model can be applied to help further our understanding of *Reoviridae* as a whole, of other non-enveloped RNA viruses and of the general nature of all viruses.

REFERENCES

Antczak, J. B., Chmelo, R., Pickup, D. J., and Joklik, W. K. (1982). Sequence at both termini of the 10 genes of reovirus serotype 3 (strain Dearing). *Virology*, **121**, 307-319.

Antczak, J. B. and Joklik, W. K. (1992). Reovirus genome segment assortment into progeny genomes studied by the use of monoclonal antibodies directed against reovirus proteins. *Virology*, **187**, 760-776.

Atmar, R. L., Neill, F. H., Romalde, J. L., Le-Guyader, F., Woodley, C. M., Metcalf, T. G., and Estes, M. K. (1995). Detection of Norwalk virus and hepatitis A virus in shellfish tissues with the PCR. *Appl. Environ. Microbiol.*,. **61**, 3014-3018.

Bartlett, N. M., Gillies, S. C., Bullivant, S., and Bellamy, A. R. (1974). Electron microscopy study of reovirus reaction cores. *J. Virol.*, **14**, 315-326.

Barton, A. F. M. (1983): Handbook of solubility parameters. CRC Press, Boca Raton.

Barton, E. S.; Forrest, J. C.; Connolly, J. L.; Chappell, J. D.; Liu, Y.; Schnell, F. J.; Nusrat, A.; Parkos, C. A. and Dermody, T. S. (2001). Junction adhesion molecule is a receptor for reovirus. *Cell*, **104**, 441-451.

Bassel-Duby, R., Nibert, M. L., Homcy, C. J., Fields, B. N., and Sawutz, D. G. (1987). Evidence that the sigma 1 protein of reovirus serotype 3 is a multimer. *J. Virol.*, **61**, 1834-1841.

Beattie, E., Denzler, K. L., Tartaglia, J., Perkus, M. E., Paoletti, E., and Jacobs, B. L. (1995). Reversal of the interferon-sensitive phenotype of a vaccinia virus lacking E3L by expression of the reovirus S4 gene. *J. Virol.*, **69**, 499-505.

Becker, M. M., Goral, M. I., Hazelton, P. R., Baer, G. S., Rodgers, S. E., Brown, E. G., Coombs, K. M., and Dermody, T. S. (2001). Reovirus sigmaNS protein is required for nucleation of viral assembly complexes and formation of viral inclusions. *J. Virol.*, **75**, 1459-1475.

Berman, D., Berg, G., and Safferman, R. S. (1981). A method for recovering viruses from sludges. *J. Virol. Methods*, **3**, 283-291.

Bisaillon, M., Bergeron, J., and Lemay, G. (1997). Characterization of the nucleoside triphosphate phosphohydrolase and helicase activities of the reovirus lambda1 protein. *J. Biol. Chem.*, **272**, 18298-18303.

Bisaillon, M. and Lemay, G. (1997a). Molecular dissection of the reovirus lambda1 protein nucleic acids binding site. *Virus Res.*, **51**, 231-237.

Bisaillon, M. and Lemay, G. (1997b). Characterization of the reovirus lambda1 protein RNA 5'-triphosphatase activity. *J. Biol. Chem.*, **272**, 29954-29957.

Bodkin, D. K. and Fields, B. N. (1989). Growth and survival of reovirus in intestinal tissue: role of the L2 and S1 genes. *J. Virol.*, **63**, 1188-1193.

Borsa, J., Morash, B. D., Sargent, M. D., Copps, T. P., Lievaart, P. A., and Szekely, J. G. (1979). Two modes of entry of reovirus particles into L cells. *J. Gen. Virol.*, **45**, 161-170.

Both, G. W., Lavi, S., and Shatkin, A. J. (1975). Synthesis of all the gene products of the reovirus genome in vivo and in vitro. *Cell*, **4**, 173-180.

Bothner, B., Dong, X. F., Bibbs, L., Johnson, J. E., and Siuzdak, G. (1998). Evidence of viral capsid dynamics using limited proteolysis and mass spectrometry. *J. Biol. Chem.*, **273**, 673-676.

Bruenn, J. A. (1991). Relationships among the positive strand and double-strand RNA viruses as viewed through their RNA-dependent RNA polymerases. *Nucleic Acids Res.*, **19**, 217-226.

Carneiro, F. A., Ferradosa, A. S., and Da Poian, A. T. (2001). Low pH-induced conformational changes in vesicular stomatitis virus glycoprotein involve dramatic structure reorganization. *J. Biol. Chem.*, **276**, 62-67.

Chakraborty, P. R., Ahmed, R., and Fields, B. N. (1979). Genetics of reovirus: the relationship of interference to complementation and reassortment of temperature-sensitive mutants at nonpermissive temperature. *Virology*, **94**, 119-127.

Chapell, J. D., Goral, M. I., Rodgers, S. E., dePamphilis, C. W., and Dermody, T. S. (1994). Sequence diversity within the reovirus S2 gene: reovirus genes reassort in nature, and their termini are predicted to form a panhandle motif. *J. Virol.*, **68**, 750-756.

Choi, A. H., Paul, R. W., and Lee, P. W. (1990). Reovirus binds to multiple plasma membrane proteins of mouse L fibroblasts. *Virology*, **178**, 316-320.

Clemens, M. J. (1996). Protein kinases that phosphorylate eIF2 and eIF2B and their role in eukaryotic cell translational control. In Mathews, M.; Sonenberg, N. (eds) *Translational Control*. Cold Spring Harbor Laboratory Press, Cold Spring Harbor, New York, pp.139-172.

Cleveland, D. R., Zarbl, H., and Millward, S. (1986). Reovirus guanylyltransferase is L2 gene product lambda 2. *J. Virol.*, **60**, 307-311.

Coffey, M. C., Strong, J. E., Forsyth, P. A., and Lee, P. W. (1998). Reovirus therapy of tumors with activated Ras pathway. *Science*, **282**, 1332-1334.

Coombs, K. M. (1996). Identification and characterization of a double-stranded RNA-reovirus temperature-sensitive mutant defective in minor core protein mu2. *J. Virol.*, **70**, 4237-4245.

Coombs, K. M. (1998). Temperature-sensitive mutants of reovirus. *Curr. Top. Microbiol. Immunol.*, **233/I**, 69-107.

Coombs, K. M., Fields, B. N., and Harrison, S. C. (1990). Crystallization of the reovirus type 3 Dearing core. Crystal packing is determined by the lambda 2 protein. *J. Mol. Biol.*, **215**, 1-5.

Coombs, K. M., Mak, S. C., and Petrycky-Cox, L. D. (1994). Studies of the major reovirus core protein sigma 2: reversion of the assembly-defective mutant tsC447 is an intragenic process and involves back mutation of Asp-383 to Asn. *J. Virol.*, **68**, 177-186.

CRC Handbook of Chemistry and Physics (1977): 57th edition. (by CRC Press, Inc. Cleveland, Ohio)

Cross, R. K. and Fields, B. N. (1972). Temperature-sensitive mutants of reovirus type 3: studies on the synthesis of viral RNA. *Virology*, **50**, 799-809.

Danis, C., Garzon, S., and Lemay, G. (1992). Further characterization of the ts453 mutant of mammalian orthoreovirus serotype 3 and nucleotide sequence of the mutated S4 gene. *Virology*, **190**, 494-498.

Drayna, D. and Fields, B. N. (1982a). Activation and characterization of the reovirus transcriptase: genetic analysis. *J. Virol.*, **41**, 110-118.

Drayna, D. and Fields, B. N. (1982b). Genetic studies on the mechanism of chemical and physical inactivation of reovirus. *J. Gen. Virol.*, **63 (Pt 1)**, 149-159.

Dryden, K. A., Wang, G., Yeager, M., Nibert, M. L., Coombs, K. M., Furlong, D. B., Fields, B. N., and Baker, T. S. (1993). Early steps in reovirus infection are associated with dramatic changes in supramolecular structure and protein conformation: analysis of virions and subviral particles by cryoelectron microscopy and image reconstruction. *J. Cell Biol.*, **122**, 1023-1041.

Duncan, R., Horne, D., Cashdollar, L. W., Joklik, W. K., and Lee, P. W. (1990). Identification of conserved domains in the cell attachment proteins of the three serotypes of reovirus. *Virology*, **174**, 399-409.

Faust, M., Hastings, K. E., and Millward, S. (1975). m7G5'ppp5'GmptcpUp at the 5' terminus of reovirus messenger RNA. *Nucleic Acids Res.*, **2**, 1329-1343.

Fernandes, J., Tang, D., Leone, G., and Lee, P. W. (1994). Binding of reovirus to receptor leads to conformational changes in viral capsid proteins that are reversible upon virus detachment. *J. Biol. Chem.*, **269**, 17043-17047.

Fields, B. N. (1971). Temperature-sensitive mutants of reovirus type 3: features of genetic recombination. *Virology*, **46**, 142-148.

Fields, B. N. and Eagle, H. (1973). The pH-dependence of reovirus synthesis. *Virology*, **52**, 581-583.

Fields, B. N. and Joklik, W. K. (1969). Isolation and preliminary genetic and biochemical characterization of temperature-sensitive mutants of reovirus. *Virology*, **37**, 335-342.

Fields, B. N., Laskov, R., and Scharff, M. D. (1972). Temperature-sensitive mutants of reovirus type 3: studies on the synthesis of viral peptides. *Virology*, **50**, 209-215.

Fields, B. N., Raine, C. S., and Baum, S. G. (1971). Temperature-sensitive mutants of reovirus type 3: defects in viral maturation as studied by immunofluorescence and electron microscopy. *Virology*, **43**, 569-578.

Fisher, A. J., and Johnson, J. E. (1993). Ordered duplex RNA controls capsid architecture in an icosahedral animal virus. *Nature*, **361**, 176-179.

Fraser, R. D., Furlong, D. B., Trus, B. L., Nibert, M. L., Fields, B. N., and Steven, A. C. (1990). Molecular structure of the cell-attachment protein of reovirus: correlation of computer-processed electron micrographs with sequence-based predictions. *J. Virol.*, **64**, 2990-3000.

Furuichi, Y., Muthukrishnan, S., and Shatkin, A. J. (1975a). 5'-Terminal m-7G(5')ppp(5')G-m-p in vivo: identification in reovirus genome RNA. *Proc. Natl. Acad. Sci. U.S.A*, **72**, 742-745.

Furuichi, Y., Morgan, M., Muthukrishnan, S., and Shatkin, A. J. (1975b). Reovirus messenger RNA contains a methylated, blocked 5'-terminal structure: m-7G(5')ppp(5')G-MpCp-. *Proc. Natl. Acad. Sci. U.S.A*, **72**, 362-366.

Gaboriaud, C., Bissery, V., Benchetrit, T., and Mornon, J. P. (1987). Hydrophobic cluster analysis: an efficient new way to compare and analyse amino acid sequences. *FEBS Lett.*, **224**, 149-155.

Garnier, J., Osguthorpe, D. J., and Robson, B. (1978). Analysis of the accuracy and implications of simple methods for predicting the secondary structure of globular proteins. *J. Mol. Biol.*, **120**, 97-120.

Gentsch, J. R. and Hatfield, J. W. (1984). Saturable attachment sites for type 3 mammalian reovirus on murine L cells and human HeLa cells. *Virus Res.*, **1**, 401-414.

Georgi, A., Mottola-Hartshorn, C., Warner, A., Fields, B., and Chen, L. B. (1990). Detection of individual fluorescently labeled reovirions in living cells. *Proc. Natl. Acad. Sci. U.S.A*, **87**, 6579-6583.

Gillies, S., Bullivant, S., and Bellamy, A. R. (1971). Viral RNA polymerases: electron microscopy of reovirus reaction cores. *Science*, **174**, 694-696.

Goldschmidt, G. (1993). An analytical approach for reducing workplace health hazards through substitution. *Am. Ind. Hyg. Assoc. J.*, **54**, 36-43.

Gomatos, P. J. and Tamm, I. (1963). The secondary structure of reovirus RNA. *Proc. Natl. Acad. Sci. U.S.A*, **49**, 707-714.

Gschwender, H. H. and Traub, P. (1978). Purification of mengovirus by freon extraction and chromatography on protein-coated controlled pore glass. *Arch. Virol.*, **56**, 327-336.

Hammond, G. W., Hazelton, P. R., Chuang, I., and Klisko, B. (1981). Improved detection of viruses by electron microscopy after direct ultracentrifuge preparation of specimens. *J. Clin. Microbiol.*, **14**, 210-221.

Hansen, C.M., Beerbower, A., 1971. Solubility parameters. In: Kirk, R.E., Othmer, D.F. (Eds.), Encyclopedia of chemical technology, Interscience Publishers, New York, pp. 889-910.

Hassard, T. H. (1991). Understanding Biostatistics. St. Louis: Mosby Year Book.

Hazelton, P. R. and Coombs, K. M. (1995). The reovirus mutant tsA279 has temperature-sensitive lesions in the M2 and L2 genes: the M2 gene is associated with decreased viral protein production and blockade in transmembrane transport. *Virology*, **207**, 46-58.

Hazelton, P. R. and Coombs, K. M. (1999). The reovirus mutant tsA279 L2 gene is associated with generation of a spikeless core particle: implications for capsid assembly. *J. Virol.*, **73**, 2298-2308.

Hooper, J. W. and Fields, B. N. (1996). Role of the mu 1 protein in reovirus stability and capacity to cause chromium release from host cells. *J. Virol.*, **70**, 459-467.

Huismans, H. and Joklik, W. K. (1976). Reovirus-coded polypeptides in infected cells: isolation of two native monomeric polypeptides with affinity for single-stranded and double- stranded RNA, respectively. *Virology*, **70**, 411-424.

Ikegami, N. and Gomatos, P. J. (1968). Temperature-sensitive conditional-lethal mutants of reovirus 3. I. Isolation and characterization. *Virology*, **36**, 447-458.

Imani, F. and Jacobs, B. L. (1988). Inhibitory activity for the interferon-induced protein kinase is associated with the reovirus serotype 1 sigma 3 protein. *Proc. Natl. Acad. Sci. U.S.A*, **85**, 7887-7891.

Ito, Y. and Joklik, W. K. (1972a). Temperature-sensitive mutants of reovirus. I. Patterns of gene expression by mutants of groups C, D, and E. *Virology*, **50**, 189-201.

Ito, Y. and Joklik, W. K. (1972b). Temperature-sensitive mutants of reovirus. 3. Evidence that mutants of group D ("RNA-negative") are structural polypeptide mutants. *Virology*, **50**, 282-286.

Jameson, B. A. and Wolf, H. (1988). The antigenic index: a novel algorithm for predicting antigenic determinants. *Comput. Appl. Biosci.*, **4**, 181-186.

Joklik, W. K. (1972). Studies on the effect of chymotrypsin on reovirions. *Virology*, **49**, 700-715.

Joklik, W. K. and Roner, M. R. (1995). What reassorts when reovirus genome segments reassort? *J. Biol. Chem.*, **270**, 4181-4184.

Keroack, M. and Fields, B. N. (1986). Viral shedding and transmission between hosts determined by reovirus L2 gene. *Science*, **232**, 1635-1638.

Koonin, E. V., Gorbalenya, A. E., and Chumakov, K. M. (1989). Tentative identification of RNA-dependent RNA polymerases of dsRNA viruses and their relationship to positive strand RNA viral polymerases. *FEBS Lett.*, **252**, 42-46.

Kozak, M. (1981). Possible role of flanking nucleotides in recognition of the AUG initiator codon by eukaryotic ribosomes. *Nucleic Acids Res.*, **9**, 5233-5262.

Kozak, M. (1982). Sequences of ribosome binding sites from the large size class of reovirus mRNA. *J. Virol.*, **42**, 467-473.

Kyte, J. and Doolittle, R. F. (1982). A simple method for displaying the hydropathic character of a protein. *J. Mol. Biol.*, **157**, 105-132.

Le-Guyader, F., Estes, M. K., Hardy, M. E., Neill, F. H., Green, J., Brown, D. W., and Atmar, R. L. (1996). Evaluation of a degenerate primer for the PCR detection of human caliciviruses. *Arch. Virol.* **141**, 2225-2235.

Lee, P. W., Hayes, E. C., and Joklik, W. K. (1981). Protein sigma 1 is the reovirus cell attachment protein. *Virology*, **108**, 156-163.

Lee, P. W., and Leone, G. (1994). Reovirus protein sigma 1: from cell attachment to protein oligomerization and folding mechanisms. *Bioessays*, **16**, 199-206.

Lemay, G. and Danis, C. (1994). Reovirus lambda 1 protein: affinity for double-stranded nucleic acids by a small amino-terminal region of the protein independent from the zinc finger motif. *J. Gen. Virol.*, **75 (Pt 11)**, 3261-3266.

Leone, G., Mah, D. C., and Lee, P. W. (1991). The incorporation of reovirus cell attachment protein sigma 1 into virions requires the N-terminal hydrophobic tail and the adjacent heptad repeat region. *Virology*, **182**, 346-350.

Lewis, J. K., Bothner, B., Smith, T. J., and Siuzdak, G. (1998a). Antiviral agent blocks breathing of the common cold virus. *Proc. Natl. Acad. Sci. U.S.A*, **95**, 6774-6778.

Lewis, J. K., Bendahmane, M., Smith, T. J., Beachy, R. N., and Siuzdak, G. (1998b). Identification of viral mutants by mass spectrometry. *Proc. Natl. Acad. Sci. U.S.A*, **95**, 8596-8601.

Lewis, J. K., Krone, J. R., and Nelson, R. W. (1998c). Mass spectrometric methods for evaluating point mutations. *Biotechniques*, **24**, 102, 104, 106, 108.

Li, Q.; Yafal, A. G.; Lee, Y. M.; Hogle, J.; Chow, M. (1994). Poliovirus neutralization by antibodies to internal epitopes of VP4 and VP1 results from reversible exposure of these sequences at physiological temperature. *J. Virol.*, **68**, 3965-3970.

Liebermann, H. and Mentel, R. (1994). Quantification of adenovirus particles. *J. Virol. Methods*, **50**, 281-291.

Lloyd, R. M. and Shatkin, A. J. (1992). Translational stimulation by reovirus polypeptide sigma 3: substitution for VAI RNA and inhibition of phosphorylation of the alpha subunit of eukaryotic initiation factor 2. *J. Virol.*, **66**, 6878-6884.

Loboda, A. V., Krutchinsky, A. N., Bromirski, M., Ens, W., and Standing, K. G. (2000). A tandem quadrupole/time-of-flight mass spectrometer with a matrix- assisted laser desorption/ionization source: design and performance. *Rapid Commun. Mass Spectrom.*, **14**, 1047-1057.

Lucia-Jandris, P., Hooper, J. W., and Fields, B. N. (1993). Reovirus M2 gene is associated with chromium release from mouse L cells. *J. Virol.*, **67**, 5339-5345.

Mah, D. C., Leone, G., Jankowski, J. M., and Lee, P. W. (1990). The N-terminal quarter of reovirus cell attachment protein sigma 1 possesses intrinsic virion-anchoring function. *Virology*, **179**, 95-103.

Mao, Z., and Joklik, W. K. (1991). Isolation and enzymatic characterization of protein λ2, the reovirus guanylyltransferase. *Virology*, **185**, 377-386.

Mayor, H. D. and Jordan, L. E. (1968). Preparation and properties of the internal capsid components of reovirus. *J. Gen. Virol.*, **3**, 233-237.

McCrae, M. A. and Joklik, W. K. (1978). The nature of the polypeptide encoded by each of the 10 double-stranded RNA segments of reovirus type 3. *Virology*, **89**, 578-593.

Mendez, I. I.; Hermann, L. L.; Hazelton, P. R.; Coombs, K. M. (2000). A comparative analysis of freon substitutes in the purification of reovirus and calicivirus. *J. Virol. Methods*, **90**, 59-67.

Metcalf, P., Cyrklaff, M., and Adrian, M. (1991). The three-dimensional structure of reovirus obtained by cryo-electron microscopy. *EMBO J.*, **10**, 3129-3136.

Miller, J. E. and Samuel, C. E. (1992). Proteolytic cleavage of the reovirus sigma 3 protein results in enhanced double-stranded RNA-binding activity: identification of a repeated basic amino acid motif within the C-terminal binding region. *J. Virol.*, **66**, 5347-5356.

Morgan, E. M. and Zweerink, H. J. (1974). Reovirus morphogenesis. Corelike particles in cells infected at 39 degrees with wild-type reovirus and temperature-sensitive mutants of groups B and G. *Virology*, **59**, 556-565.

Morgan, E. M. and Zweerink, H. J. (1975). Characterization of transcriptase and replicase particles isolated from reovirus-infected cells. *Virology*, **68**, 455-466.

Morozov, S. Y. (1989). A possible relationship of reovirus putative RNA polymerase to polymerases of positive-strand RNA viruses. *Nucleic Acids Res.*, **17**, 5394-

Mustoe, T. A., Ramig, R. F., Sharpe, A. H., and Fields, B. N. (1978a). A genetic map of reovirus. III. Assignment of the double-stranded RNA- positive mutant groups A, B, and G to genome segments. *Virology*, **85**, 545-556.

Mustoe, T. A., Ramig, R. F., Sharpe, A. H., and Fields, B. N. (1978b). Genetics of reovirus: identification of the ds RNA segments encoding the polypeptides of the mu and sigma size classes. *Virology*, **89**, 594-604.

Nibert, M. L. and Fields, B. N. (1992). A carboxy-terminal fragment of protein mu 1/mu 1C is present in infectious subvirion particles of mammalian reoviruses and is proposed to have a role in penetration. *J. Virol.*, **66**, 6408-6418.

Nibert, M. L., Margraf, R. L., and Coombs, K. M. (1996). Nonrandom segregation of parental alleles in reovirus reassortants. *J. Virol.*, **70**, 7295-7300.

Nibert, M. L., Schiff, L. A., and Fields, B. N. (1991). Mammalian reoviruses contain a myristoylated structural protein. *J. Virol.*, **65**, 1960-1967.

Noble, S. and Nibert, M. L. (1997). Core protein mu2 is a second determinant of nucleoside triphosphatase activities by reovirus cores. *J. Virol.*, **71**, 7728-7735.

Norman, K. L. and Lee, P. W. (2000). Reovirus as a novel oncolytic agent. *J. Clin. Invest,* **105**, 1035-1038.

Olland, A. M., Jane-Valbuena, J., Schiff, L. A., Nibert, M. L., and Harrison, S. C. (2001). Structure of the reovirus outer capsid and dsRNA-binding protein sigma3 at 1.8 Å resolution. *EMBO J.*, **20**, 979-989.

Paul, R. W., Choi, A. H., and Lee, P. W. (1989). The alpha-anomeric form of sialic acid is the minimal receptor determinant recognized by reovirus. *Virology,* **172**, 382-385.

Phinney, B. S., Blackburn, K., and Brown, D. T. (2000). The surface conformation of Sindbis virus glycoproteins E1 and E2 at neutral and low pH, as determined by mass spectrometry-based mapping. *J. Virol.*, **74**, 5667-5678.

Ramig, R. F. and Fields, B. N. (1979). Revertants of temperature-sensitive mutants of reovirus: evidence for frequent extragenic suppression. *Virology,* **92**, 155-167.

Ramig, R. F., Mustoe, T. A., Sharpe, A. H., and Fields, B. N. (1978). A genetic map of reovirus. II. Assignment of the double-stranded RNA- negative mutant groups C, D, and E to genome segments. *Virology,* **85**, 531-534.

Reinisch, K. M., Nibert, M. L., and Harrison, S. C. (2000). Structure of the reovirus core at 3.6 Å resolution. *Nature*, **404**, 960-967.

Richt, J. A., Clements, J. E., Herzog, S., Pyper, J., Wahn, K., and Becht, H. (1993). Analysis of virus-specific RNA species and proteins in Freon-113 preparations of the Borna disease virus. *Med. Microbiol. Immunol. (Berl)*, **182**, 271-280.

Roner, M. R., Sutphin, L. A., and Joklik, W. K. (1990). Reovirus RNA is infectious. *Virology*, **179**, 845-852.

Rosen, L. (1962). Reoviruses in animals other than man. *Ann. NY Acad. Sci.*, **101**, 461-465.

Rubin, D. H., Weiner, D. B., Dworkin, C., Greene, M. I., Maul, G. G., and Williams, W. V. (1992). Receptor utilization by reovirus type 3: distinct binding sites on thymoma and fibroblast cell lines result in differential compartmentalization of virions. *Microb. Pathog.*, **12**, 351-365.

Sabin A. B. (1959). Reoviruses. *Science*, **130**, 1387-1389.

Schmechel, S., Chute, M., Skinner, P., Anderson, R., and Schiff, L. (1997). Preferential translation of reovirus mRNA by a sigma3-dependent mechanism. *Virology*, **232**, 62-73.

Seliger, L. S., Zheng, K., and Shatkin, A. J. (1987). Complete nucleotide sequence of reovirus L2 gene and deduced amino acid sequence of viral mRNA guanylyltransferase. *J. Biol. Chem.*, **262**, 16289-16293.

Sharpe, A. H. and Fields, B. N. (1982). Reovirus inhibition of cellular RNA and protein synthesis: role of the S4 gene. *Virology*, **122**, 381-391.

Sharpe, A. H., Ramig, R. F., Mustoe, T. A., and Fields, B. N. (1978). A genetic map of reovirus. 1. Correlation of genome RNAs between serotypes 1, 2, and 3. *Virology*, **84**, 63-74.

Shatkin, A. J., Furuichi, Y., LaFiandra, A. J., and Yamakawa, M. (1983). Double-stranded RNA viruses. In Compans, R.W.; Bishop, D. H. L. eds. Elsevier, New York pp:43-54.

Shatkin, A. J., Sipe, J. D., and Loh, P. (1968). Separation of ten reovirus genome segments by polyacrylamide gel electrophoresis. *J. Virol.*, **2**, 986-991.

Shepard, D. A., Ehnstrom, J. G., and Schiff, L. A. (1995). Association of reovirus outer capsid proteins sigma 3 and mu 1 causes a conformational change that renders sigma 3 protease sensitive. *J. Virol.*, **69**, 8180-8184.

Shevchenko, A., Loboda, A., Shevchenko, A., Ens, W., and Standing, K. G. (2000). MALDI quadrupole time-of-flight mass spectrometry: a powerful tool for proteomic research. *Anal. Chem.*, **72**, 2132-2141.

Shing, M. and Coombs, K. M. (1996). Assembly of the reovirus outer capsid requires mu 1/sigma 3 interactions which are prevented by misfolded sigma 3 protein in temperature-sensitive mutant tsG453. *Virus Res.*, **46**, 19-29.

Silverstein S.C. and Dales, S. (1968). The penetration of reovirus RNA and initiation of its genomic function in L-strain fibroblasts. *J. Cell Biol.*, **36**, 197-230.

Siuzdak, G. (1998). Probing viruses with mass spectrometry. *J. Mass Spectrom.*, **33**, 203-211.

Skehel, J. J. and Joklik, W. K. (1969). Studies on the in vitro transcription of reovirus RNA catalyzed by reovirus cores. *Virology*, **39**, 822-831.

Smith, R. E., Zweerink, H. J., and Joklik, W. K. (1969). Polypeptide components of virions, top component and cores of reovirus type 3. *Virology*, **39**, 791-810.

Stanley, N. F. (1967). Reoviruses. *Br. Med. Bull.*, **23**, 150-154.

Starnes, M. C. and Joklik, W. K. (1993). Reovirus protein lambda 3 is a poly(C)-dependent poly(G) polymerase. *Virology*, **193**, 356-366.

Strong, J. E., Leone, G., Duncan, R., Sharma, R. K., and Lee, P. W. (1991). Biochemical and biophysical characterization of the reovirus cell attachment protein sigma 1: evidence that it is a homotrimer. *Virology*, **184**, 23-32.

Tang, D., Strong, J. E., and Lee, P. W. (1993). Recognition of the epidermal growth factor receptor by reovirus. *Virology*, **197**, 412-414.

Tao, Y., Nibert, M. L., and Harrison, S. C. (2000). Crystal structure of reovirus polymerase lambda3 at 2.5 Å resolution. *Seventh International Symposium of Double-Stranded RNA Viruses*, Aruba. W4-2.

Taylor, A. E. (1996). Cardiovascular effects of environmental chemicals. *Otolaryngol. Head Neck Surg.*, **114**, 209-211.

The Merck Index (1983): 10th edition, Merck and Co., Inc. Rathway, NJ.

Tosteson, M. T., Nibert, M. L., and Fields, B. N. (1993). Ion channels induced in lipid bilayers by subvirion particles of the nonenveloped mammalian reoviruses. *Proc. Natl. Acad. Sci. U.S.A.*, **90**, 10549-10552.

Traore, O., Arnal, C., Mignotte, B., Maul, A., Laveran, H., Billaudel, S., and Schwartzbrod, L. (1998). Reverse transcriptase PCR detection of astrovirus, hepatitis A virus, and poliovirus in experimentally contaminated mussels: comparison of several extraction and concentration methods. *Appl. Environ. Microbiol.* **64**, 3118-3122.

Turner, D. L., Duncan, R., and Lee, P. W. (1992). Site-directed mutagenesis of the C-terminal portion of reovirus protein sigma 1: evidence for a conformation-dependent receptor binding domain. *Virology*, **186**, 219-227.

van Regenmortel, M. H. V., Fauquet, C. M., Bishop, D. H. L., Carstens, E. B., Ester, M. K., Lemon, S. M., Maniloff, J., Mayo, M. A., McGeoch, D. J., Pringle, C. R., and Wickner, R. B. (eds.) (2000). Reoviridae. In *Virus Taxonomy: Seventh report of the International Committee on Taxonomy of Viruses*. Academic Press, San Diego, CA. pp: 395-480.

Vander, A. J., Sherman, J. H., and Luciano, D. S. (1994). Human physiology: the mechanism of body function. 6th edition. Prancan, K. M.; Bradley, J. W. eds. New York, McGraw-Hill, Inc. pp:561-600.

Vertrel XF technical bulletin (1999): DuPont Chemicals, Wilmington, Delaware, U.S.A.

Virgin, H. W., Mann, M. A., and Tyler, K. L. (1994). Protective antibodies inhibit reovirus internalization and uncoating by intracellular proteases. *J. Virol.*, **68**, 6719-6729.

Wiener, J. R., Bartlett, J. A., and Joklik, W. K. (1989). The sequences of reovirus serotype 3 genome segments M1 and M3 encoding the minor protein mu 2 and the major nonstructural protein mu NS, respectively. *Virology*, **169**, 293-304.

Wiener, J. R. and Joklik, W. K. (1989). The sequences of the reovirus serotype 1, 2, and 3 L1 genome segments and analysis of the mode of divergence of the reovirus serotypes. *Virology*, **169**, 194-203.

Xu, P., Miller, S. E., and Joklik, W. K. (1993).Generation of reovirus core-like particles in cells infected with hybrid vaccinia viruses that express genome segments L1, L2, L3, and S2. *Virology*, **197**, 726-731.

Yeager, M., Weiner, S., and Coombs, K. M. (1996). Transcriptionally active reovirus core particles visualized by electron cryo-microscopy and image reconstruction. *Biophys.* **70**, A116.

Yin, P., Cheang, M., and Coombs, K. M. (1996). The M1 gene is associated with differences in the temperature optimum of the transcriptase activity in reovirus core particles. *J. Virol.*, **70**, 1223-1227.

Yue, Z. and Shatkin, A. J. (1997). Double-stranded RNA-dependent protein kinase (PKR) is regulated by reovirus structural proteins. *Virology*, **234**, 364-371.

Zarbl, H., Skup, S., and Millward, S. (1980). Reovirus progeny subviral particles synthesize uncapped mRNA. *J. Virol.*, **34**, 497-505.

Zarbl, H. and Millward, S. (1983). The Reoviridae. 107-196.

Zou, S. and Brown, E. G. (1992). Identification of sequence elements containing signals for replication and encapsidation of the reovirus M1 genome segment. *Virology*, **186**, 377-388.

Zweerink, H. J., Ito, Y., and Matsuhisa, T. (1972). Synthesis of reovirus double-stranded RNA within virion like particles. *Virology*, **50**, 349-358.